This is not a peer-reviewed article.
Jack C. Wiley and Reed J. Turner. 2008. Power Hop Instability of Tractors. ASABE Distinguished Lecture No. 32, pp. 1-64. Agricultural Equipment Technologcy Conference, 10-13 February 2008, Louisville, Kentucky, USA. ASABE Publication Number 913C0108.

Power Hop Instability of Tractors

Jack C. Wiley
Principal Engineer, Retired
Deere & Company Technology Center
Moline, Illinois

Reed J. Turner
Project Engineer, Retired
The Agricultural Technology Centre
(formerly the Alberta Farm Machinery Research Centre)
Lethbridge, Alberta, Canada

For presentation at the 2008 Agricultural Equipment Technology Conference
Louisville, Kentucky, USA 10-13 February 2008

Published by the
American Society of
Agricultural and Biological Engineers
2950 Niles Road, St. Joseph, MI 49085-9659 USA

The Lectures Series has been developed by the Power and Machinery Division Tractor Committee (PM-47) of ASABE to provide in-depth design resource information for engineers in agricultural industry. Topics shall be related to the power plant, power train, hydraulic system, and chassis components such as operator environment, tires, and electrical equipment for agricultural or industrial tractors or self-propelled agricultural equipment.

ASABE is grateful to Deere & Co. for sponsoring the ASABE Distinguished Lecture Series.

For information, contact:

ASABE, 2950 Niles Rd., St. Joseph, MI 49085-9659 USA.

Phone: 269 429 0300 Fax: 269 429 3852 E-mail: hq@asabe.org

ASABE is an educational and scientific organization dedicated to the advancement
of engineering applicable to agricultural, food, and biological systems.
For more information visit www.asabe.org.

ASABE Publication Number 913C0108

Contents

Power Hop Instability of Tractors

Jack C. Wiley
Principal Engineer, Retired
Deere & Company Technology Center
Moline, Illinois

Reed J. Turner
Project Engineer, Retired
The Agricultural Technology Centre
(formerly the Alberta Farm Machinery Research Centre)
Lethbridge, Alberta, Canada

Abstract. *Power hop is a "porpoising" type of pitch/bounce oscillation superimposed on the forward motion of tractors equipped with pneumatic tires. It is most often observed with tractors having two powered axles pulling towed implements in moderate to high draft field operations on dry soils. As power hop begins, the tractor exhibits gradually increasing vibration amplitudes until the operator, of necessity, has to take action to maintain control of the vehicle. In this paper, the phenomenon is shown to be a self-excited vibration. This result follows from a stability analysis of a mathematical model of the tractor-implement system. The model results were confirmed with extensive tests conducted on both concrete test tracks and in numerous different soil conditions. Adjustments of fore-aft weight distribution and of front and rear vertical stiffnesses as influenced by tire inflation pressures are shown to be required for power hop control. During the course of research conducted in collaboration with several tractor tire manufacturers, it was found necessary to extend the tire load-inflation pressure tables to lower pressure limits in order to reduce stiffnesses enough to control power hop. The new tables were introduced early in 1992 and are now being used worldwide. In addition to controlling power hop, use of these lower inflation pressures has been shown to significantly increase tractor productivity and fuel economy, reduce soil compaction, improve ride quality, and reduce tire wear.*

Keywords: *Tractor, Vibrations, Power hop, Traction, Stability, Tires, Ballast, Tractor performance.*

Authors' Note: This paper was discussed and planned by both authors, then substantially prepared by the first author with subsequent additions by the second author and editing by both authors. Content authorship is noted using the active author's initials at the beginning of each section where there is a change in authorship.

The Power Hop Phenomenon

Basic Description

JCW—Power hop is a type of dynamic instability that can occur when a tractor is operating under moderate to high draft loads in the field. It has also been called "wheel hop," "tire hop," and "tractor hop," but the term "power hop" is most appropriate since it indicates that the phenomenon occurs when the tractor is delivering power to the ground in field operations. It is characterized by the gradual onset of an oscillatory motion having the general appearance of a combination of bounce and pitch modes of vibration that observers often describe as "porpoising." The oscillation amplitude increases with each cycle until it ultimately attains a steady-state value (limit cycle) determined by geometric constraints or power limits. Usually the tractor operator will reduce power as soon as possible after the unstable motion begins in order to stop the instability before maximum amplitude is reached. The motions can become so severe that the operator can lose contact with the seat and controls, so throttling back before this happens is a necessity.

Since power hop is a dramatic and unusual dynamic phenomenon, either seeing it on video or witnessing it live is essential to grasping the concept. The film clips of the destruction of the Tacoma Narrows Bridge serve as a perfect example of this point. Virtually everyone who has seen those movie clips can remember the bridge oscillations vividly, but most would find it difficult to describe the behavior to others in mere words. For that reason, a DVD with many video clips of power hop is included with the printed copies of this Lecture that are available for purchase from ASABE. Any reader who has not seen power hop is urged to watch the video clips before proceeding

further since this will clarify many aspects of this intriguing phenomenon that words cannot easily convey.

Power Hop Is Not Road Lope

Road lope is a different type of dynamic phenomenon that can occur at typical transport travel speeds. It is a forced vehicle vibration excited by a geometrically out-of-round tire, wheel, or hub, or a combination of these three. In a relatively small critical speed range, the frequency of excitation is close to or coincides with a natural frequency of vibration (pitch or bounce) which produces large amplitude motions if the out-of-roundness is sufficiently high. Usually these large motions begin to subside and then vanish as the travel speed is increased beyond this critical range. This is an example of the well-known condition called resonance and occurs in typical vibrating systems subjected to a periodic external excitation. Road lope occurs during high-speed transport—not at field working speeds with typical draft loads acting on the tractor.

Terminology

Vehicle Terms

Throughout this document and on the accompanying DVD, the terms MFWD, 4WD, and 2WD are used with the following meanings unless otherwise noted.

- MFWD (mechanical front-wheel drive) tractor—A tractor with powered front and rear axles. The front tires are smaller in diameter than the rear tires, and the tractor is steered with the front wheels. It is assumed to *not* have a front suspension system unless specifically indicated to the contrary.
- 4WD (four-wheel drive) tractor—A tractor with powered front and rear axles. The tires are all equal in diameter, and the tractor is steered by a center frame articulation joint or, less frequently, by coordinated front and rear steer wheels. It is assumed to *not* have a suspension system.
- 2WD (two-wheel drive) tractor—A tractor whose rear axle only is powered. The front tires are smaller in diameter than the rear tires, and the tractor is steered with the front wheels. It is assumed to *not* have a suspension system.

Traction Terms

RJT—Over the years, traction terminology has varied as the understanding of traction parameters has developed. While the authors recognize the current standard terminology defined by ASABE S296.5 (2003), no effort has been made to standardize these terms across the spectrum of work reported in this document. Table 1 is presented to assist the reader in relating older or previous terms to the current standard ones.

Table 1. Tractor and traction term equivalencies.

ASABE Standard Term	Common or Prior Usage Term
Static Load (Tire)	Weight per tire, normal force per tire
Dynamic Load (Tire)	Normal force while operating, Static Load + Weight Transfer
Static Load (Vehicle)	Weight, Vehicle Weight
Motion Resistance	Towing Force, Rolling Resistance
Motion Resistance Ratio	Rolling Resistance Ratio
Travel Reduction	Slip, % Slip
Traction Ratio	Pull/Weight Ratio, P/W
Vehicle Output Power	Drawbar Power

Observations about Power Hop

Vehicle Types

JCW—Power hop was apparently first observed soon after 4WD tractors began to appear in North America in the 1950s. The earliest incidence of power hop reported by John Deere engineers occurred in 1958 during tests of a prototype of the model 8010 4WD tractor (Figure 1), the first 4WD tractor designed by John Deere. The test engineers had not seen this behavior before and did not know what to call it. In their test reports, they referred to it as "bunny hop," the name of a dance that was popular with teenagers at the time. Later, power hop was also observed when MFWD tractors were introduced in the 1970s. Power hop can occur on MFWD tractors equipped with front suspension systems, but is far less likely than with unsuspended tractors. Although power hop can occur with 2WD tractors, it is extremely rare in field applications. It has been observed at very high pull levels in tests of 2WD tractors on soil and on concrete. It is likely to be the instability sometimes cited in Nebraska tractor test reports as "pull in *n*th gear was limited by tractor stability." Power hop also can occur in 4WD trucks, 4WD automobiles, and certain types of multi-axle drive military vehicles all operating in off-road high draft conditions.

Figure 1. John Deere 8010 4WD tractor introduced in 1959.

Tire Types

Early 4WD and MFWD tractors were only equipped with bias ply tires, and, as noted previously, these tractors exhibited power hop in certain soil and test conditions. Later when radial ply tires were introduced, the incidence of power hop increased which caused some people to place blame on the radial tires. One possible explanation is that the internal damping rate of bias ply tires is higher than that of radial ply tires which would tend to quell or diminish vibrations. Although data on this is sparse, Kutzbach and Schrogl (1987) found that at typical field working speeds, the internal damping of bias ply tires on a firm surface was about 50% higher than that of radial ply tires. Now (2007) almost all high power field-working tractors with tires are equipped with radial tires, so the question of the difference in tractor stability behavior due to tire construction is essentially moot.

Implement Types

Power hop occurs predominately with implements towed from the tractor drawbar. It typically does not occur with standard 3-point hitch mounted implements. Presumably this is the result of the damping/dissipation effect of the attached implement that resists the pitch motions of the tractor/implement combination. It can occur with semi-mounted implements since the draft links essentially serve as a drawbar with this type of mounting arrangement.

RJT—The lack of power hop with mounted implements may also be the result of the steeper draft angle, the center of mass location change because of the load, or the increased rear tire inflation pressures required because of the weight of the mounted implement.

Tillage Practices and Terrain

JCW—Power hop can occur on soils which are either firm or are loose on top as the result of either a secondary tillage pass or because that is just the nature of the particular soil type. Often the scenario in dryland farming areas of North America is that the tractor operates without incidence when pulling a chisel plow or similar tillage tool in wheat stubble, but experiences power hop during a second-pass tillage operation in the same field. The loose soil on top of the hard under-layer may be 100-200 mm (4-8 in) deep in such cases, and often this means that the draft load increases on the second pass. In addition to increased draft and the resulting changes produced in weight transfer and slip, other changes in the tilled soil, including different traction conditions and different stiffness and damping properties of the loosened soil, also come into play. This change of behavior from stable on untilled soil to unstable on tilled soil in the same field has been a major source of frustration for tractor operators.

The likelihood of encountering power hop also increases when the tractor is pulling up a slope or turning with the tillage implement still in the ground, a common practice in some parts of North America. These also imply increases in draft load beyond that required for level straight-ahead operations. It will become clear in the analysis and test results presented later that the onset of power hop instability is very much related to the draft load on the tractor. However, power hop has also been observed on an International Harvester 2+2 style 4WD tractor climbing a steep hill on loose soil without pulling any implement. The downslope component of the tractor weight was enough of a "draft load" to induce the instability. See the accompanying DVD which shows this unusual behavior.

Soil Conditions

Soil moisture and texture have major influences on power hop. The drier the soil, the more likely it is that power hop will occur. Dry soils correlate with areas of North America and the rest of the world where incidences of power hop are most frequent. Presumably, this is due to the way in which moisture influences the damping characteristics of the soil. Power hop is extremely rare or non-existent when operating on soils that are very moist most of the time, e.g. drained rice checks. However, even in soils that are only somewhat moist most of the time, e.g., soils in the central U. S. Midwest, power hop is a rare occurrence. The fact that tractors can be operated hop-free in most parts of the world with little attention paid to the control recommendations for inflation pressures and ballasting now being recommended is probably due to the amount of moisture present during tillage operations in the vast amount of arable soils. Most tractors never experience power hop in their entire working life, but where the soil moisture content tends to be low, the incidence of power hop dramatically increases.

The location of the moisture within the soil also has a very significant influence on power hop incidence. Two personal experiences of the first author illustrate this point. The first occurred at the Firestone Fort Stockton, Texas, Proving Grounds in 1990. The previous fall, John Deere and Firestone engineers had conducted numerous power hop tests of an MFWD tractor at that location. Power hop occurred readily on this very dry and loose Caliche soil. The following year in late March, tests of a 4WD tractor were initiated in the same field. No matter what combinations of inflation pressures were used, power hop did not occur at any drawbar load. Rain had fallen on the location several weeks prior to the test, but the soil was very dry and loose on top. It appeared to be just as dry as it was the previous fall, and dust was easily stirred up by the test tractor and associated equipment. Several holes were dug in the field to look for moisture. The first traces of slightly moist soil were about 200 mm (8 in) below the average surface level and the moisture content gradually increased with further depth. Thus the damping effect of the moisture which was quelling the hop was coming from well below the loose layer at the top.

A second revealing event occurred while testing a 4WD tractor in the San Joaquin Valley of California in May of 1990. The tractor was pulling a five-shank towed ripper operating 400-460 mm (16-18 in) deep in a level field where a crop of lettuce had just been harvested. While the crop was growing, the field had been irrigated with open-flow surface water between each row of lettuce. The entire square field was bordered by a deep irrigation ditch, and another deep irrigation ditch crossed through the middle of the field. An early crop of lettuce was planted on one side of the cross channel and a later crop was planted on the other side. Prior to harvesting each crop, the irrigation was stopped to allow the soil to dry. The irrigation water for the later crop was in place two weeks longer than for the first crop. After both crops were harvested, the ditches were filled and the entire field disked with a stubble disk. The power hop testing in this field occurred two weeks after the final lettuce harvest. Passes through the field crossed alternately from the early crop area to the later crop area. For most front and rear inflation pressure combinations, power hop occurred readily on the drier side of the field. However, as soon as the tractor passed to the side that had been harvested last and thus had more subsoil moisture, hop would cease immediately. With either extremely high front inflation pressures or extremely high rear inflation pressures, power hop was controlled on both sides of the field. This was very convincing evidence that the moisture content of the soil well below the surface was the factor determining tractor stability.

Soil texture is an additional factor influencing power hop. Tractors operating on lighter soils experience more power hop than those on heavier soils. In many cases, areas with lighter soils are also drier so these factors may be linked.

RJT—Stiff or motion-resistant soils, those with high interstitial friction or significant interlocking between the constituent particles, such as the volcanics found in parts of the Northwest, are also more prone to power hop.

JCW—Power hop is not as common in Europe as in North America. This is probably because (a) European soils tend to be moist and are often tilled with much higher moisture content than would be the case in most of North America, and (b) most high draft tillage tools used in Europe are 3-point hitch mounted. Of course there are exceptions where power hop does occur routinely, including portions of Spain and Italy. It also occurs in other countries with dry soil conditions such as Israel.

In summary, the soil has a major influence on the incidence and ease of control of power hop. Variations of soil properties and conditions mean that adjustments of the tractor ballast and/or tire inflation pressures are required for control. Obviously, humans can control the tractor and tires but not the soil.

Other Factors

The incidence of power hop also increases as tractor travel speed increases. It is also more likely to occur with 4WD tractors ballasted with a low weight-to-power ratio. These factors were not recognized prior to the mid-1990s. Both are discussed later in the section dealing with power hop control of 4WD tractors.

Conjectures about Power Hop

Beginning with the first power hop incidents in the late 1950s and continuing forward to the present, numerous conjectures have been advanced to try to explain it or to identify a possible cause. Some of the first to be offered placed blame on the implement, and in particular, on the incessant partial tripping and resetting action of the shanks of chisel plows and cultivators in some field conditions. Another suspected implement problem was improperly adjusted gauge wheels. The height of the tractor drawbar above ground was also considered a possible factor. Another alternative that was seriously investigated was "terrain molding" with 4WD tractors—a concept similar to the washboarding effect of cars and trucks on gravel roads. It was based on the premise that as a result of vehicle motions, the front tires could imprint a "wavy" shape into the soil that the rear tires would have to follow creating a situation in which the amplitude of tractor motion would grow with time. A similar effect can occur with a bulldozer if the operator does not continuously "feather" the blade height. If the operator does not modulate the height, a progressively more wavy set of gouges can be created in the soil. The specific amount of lead or lag of the front wheel speed relative to the rear of MFWD tractors was also cited as a possibility along with a resultant "difference in traction" between the front and rear tires. There were numerous power train related suggestions starting with engine governor surge. Surge was followed by power train torsional oscillations, tire windup, and stick-slip soil/tire interactions. The influence of tire construction, i.e., bias ply vs. radial ply, on power hop was also hotly debated. All of these factors can have some influence on power hop, but none ultimately surfaced as a prime factor. However, this wide range of speculations about possibilities made it difficult to formulate either an analytical or an experimental investigation in the early years.

Power Hop Investigations

Relatively little about power hop has been published over the years. Starting in the early 1970s and continuing to the present, service bulletins on power hop have been issued by tractor and tire manufacturers to their dealers. These documents often contained what now have come to be recognized as glaring errors in describing what it was or what to do about it. The subject was treated very cautiously

and quietly by tractor and tire manufacturers because there was a general feeling of embarrassment that there was a problem in the first place, and second, that there was no certain way to deal with it.

The first research publications on power hop were written by Professor J. B. Liljedahl and his students at Purdue University; see Kirby et al. (1968) and Al-Deen et al. (1977, 1978). They used the phrase "jumping phenomena of tractors" but did also mention the word "hop" in their list of keywords. They explain that this problem had been observed by "some farmers, test engineers, and contractors," but they made no claim as to having actually seen it themselves. Single-wheel and two-wheel test rigs were built to try to show the phenomenon and compare results to mathematical models, but the outcomes were limited. In a short article in the August, 1974, issue of *Agricultural Engineering*, Professor Liljedahl (1974) also quotes remarks about power hop that R. N. Coleman of International Harvester made during a session on tractor tire vibrations at the 1974 ASAE Annual Meeting. Coleman also showed a short movie of power hop at that meeting.

RJT—The authors received letters from L. T. Scura and R. A. Michael discussing their power hop modeling efforts at the John Deere Product Engineering Center (PEC) at Waterloo, Iowa. While this work was not published, their early efforts provided points on a path that ultimately led to the hop modeling approach discussed in this lecture, and they have generously made summaries available for the purpose of the lecture.

As recorded by Scura, around 1979 a subjective evaluation was undertaken by the PEC to evaluate the factors that contributed to power hop on an MFWD tractor. The study concluded that tire pressures, ballast levels, weight distribution, foam-filled tires, liquid ballast, and travel speed all affected power hop. It found that front tire overspeeds, tread width settings, duals front or rear, blocked front axle oscillation, drawbar heights, and implement isolation had no effect on power hop. The video sequence "Power Hop from the 1970s" on the Lecture DVD is actually shots of tractors tested during this program.

Concurrent with this test program, Scura was asked to further study Al-Deen's two degree of freedom model. He exercised it using the IBM mainframe computer-based Continuous System Modeling Program (CSMP), and investigated the model response to various ranges of inputs, including the effects of tire spring rates, tire damping rates, and chassis weight distributions. He was one of the first investigators to recognize the importance of a coordinate coupling coefficient in the hop model and to investigate and show its effect on predicting the stability of the vehicle. He showed that with certain tire spring rate and vehicle weight distribution combinations, the tractor system could become unstable, and found that detuning the system was an effective way of controlling the instability.

In 1981, Michael developed a three degree of freedom model of a tractor, adding fore-aft translation to the previously used vertical translation and pitch rotation degrees of freedom. He approached the project using a classical control systems analysis that examined the complex roots of the characteristic equation of the system, a similar approach to one Scura had tried along with his time domain CSMP simulations. He found it was necessary to include both static sinkage of the tire into the soil and sinkage due to slip to achieve a good correlation between the model predictions and field test results.

JCW—In 1982, Erickson et al. (1982) presented a paper on 4WD tractor axle and drawbar horsepower measurements at the ASAE Summer Meeting. In it they briefly mention "severe harmonic vibrations" encountered in field testing at high draft loads and in turns. This probably was power hop although they did not use that term. However, when this paper was ultimately published in the *ASAE Transactions* (Erickson et al., 1983), this point was omitted for some reason.

There have been several publications by engineers from Deere. Volfson's research is based on his conjecture that there is a stick-slip phenomenon occurring at the soil-tire interface (see Volfson, 1983, 1986, 1988, and 1999). Wiley et al. (1979), Smith et al. (1982), and Orlandea (1988) published some results from extensive simulations of full 3D models of 4WD tractors using Orlandea's personal version of ADAMS (Automated Dynamic Analysis of Mechanical Systems), a general purpose dynamic simulation software package he had written as part of his Ph.D. thesis at the University of Michigan (Orlandea, 1973). This thesis later became the basis for the commercial version of ADAMS (see Orlandea et al., 1977, and MSC Software, 2007). The ADAMS simulations were coupled with 3D graphic animations which clearly showed power hop occurring or a stable tractor depending on inflation pressure combinations. A variety of power train configurations were also examined. One of the most interesting results produced by the ADAMS simulations is that the front tire-soil damping plays a more important role than the rear tire-soil damping in controlling power hop (see Orlandea, 1988). Later Wiley et al. (1992) presented the results of a collaborative test program with Deere and the major agricultural tire manufacturers which prefaced the introduction of the load-inflation pressure tables that were extended downward to lower pressures. These tables, introduced by Deere and the major agricultural tire manufacturers early in 1992, provided a much needed breakthrough in power hop control. Zoz (2007) offered the conjecture that tangential deflection of the tire is a cause of power hop. Directly related to this is another paper on tire behavior by Burt et al. (1999).

Zhuang et al. (1990) created a mathematical model of a 4WD utility vehicle towing a draft load on sand. They focused on the interactions of the vehicle suspension system and the power train dynamics.

Professor Kenshi Sakai and his colleagues have produced a number of publications on power hop (see Sakai et al., 1998, 1999; Garciano, 2002). Their studies are based on chaos theory.

The question of determining the appropriate gear ratio between front and rear axles of MFWD tractors has been addressed by several researchers in the past, but one study that specifically focuses on power hop was presented by Schlosser et al. (2001).

Professor Karl Th. Renius, who gave the 2005 ASABE Distinguished Lecture (Renius and Resch, 2005), provided us the following information regarding work of his students that bears some relation to power hop. We paraphrase his communications to us as follows. Professor Renius says that "Although power hop is not often considered to be a problem in mid-Europe, we have collected in my former Institute at TU München some experience with power hop**.** This was within a large research program on optimized power distribution between rear and front axles. The basic problem was that with a rigid shaft connection of both axles with MFWD engaged—as is the usual case for agricultural tractors—it only works well when pulling straight ahead on soft soils, but does not work well under many other conditions such as pulling at higher speeds (circulating power) or pulling in turns (front axle speed too low, creates braking, reduces pull, creates high tire wear) or pulling a trailer uphill on hard soils (power hop). All tractor companies thus introduced for transport speeds and sharp turns an automatic disconnection of the front axle, but they are not pleased with this 'solution.' Two well-accepted Ph.D. theses under my guidance have been published as books on the related fundamentals and on a solution of the well-known problems (Grad, 1996, and Brenninger, 2002)."

Going on, he says, "The Grad thesis is focused on the fundamentals, but does present a solution by replacing the conventional 'rigid' MFWD drive shaft (gear box output to front axle) by an infinitely variable power split transmission designed and built in my institute. This transmission worked almost mechanically in a straight forward mode (with high efficiency), hydrostatic power portion increases in turns giving 'pull-in-turn' ability and prevents circulating power on the road. A torque distribution control was developed. The system worked well preventing all the indicated problems and we could not create power hop. The control of the first approach was, however, not very fast, mainly in turns. Brenninger's thesis was focused on improving the system regarding the transmission structure and control. First, the results of Karl Grad were confirmed and refined. The control system was improved considerably by highly sophisticated digital algorithms. He also asserted that power hop can be prevented by his infinitely variable MFWD control system."

Dominique Dessèvre (2005) of Michelin Research and Development in Clermont-Ferrand, France, presented results of his 2D simulation model and compared them to experimental results showing general agreement. At the conclusion, he made the interesting observation, "Other simulations, not described in detail in this paper, tend to demonstrate the limited impact of reasonable changes in the tire conceptions."

Finally, the following U. S. Patent and Patent Applications are relevant to power hop. The information is taken directly from the documents themselves without editing.

1. U. S. Patent Number 6,589,135. System and method for reducing vehicle bouncing. Inventor: James A. Miller. Assignee: Deere & Company. Issued: July 8, 2003.

This invention relates to a method for controlling an internal combustion engine of a vehicle in order to reduce low frequency bouncing oscillations of the vehicle, which is a phenomenon known as "road lope." (Note: The term power hop is also used in the Background of the Invention in the Patent.)

A system and method is described for controlling vehicle bouncing of a vehicle having an engine driving wheels through a transmission having multiple gear ratios. The vehicle has a fuel control unit for supplying a variable amount of fuel to the engine in response to fuel control signals generated by an engine control unit. The method includes generating a control code as a function of a gear ratio of the transmission; sensing vehicle acceleration with an accelerometer mounted on the vehicle and generating an acceleration signal in response to motion of the vehicle. The fuel control signal is generated as a function of the control code, the acceleration signal and a frequency dependent transfer function value. The fuel delivered to the engine is modified as a function of the fuel control signal.

2. Patent Application Number 20060009897. Tractor power hop control system and method. Inventors: Troy Eugene Schick and Boris P. Volfson, Assignee: Deere & Company, January, 2006.

A control system performs a method for controlling pitching and bouncing of a vehicle having an engine driving wheels through a transmission and having a fuel control unit for supplying a variable amount of fuel to the engine in response to fuel control signals generated by an engine control unit. The method includes, from front and rear acceleration signals, generating vehicle pitch and bounce signals, converting the pitch and bounce signals to RMS pitch and bounce values, generating a fuel offset value as a function of the RMS pitch and bounce values, and modifying fuel delivered to the engine as a function of the fuel offset value. The fuel offset value is operated on by a bi-linear gain function wherein negative values are multiplied by a larger gain and positive values are multiplied by a smaller gain.

The Mathematical Model: An Overview

Modeling Approaches

"A problem well stated is a problem half solved."

Charles F. Kettering

Power hop was and remains an intriguing dynamic phenomenon. It was natural that engineers would turn to the principles of rigid body dynamics to develop an understanding of power hop as a first step in determining an appropriate strategy for either eliminating it from happening by design or to know how to control it with appropriate system adjustments. Thus an obvious approach was the classical method of developing a free body diagram of an off-road vehicle including all the external forces and using a time domain integration technique to numerically solve the resulting differential equations of motion. By varying parameters such as the applied drawbar load, tire stiffnesses and damping, the vehicle center of gravity location, etc., one would hope to be able to reproduce power hop analytically and thus have a powerful tool for investigating it. During the 1970s and 1980s, a number of Deere engineers took up the challenge of modeling power hop using this time domain approach. The vast majority of their work was published only as internal company reports, but some was published externally as noted previously.

A major challenge in doing mathematical simulations was the lack of understanding of the specific circumstances in the field when power hop occurred, i.e., what exactly needed to be accounted for in the simulations that related to tractors operating in real field conditions. Up until the late 1980s, power hop was very much a "ghost" type phenomenon in that when occurrences of hop were reported in the field and an engineer was sent to investigate, usually a change in soil conditions or operating conditions made it impossible to reproduce hop. Clearly a more systematic means for being able to consistently induce hop for experimental purposes was needed.

This breakthrough occurred in the early spring of 1989 when Firestone engineers used a motor grader as a hold-back loading device to gradually increase the drawbar load on a MFWD tractor operating on Caliche soil at the Firestone Fort Stockton, Texas, Proving Grounds. Power hop occurred with several different combinations of front and rear inflation pressures. These tests also showed that hop could be controlled by increasing the inflation pressure of the front tires while lowering the inflation pressure of the rear tires.

When the results of the Firestone tests were communicated to Deere personnel in mid-spring of 1989, a new effort was initiated to understand hop from an analytical standpoint. But instead of using a time domain approach, a stability analysis was developed. It is similar to the approach often used in the analysis of control systems and to determine the dynamic stability of elastic systems. This provided the major breakthrough for a greatly improved understanding of power hop. Some of the earlier analytical investigators within Deere had suggested this approach but had not fully utilized its power for understanding the hop phenomenon.

The Stability Analysis Approach

The theory of stability analysis and many practical examples are provided in the books by Bolotin (1963), Bolotin (1964), Panovko and Gubanova (1965), and Ziegler (1968), to cite just a few of the most well-known classical references. The general approach most widely employed is to investigate disturbances (small motions) about a static equilibrium position or about a steady-state configuration (operating point) in a dynamic system. If these small motions decay with time, the system is stable. If they begin to increase with time, the system is unstable.

The first step in using this approach is to determine the steady state equilibrium configuration or *operating point* of the dynamic system being investigated. This requires that system geometric and other nonlinearities be included unless the location of the equilibrium configuration or operating point is readily determined by inspection.

The next step is to develop the linearized differential equations that govern small motions of the system about the equilibrium configuration or operating point. Then the eigenvalues of these linear differential equations are examined to determine the nature of small oscillations of the system about the operating point that would result from any kind of small disturbance or perturbation from the equilibrium configuration. These disturbances are slight "nudges" from the equilibrium position—not a periodic external excitation from some source. Such disturbances are always present in nature.

If the resulting motion tends to decay with time, the system is said to be *asymptotically stable* as shown in Figure 2. This behavior is typical of most well-known free vibration systems.

If the resulting motion tends to grow with time without oscillation, the system is said to exhibit *static instability* or *divergence* as shown in Figure 3. A simple example of a system exhibiting this type of behavior is the buckling of a beam column subjected to an axial load.

If the resulting motion tends to grow with time in an oscillatory manner, the system is said to exhibit a *dynamic instability* (sometimes called *flutter*) as illustrated in Figure 4. Some examples of dynamic instability include flutter of airplane wings (Scanlan and Rosenbaum, 1968); extreme oscillations in suspension bridges and cables (Billah and Scanlan, 1991); galloping power lines and fluttering "STOP" signs in a steady wind (Den Hartog, 1956); weaving towed trailers, shimmying caster wheels and shimmying automotive steering systems (Rocard, 1957; Ziegler, 1968); "hunting" of rail car wheels on railroad rails (Rocard, 1960); brake chatter and machine tool chatter. These

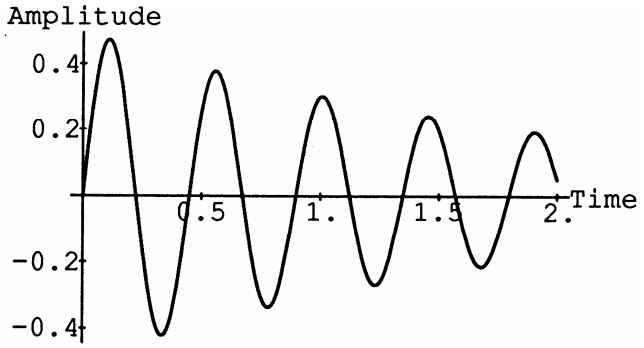

Figure 2. Asymptotically stable motion behavior.

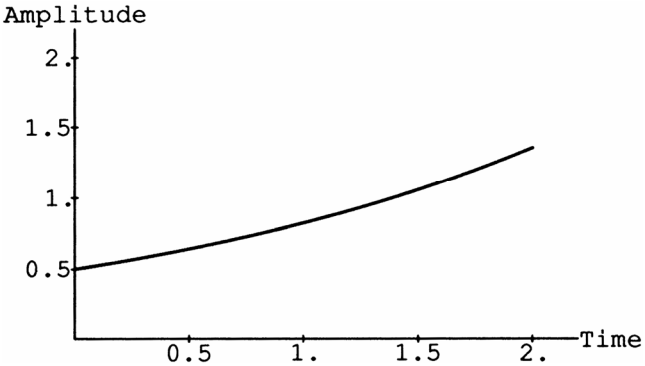

Figure 3. Divergence instability motion behavior.

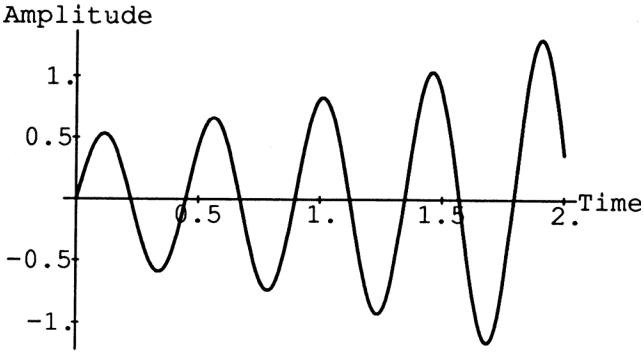

Figure 4. Flutter instability motion behavior.

are all examples of *Self-Excited Vibrations*. This terminology was established to clearly distinguish the flutter phenomena from the more well-known condition of *Resonance.* Resonance occurs when the frequency of an *external* periodic excitation is near one of the system natural frequencies resulting in amplitudes of motion that can become large. See Billah and Scanlan (1991) for an especially clear presentation of this distinction and of the errors made by many prior investigators who incorrectly tried to explain the failure of the Tacoma Narrows Bridge as a resonance phenomenon instead of recognizing it correctly as a dynamic instability. Also see Feldman (2003) for additional comments on Billah and Scanlan's presentation.

Before proceeding further, we pause to provide several statements that can be helpful in thinking about self-excited vibrations. The following quote is from J. P. Den Hartog, one of the most well-known early authorities on the subject; see Den Hartog (1956) and Chapter 5 of Harris (2002).

> "In a self-excited vibration, the alternating forces that sustain the motion are created or controlled by the motion itself; when the motion stops the alternating forces disappear.
>
> In a forced vibration, the sustaining alternating force or forces exists independently of the motion and persist even when the vibratory motion is stopped."

In a somewhat simplified form, we can say that a self-sustained oscillation amplitude gets larger on *this* cycle because it got larger on the *last* cycle. This increase continues until geometric or power constraints ultimately limit the amplitude of motion. Another statement often used is that in a self-excited vibration, some positive feedback mechanism allows energy from an external uniform or steady source to be absorbed into the vibration itself. This form is particularly meaningful when studying vibrations of pipes, cables, or structures induced by an external or internal flow of fluid.

In carrying out a stability analysis, it is not necessary to take the solution of the differential equations to completion by specifying initial conditions and performing a time domain integration of the equations. All of the information about stability is contained in the location of the roots (eigenvalues which, in general, are complex numbers $s = a + j\omega$) of the characteristic equation in the complex plane and in the relative amplitudes (eigenvectors or modes of vibration) of the system coordinates (or degrees of freedom) governed by these roots.

Typically the eigenvalues are plotted in the complex plane as illustrated in Figure 5 where the real part of the root is plotted on the horizontal axis with the imaginary part plotted on the vertical axis. It can be shown that the roots are always real or occur as complex conjugate pairs. A complex conjugate pair $a \pm j\omega$ corresponds to a time domain solution of the form $Ae^{at}\sin\omega t$. Thus if the real part of the root, a, is positive, the solution will increase with time (Figure 4) while if the real part is negative, the solution will decay with time (Figure 2). The imaginary part of the root determines the frequency, ω, of the oscillatory part of the motion. Thus for system stability, the real parts of the roots should lie in the left half of the complex plane or on the imaginary axis. A root with only a real part will lie on the horizontal axis with a positive root producing the divergent time domain behavior shown in Figure 3. A complex conjugate pair with a zero real part represents a sinusoidal oscillation of constant amplitude.

Each root is associated with an eigenvector or mode shape. For a linear system, the system's time response can be represented as a linear combination of the eigenvectors associated with the corresponding eigenvalues.

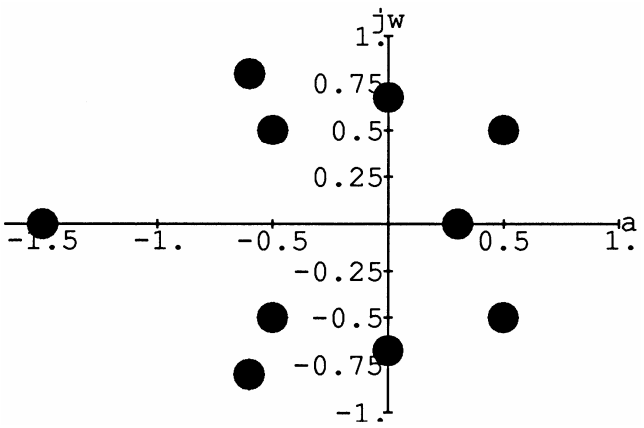

Figure 5. Example of typical eigenvalues in the complex plane.

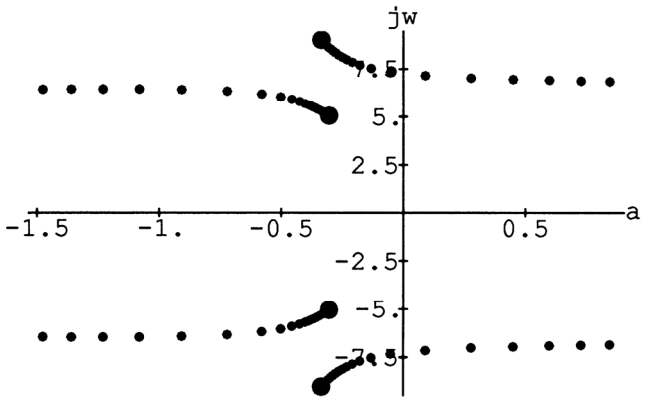

Figure 6. Example of root-locus behavior with two pairs of complex conjugate roots.

Usually, the system being investigated is under the influence of some non-oscillatory loading, motion generator (linear or angular velocity) or gain parameter. The value of this parameter dictates the system's stability as indicated by the eigenvalues which vary as the parameter is increased. Normally when the parameter is small, the system is stable. When the parameter is increased past some critical value, the system becomes unstable. This behavior is indicated by the real parts of at least one of the eigenvalue pairs migrating into the right half of the complex plane.

The ultimate task of the stability analysis is to determine how the system stability changes as the system parameter(s) are changed and includes determination of the critical condition at which the transition from stability to instability occurs. Note that the operating point also changes as a function of the system parameter(s).

A convenient means of illustrating the nature of the stability of the system is a root locus plot (sometimes called a pole plot) of the eigenvalues of the characteristic equation as a function of the parameter(s). Such a root locus plot is shown in Figure 6 for a two degree of freedom system having four roots. In this example the roots occur as complex conjugate pairs (equal real parts but imaginary parts of opposite sign). The large dots indicate the initial value of each of the four roots. As the parameter increases in specified increments, the roots follow the paths indicated by the smaller dots. In this example, two of the roots have real parts becoming more negative (greater stability) while two have real parts becoming more positive. When the real parts cross into the right half of the complex plane, the system becomes unstable. Note that only one of the pairs has to exhibit this behavior to produce an unstable system.

It is important to note that the approach outlined above does not predict what will happen *after* the onset of instability since it is only valid for small oscillations around the operating point. As the amplitude of the vibration increases, it is likely that the assumptions used to linearize the differential equations of motion are no longer valid. But the purpose of the analysis is only to predict the onset of instability, not what happens after it occurs.

Care must be exercised in modeling the dynamics of the system both to accurately determine the operating point and to then linearize the differential equations of motion for small oscillations about the operating point. In the formulation of the stability problem, one must be very careful to avoid making assumptions about the magnitudes, directions, and phase angles of forces or other effects that can change dramatically or come into play only after the onset of instability and then incorporating these concepts into the linearized model. The correct and safe approach is to think in terms of modeling a system that is well-behaved and undergoing small oscillations. The model has to include the basic physical phenomena that are relevant and operative in the stable regime and nothing more. The model is then exercised to determine the conditions under which it ceases to be stable. That is, the stability boundary is approached by going from the stable side to the unstable side.

The System Model: Basic Assumptions

The development of the mathematical model is rather detailed and lengthy. Consequently, the complete derivation and analysis are placed in the Appendix with only a basic sketch of the essential elements provided here to enhance readability. Some references to details in the Appendix will still be required to understand this outline, but they will be obvious to the reader.

The system model considers the motions of a four-wheel drive tractor in its plane of forward motion. The tractor has neither a front nor a rear suspension system other than the effects of the tires. Either a row crop MFWD tractor configuration or a 4WD tractor configuration can be represented by appropriate choices of parameters. The tractor is pulling a draft load and moving at a constant velocity V. Three degrees of freedom are all measured from the operating point position and orientation as illustrated in Figure 7.

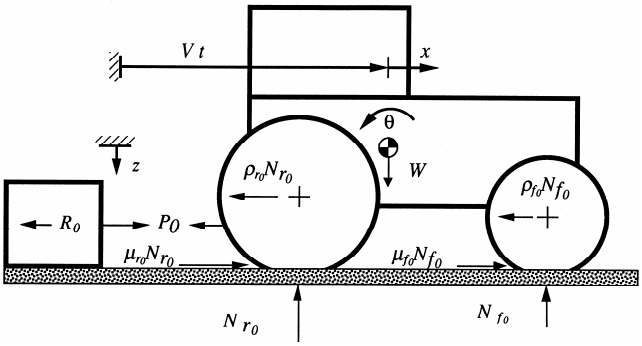

Figure 7. Operating point free-body diagram.

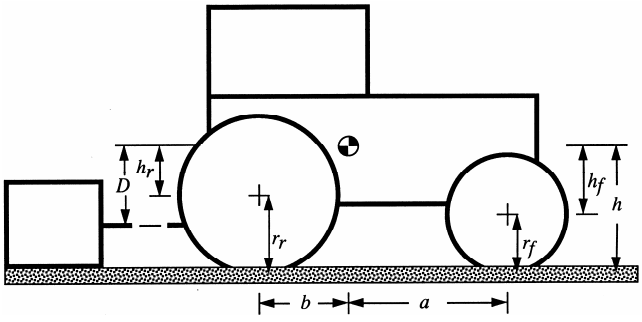

Figure 8. Basic system geometry parameters.

These are:

x, fore-aft translational motion (surge) of the center of gravity with respect to a coordinate system translating forward at the constant velocity *V* corresponding to the operating point forward velocity. With respect to the ground, the location of the center of gravity is given by $X = Vt + x$ where *t* is time. Thus a positive *x* displacement is in the direction of forward motion.

z, vertical translational motion of the center of gravity with respect to a datum located at the operating point height of the center of gravity above the ground surface. A positive *z* displacement is downward.

θ, pitch rotational motion of the vehicle with a counterclockwise displacement being considered positive. This pitch motion is measured from the operating point pitch orientation of the vehicle.

Thus, all three degrees of freedom have zero displacements and velocities at the operating point position.

The choice of the degrees of freedom here is significant in that additional degrees of freedom could have been considered. It has been postulated by some that power hop might have a power train related cause such as engine torque variations created by the engine governor, torsional oscillations in the power train and/or torsional oscillations in the drive tires. If the power hop instability is directly related to these degrees of freedom and they are not considered, the model will not be capable of predicting power hop. However, as the subsequent development shows, the model with just these three degrees of freedom does predict power hop.

The next step in the development of the model is to create a free body diagram of the vehicle including all the external forces. In doing so, the drive wheel mechanics used in Chapters 13 and 14 of Goering et al. (2003) are used. The traction and motion resistance forces for the front and rear wheels are shown appropriately in Figure 7. For operation on soils, the traction and motion resistance formulations of Brixius (1987) are used. For operation on concrete, the corresponding equations suggested by Zoz and Brixius (1979) are used.

System Geometric Parameters

The geometric parameters needed to describe the system are shown in Figure 8.

Determination of Operating Point Conditions

Referring to Figure 7, by writing out (a) Newton's equations of static equilibrium for the steady-state operating point condition, (b) the traction and motion resistance equations, and (c) the kinematics that relate the front wheel slip, the rear wheel slip and the tractor forward velocity *V*, we arrive at a set of 14 non-linear algebraic equations in 14 unknowns. This development parallels that shown in Chapter 14 of Goering et al. (2003).

Perturbed Motion about the Operating Point

The next step is to apply Newton's laws of motion to derive the differential equations describing small oscillations about the operating point in terms of the three generalized coordinates. The free-body diagram is the same as in Figure 7 except that the subscripts *0* indicating the operating point values are dropped to indicate general values instead of the specific values at the operating point. Once these equations are written out in base form, it is necessary to express them in terms of the degrees of freedom (x, z, θ), i.e., the external forces acting on the system must be represented in terms of them. The process is illustrated here only for the case of the front and rear normal forces. See the Appendix for all others.

The normal forces are modeled as a parallel spring-damper combination to reflect the tire's spring and damping properties. In doing so, the tire stiffness is taken as the slope (k_i, i = *f* or *r*) of its vertical load-deflection relation at the operating point deflection δ_{i0} as shown in Figure 9.

This stiffness model is really valid only for operation on a firm surface. For operation in deformable soil conditions, the spring and damping values used should reflect the tire/soil combination. This is an important point to remember when comparing analytical and experimental results, i.e., they will be most accurate for operation on firm surfaces. Mathematical models and/or experimental data describing the combined stiffness and damping effects of the tire/soil combination while tires are delivering traction on soft soils are unavailable.

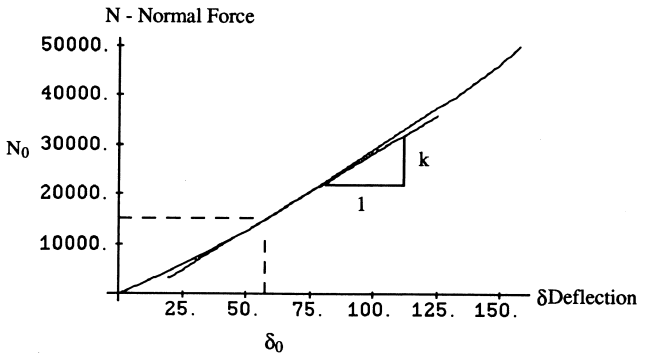

Figure 9. Typical vertical load-deflection relationship of a tire on a firm surface.

For firm surfaces the normal force can then be expressed as

$$N_i = N_{i0} + k_i(\delta_i - \delta_{i0}) + c_i\dot{\delta}_i$$

where c_i is the viscous damping value. Note k_i and c_i represent the total vertical stiffness and damping at the front or rear axle. For springs (or dampers) in parallel (the case for multiple tires on an axle), the individual stiffnesses (damping rates) add to determine the equivalent total stiffness (damping) at the axle.

The process of defining the linearized values of all of the other external forces at the operating point is similar. Once these are complete and linearized, the three differential equations of perturbed motion about the operating point can be expressed in vector-matrix form as:

$$[M]\begin{Bmatrix}\ddot{z}\\ \ddot{\theta}\\ \ddot{x}\end{Bmatrix} + [C]\begin{Bmatrix}\dot{z}\\ \dot{\theta}\\ \dot{x}\end{Bmatrix} + [K]\begin{Bmatrix}z\\ \theta\\ x\end{Bmatrix} = \begin{Bmatrix}0\\ 0\\ 0\end{Bmatrix} \qquad (1)$$

where [*M*], [*C*], and [*K*] are termed the mass, damping and stiffness matrices respectively. See Equation (A-16) in the Appendix for the complete definitions of the elements of these matrices.

System Stability Calculations

The previous two sections outline the derivation of the system of equations determining the operating point and the three linearized differential equations of motion about that operating point. A *Mathematica*-based (see Wolfram, 2007) procedure was set up to automate this task using the drawbar pull force (or slip) as a parameter. This procedure is outlined in Figure 10.

First the vehicle parameters are defined. For a given drawbar pull level exerted on the vehicle (or alternatively for a given slip value), the system of equations determining the operating point are solved using an iterative technique to determine the operating point values. These values are then entered into the mass, damping and stiffness matrices defined in Equation (A-16) of the Appendix. The eigenvalues and eigenvectors of the system differential equations are then computed numerically using standard *Mathematica* routines. This procedure is repeated for incrementally increased values of the drawbar pull (or slip). A root locus

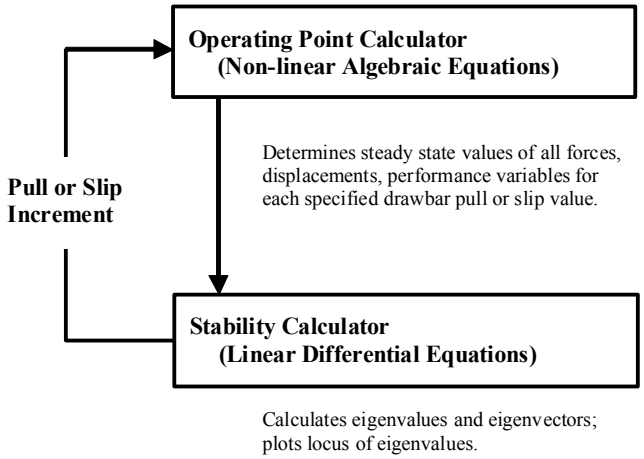

Figure 10. Algorithm for calculation of the operating point and determination of stability.

plot is produced to illustrate how the eigenvalues are affected by the changing drawbar pull (or slip) value. As outlined above, a complex conjugate pair of eigenvalues which move into the right half of the complex plane then indicates the presence of power hop. An example of the complete set of computational results follows later.

This frequency domain approach proved of tremendous value in better understanding the power hop phenomenon and provided a sound basis for the extensive experimental work that followed. Later, the commercial version of the multibody dynamics program ADAMS (see MSC Software, 2007) was used to again study power hop using a time domain approach. An ADAMS model was set up very closely paralleling the three degree of freedom model described above including use of the same equations for the gross tractive and motion resistance force coefficients. An increasing drawbar load was applied reaching a steady state value that should have resulted in the initiation of power hop. However the time domain results indicated the system was remaining stable. Further investigation indicated that a smaller integration error tolerance was necessary for the time domain solution to reflect the development of hop. In effect, "numerical damping" in the integration procedure had been damping out the hop signal. When this situation was realized and corrected with a tighter integration error tolerance, the time domain results agreed very well with the frequency domain predictions in both prediction of the operating point values and the stability of the system. But this example shows how difficult it can be to be able to produce the hop phenomenon with a time domain technique. The user of the simulation software has to understand the necessity of constantly rechecking to assure that the error tolerance is tight enough to allow the true motions to be calculated. ADAMS also has the capability to linearize a dynamic system at a given point in time and then determine the system eigenvalues. This capability was used by Sohoni and Smith (1995) to show the development of power hop as the drawbar load was increased on a 4WD tractor.

Observations about the Structure of the Differential Equations of Perturbed Motion

The three coupled linear differential equations (1) of perturbed motion about the operating point are autonomous, i.e., there is no explicit dependence on the time, t. Note, in particular, that there are no periodic "forcing functions" present, and thus, no possibility of resonance or large amplitude motions resulting from excitation by a periodic input with a frequency near a system natural frequency. Forced resonance is the type of large amplitude motion in physical systems dealt with in most basic vibration texts. However, since there are no periodic forcing functions in the stability equations for the tractor/implement system here, power hop is not the result of a resonance condition.

Inspection of the structures of the mass, damping, and stiffness matrices in Equation (A-16) in the Appendix reveals the following properties:

- The mass matrix is symmetric and positive-definite.
- The damping matrix is unsymmetric.
- The stiffness matrix is unsymmetric and semi-definite. The semi-definiteness is indicated by the null third column.

The semi-definiteness of the stiffness matrix is a result of the fact that the surge degree of freedom, x, is not restrained by a spring to ground. This has no effect on the overall stability of the system and poses no problems in the analytical or numerical computation of eigenvalues of the system.

In the analysis of free vibrations presented in most standard texts (and in most real-world vibrating systems), the mass, damping, and stiffness matrices are all positive-definite and symmetric. These symmetry and definiteness properties occur in linear systems that oscillate about a position of stable static equilibrium. It can be shown that as a result of these properties, the eigenvalues are either real or are complex with negative imaginary parts. Thus these systems cannot exhibit an oscillatory dynamic instability (see Meirovitch, 1967; Ziegler, 1968).

Since the stiffness and damping matrices in the power hop analysis under consideration here are not symmetric, some of the eigenvalues may have positive real parts for certain values of the system parameters. If there is at least one complex conjugate pair of roots with positive real parts, the system will exhibit flutter instability. In other words, if the model parameters that describe a particular tractor/implement system produce at least one pair of eigenvalues with positive real parts for a given load or slip, the system is dynamically unstable and exhibits self-excited vibrations. As will be shown in the next section, this is precisely the phenomenon called power hop.

Analytical Stability Results

Closed-form results for the eigenvalues and eigenvectors are available by making one of the standard assumptions employed in the classical analysis of stability of dynamic systems, i.e., that the velocity-dependent forces are small in comparison to the inertial and stiffness forces (see Bolotin, 1963; Ziegler, 1968). This is done in the Appendix by completely neglecting the damping matrix [C] in the general differential equations for perturbed motions. However, note that in the numerical computations of stability, the damping matrix is not neglected.

The algebraic manipulations required to solve the differential equations are presented in complete detail in the Appendix. The essential results are summarized here. In the solution process, the eigenvalues are ultimately calculated as the roots of a 4th order polynomial. These roots occur as complex conjugate pairs. From the algebraic equations for these roots, an equation is derived that is a *sufficient* condition to prevent the occurrence of a pair with positive real parts. We define this as the *Hop Function*

$$H \triangleq k_f a - k_r b \tag{2}$$

Recall that k_f and k_r are, respectively, the front and rear combined stiffness of the tire and soil, a is the horizontal distance of the tractor center of gravity behind the front axle, and b is the horizontal distance of the tractor center of gravity ahead of the rear axle.

Then a *sufficient* condition for stability is as follows. If

$$H \triangleq k_f a - k_r b > 0 \tag{3}$$

throughout the pull-slip range of interest for this tractor/implement system with negligible velocity-dependent forces, power hop cannot occur. Note again that this was derived for tractors *without* suspension systems beyond that of the tires. In the discussion of analytical and experimental results, it will become evident that this criterion plays a very important role in the practical considerations of power hop control. However, it is also very important to note that this is *not a necessary* condition. In other words, this condition does not have to be satisfied for the tractor to be stable. It could be stable due to the presence of sufficient damping or to other system parameter combinations that simply do not allow any complex conjugate pair of eigenvalues to migrate to the right half plane (see Equation A-44 in the Appendix).

Observations about the Stability Analysis and Criteria

The analytical results clearly show that the model is capable of predicting dynamic instability of the tractor-implement system. As discussed in greater depth below, the complete numerical stability analysis also predicts dynamic instability for certain parameter combinations. Thus, power hop is an example of a self-excited vibration. In early May

of 1989 when it was first discovered that this mathematical model could predict power hop, the engineers involved were both exhilarated and humbled. This event was the culmination of many years of research and truly was one of the high points of their technical careers.

This model incorporates only those basic elements, e.g. masses and geometry, vertical tire/soil stiffnesses, etc. that are essential to predict the instability phenomenon. Some investigators have offered conjectures about other possible elements that might contribute to power hop such as drive train wind-up, circumferential tire wind-up, tangential tire deflection, stick-slip soil/tire interactions, governor surges, and chaos theories. However, since these elements are not included in the present model, and this model is capable of predicting power hop, these other elements cannot be primal. They may come into play as refinements, but they are not fundamental to predicting basic power hop instability in tractors.

The sufficient condition for stability, Equation (3), offers basic insights into the nature of power hop control. It involves only three elements: (1) the fore-aft location of the tractor center of gravity, (2) the radial stiffness of the tire/soil combination in the front and (3) the radial stiffness of the tire/soil combination in the rear. Tire stiffnesses as influenced by tire inflation pressures (but not *total* tire/soil stiffnesses) were recognized to be factors that influenced power hop control as a result of trial-and-error efforts with real tractors in the field prior to the development of this model. It was very comforting to find that the stability criterion that emerged from the mathematical model was not inconsistent with prior field experiences. However, the critical importance of tractor center of gravity location in influencing power hop had not been previously recognized.

A careful examination of the sufficient stability criterion, Equation (3), indicates that hop sensitivity is increased as the tractor center of gravity is moved forward. Furthermore, it indicates that higher radial stiffness in the front and lower radial stiffnesses in the rear are important in controlling power hop. The radial stiffnesses are actually the result of the tire and soil acting as springs in series. The tire stiffness can be controlled by inflation pressure and the amount of liquid ballast they contain, but the soil stiffness is not under human control. Furthermore, very little experimental evidence is available about modeling the complex stiffness (and damping) effects in the combined tire and soil system when the tire is pulling. Thus it is very difficult to estimate how the total front and total rear stiffnesses vary on soft soil. However, if the tractor is pulling on a concrete test track or firm soil, the radial stiffness is basically due to the tires alone and information about how this stiffness varies with inflation pressure and normal force is available from tire manufacturers. Thus tests on firm surfaces should produce the "cleanest" data for comparing theory and experiment.

It is also important to note here that the Hop Function H varies with drawbar pull. The dimensions a and b appearing in H which locate the tractor center of gravity are constants, but the stiffnesses vary as a result of the non-linear load deflection characteristics of the tires and the changing values of the normal forces. Obviously as pull is increased, the front normal force decreases and the rear increases. As Figure 9 indicates, the tire vertical stiffness tends to increase as the normal force increases and vice versa. The net consequence is that H continuously decreases with pull-to-weight ratio as shown in the series of several possible curves in Figure 11.

The top curve represents the case where H remains positive throughout the entire pull range which indicates that power hop cannot occur. For the case represented by the middle curve, power hop cannot occur while H is in the positive range, but it either may or may not occur thereafter. Nothing can be said about whether power hop cannot occur for the third curve where H is entirely negative throughout the pull range.

At first glance, it might appear that all that is required for power hop control is to adjust the tractor to make the Hop Function positive. Note what that would involve. The fore/aft location of the center of gravity can be controlled by ballast locations and amounts and the tire inflation pressures can be adjusted (within practical limits). However, on soil, the stiffnesses appearing in H are the *total* of the series combination of tire stiffnesses and soil stiffnesses, and the soil stiffnesses are not at all controllable by humans. Thus extensive experimentation on both concrete test tracks and a variety of soils was required to determine the most practical approaches for using the parameters we do have available (tire stiffnesses and center of gravity location) to control power hop in tractors without suspension systems. In each of these tests, the drawbar load on the tractor was gradually increased to determine if power hop would occur exactly mirroring the numerical process outlined in Figure 10.

We also note that all of the previous analyses hold for 2WD tractors by simply dropping out the front traction expressions while retaining the front motion resistance terms in the calculations. Doing so does not change the unsymmetric structure of the equations, so power hop is still a possibility in 2WD tractors. While power hop in real

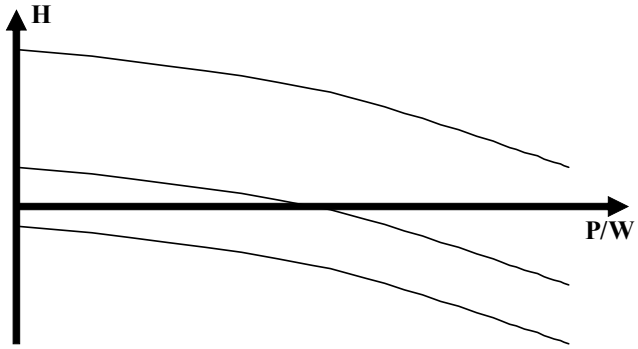

Figure 11. Variation of the hop function with pull-to-weight ratio.

2WD tractors operating on typical soils is an extremely rare occurrence, it has been observed in test conditions. The Nebraska Test Reports for both 2WD and 4WD tractors sometimes indicate "pull in nth gear was limited by tractor stability."

There is an interesting analogy here between power hop and steering directional stability of a vehicle. The directional stability characteristics of a vehicle based on a 2D model leads to a condition that determines whether the vehicle will oversteer or understeer. See Goering, et al. (2003) and Pacejka (2005). This condition is

$$S = C_{\alpha f} a - C_{\alpha r} b > 0$$

where the C coefficients are the front and rear axle lateral cornering stiffnesses, and a and b are the same dimensions from the center of mass to the front and rear as used in the power hop model. The structures of the sufficient condition for stability, the Hop Function (Equation 3), and the steering condition S are identical, i.e., a difference of two products involving a tire stiffness and center of mass location. A positive value of the steering parameter S indicates oversteer. With oversteer there is also the possibility of directional instability above a forward critical speed determined by other parameters (Pacejka, 2005). For a given vehicle and operating surface condition, the critical parameter at which instability is reached is a *force* for power hop while it is a forward *speed* for directional stability. Power hop is a *flutter* type (Figure 4) of instability while directional instability is a *divergence* (Figure 3).

Numerical Stability and Performance Results

To illustrate typical results of the *Mathematica*-based stability calculations, a model of the John Deere 4450 mechanical front-wheel drive (MFWD) tractor pulling on concrete will be used. The tractor is equipped with 14.9R30 front tires and dual 18.4R42 rear tires. The wheelbase is 2710 mm, the horizontal distance from the front axle to the tractor CG is 1819 mm so the static weight split is 33/67 (33% on the front axle and 67% on the rear). The mass is 7315 kg and the moment of inertia about the center of mass is 10,500 kg-m^2.

From the firm surface load-deflection data provided by the tire manufacturer (Firestone in this case), the stiffness for each tire as a function of deflection is obtained by differentiation of the fitted curves. The load-deflection and stiffness-deflection curves are shown in Figures 12 and 13. Note that each curve is parameterized on inflation pressure. For Case 1 we select front inflation pressures of 221 kPa (32 psi) and rear inflation pressures of 110 kPa (16 psi). The resulting root locus plot is shown in Figure 14. Each small dot represents a root (eigenvalue) location and the paths of the dots result from incrementing the drawbar pull. The four large dots in the left half plane are the roots at *no* drawbar load, and the large dot at the origin corresponds to the surge degree of freedom.

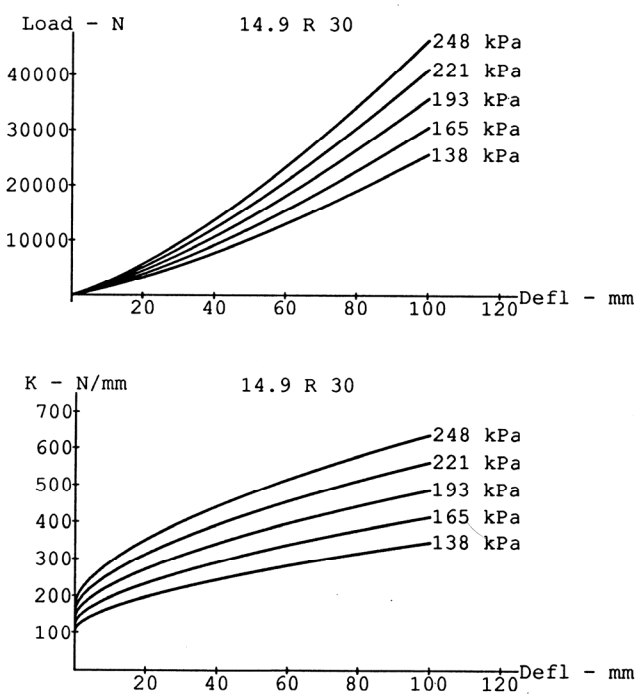

Figure 12. Load and stiffness as functions of deflection for a 14.9R30 front tire on a firm surface.

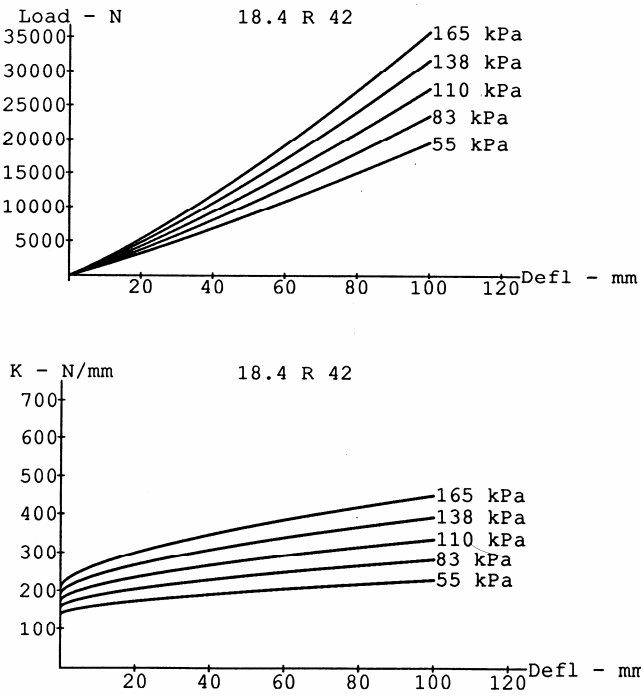

Figure 13. Load and stiffness as functions of deflection for an 18.4.R42 rear tire on a firm surface.

Line drawing representations of the pitch and bounce modes of vibration when there is *no* drawbar load are shown in Figures 15 and 16. The path of the tractor CG is the line tilted at approximately 45 degrees in Figure 15 and

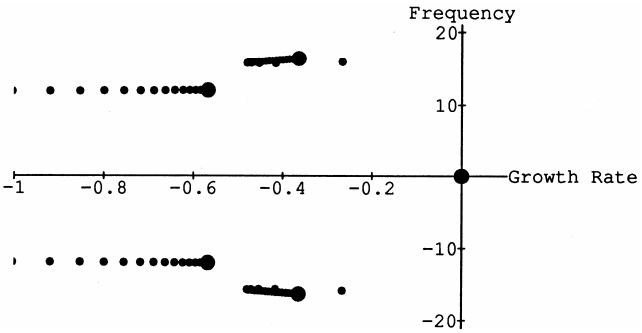

Figure 14. Root locus plot for Case 1: 221 kPa (32 psi) front and 110 kPa (16 psi) rear.

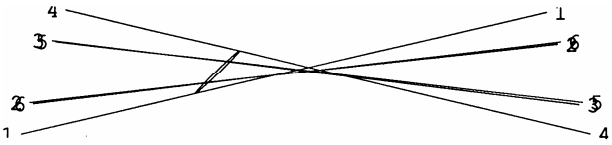

Figure 15. Unloaded pitch mode of vibration at 1.9 Hz for Case 1.

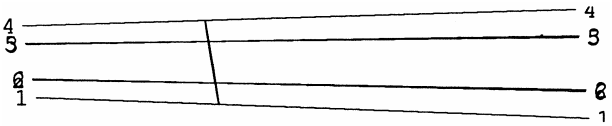

Figure 16. Unloaded bounce mode of vibration at 2.6 Hz for Case 1.

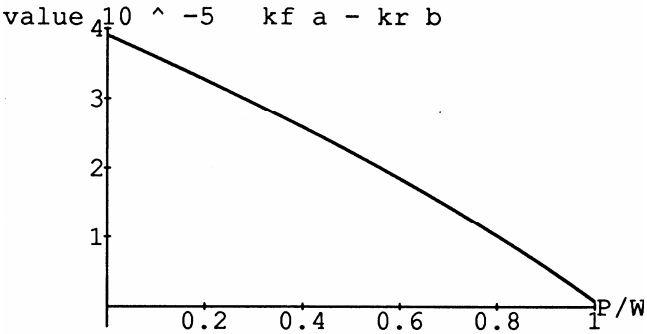

Figure 17. Hop Function vs. tractor pull/weight ratio for Case 1.

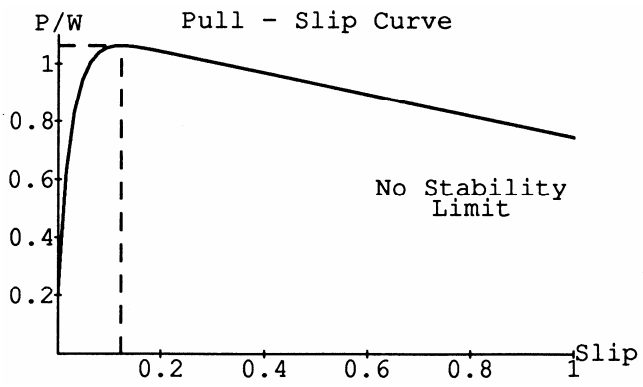

Figure 18. Pull-slip curve for Case 1.

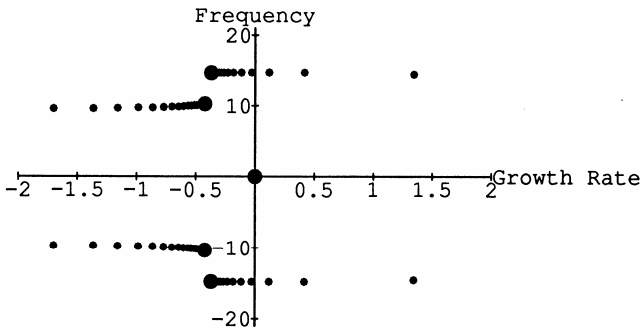

Figure 19. Root locus plot for Case 2: 110 kPa (16 psi) in all 6 tires.

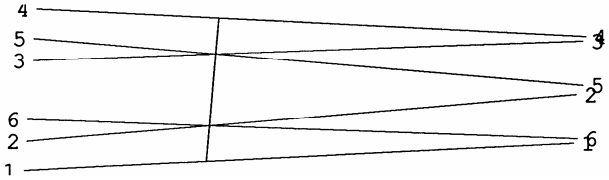

Figure 20. Hop mode shape at the critical pull when hop begins for Case 2.

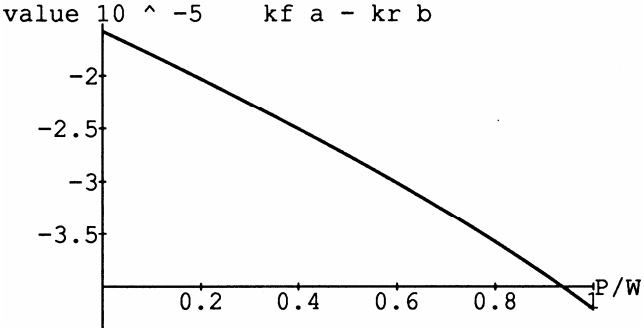

Figure 21. Hop Function vs. tractor pull/weight ratio for Case 2.

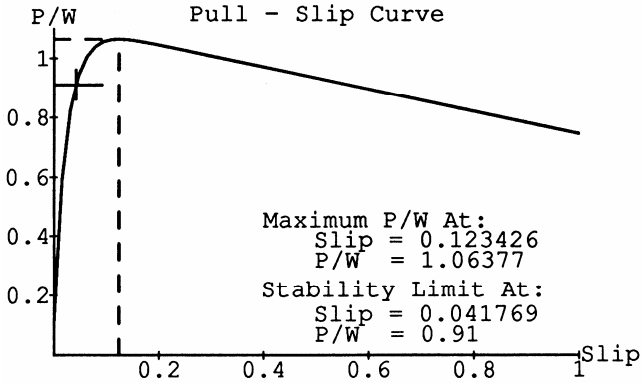

Figure 22. Pull-slip curve for Case 2.

nearly vertical in Figure 16. The lines connecting the same number on the left and right in each figure show the pitch of the chassis. The small numbers at each end indicate the sequence through one cycle. Some of these numbers are necessarily overwritten by others due to the symmetry of the vibration on the second half of the cycle.

Referring to Figure 14, as the drawbar load is incrementally increased, the complex conjugate pair of roots at the lowest frequency (the pitch mode of vibration) move to the left into the region of greater stability. The other complex conjugate pair (representing the bounce mode of vibration) initially moves to the left, but then turns back and moves toward the right but does not cross into the right half plane.

The computed Hop Function shown in Figure 17 is clearly positive throughout the full ascent up to the peak of the pull-slip curve shown in Figure 18. Thus no power hop can occur at this combination of front and rear inflation pressures. Of course, this is also clear from the root locus plot of Figure 14 since no root passed into the right half plane.

For Case 2 we set *both* the front and rear inflation pressures to 110 kPa (16 psi) and repeat the calculations. The root locus plot shown in Figure 19 now is quite different from Case 1. The complex conjugate pair that initially started as the bounce mode now crosses over into the right half plane at a pull-to-weight ratio of 0.91 indicating the onset of power hop (see Figure 22). The mode shape line representation corresponding to this point is provided in Figure 20. Again the nearly vertical line is the path of the tractor CG and the nearly horizontal lines indicate the chassis pitch. By following the sequence numbers, it is easy to visualize that this mode has the same "porpoising" appearance that is seen when a tractor begins to power hop.

The computed Hop Function shown in Figure 21 is negative throughout the full ascent up to the peak of the pull-slip curve shown in Figure 22. However, it is important to note here that just because the Hop Function is not positive, it does not provide any information as to whether the tractor is stable. It is only clear from the root locus plot in Figure 19 that hop occurs beyond a pull-to-weight ratio of P/W=0.91.

The *Mathematica* computational results are similar when modeling 4WD tractors.

Experimental Tests on Concrete Tracks

Test Plan and Process

After the first mathematical model calculations showed that power hop could be predicted, it was necessary to conduct experimental tests for verification. The initial tests were conducted on a concrete test track for convenience of location and because concrete provided a known consistent condition of stiffness, i.e., it could be regarded as non-deformable, and, thus, only the tires contributed to the stiffnesses.

Plans for the experimental tests were strongly guided by the results of the mathematical model. At the outset, a loading system was designed to allow an independent test operator to gradually increase or decrease the drawbar load on the test tractor to determine if power hop would begin at some point before the peak drawbar load was attained. The tests focused on determining the influences of tractor center of gravity location, front stiffness, and rear stiffness on power hop sensitivity and controllability.

The equipment used in almost all tests that were begun in the late summer of 1989 is shown in Figure 23 and represented schematically in Figure 24. The test data acquisition computer and load controls for a towed electrical retarder were located in the instrument tractor operated by the test engineer. This was followed by another load unit tractor (a "wheezer") providing resistance by means of engine compression. Finally, when it was necessary to generate very high draft loads on concrete, another operating tractor was used as the last vehicle in the train. The operator of the last tractor could throttle back as needed to provide additional draft load. The test tractor towed the train with a 29 mm (1.12 in) steel cable that passed below the front axle of the instrument tractor and was connected to a load cell to measure drawbar pull. The load cell was attached to the instrument tractor's main drawbar pivot pin beneath the rear axle housing.

When planning for these initial tests, there was concern that the test tractor operator might be repeatedly subjected to severe rough ride conditions during hop. This led to the design of a remote-control operating system for the test tractor operator. An operator's platform was placed atop the front of the instrument tractor and controls for the power steering, clutch, brakes, powershift transmission, and throttle were connected by an "umbilical cord" of hoses and wire bundles to the test tractor (see Figure 28). It worked well, but most test operators ultimately chose to operate the test tractor from inside the cab especially when operating in dusty conditions.

The test tractor was equipped with an on-board radar system and monitor to display both slip and true ground speed. In addition, a fifth wheel to measure true ground speed and a tractor rear axle speed sensor were used to calculate slip independent of the radar system. This data was captured by the instrumentation computer. In some cases, chassis accelerations were also recorded, but it soon became obvious that the onset of power hop could be easily recognized in the measured pull data, felt by the test tractor operator, and seen by outside observers. Thus it was deemed unnecessary to continue to capture acceleration data. Any level of hop whether dramatic and violent or simply obnoxious and uncomfortable was considered unacceptable to the operator.

Figure 23. Test tractor, instrument tractor, and load units on concrete test track—1989.

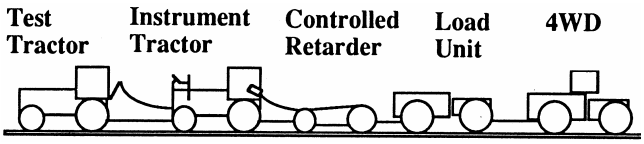

Figure 24. Load train schematic.

A portable VHF radio setup allowed for communication among the test tractor operator, the test engineer, and a video camera operator in a van or pickup truck driving alongside the test or at a stationary position on the ground. All tests were recorded on video tape with open radio microphones to capture the dynamic events along with the "play-by-play" description provided by the test tractor operator. He continuously called out the slip and ground speed being displayed, engine speed, operating gear, whether the tractor was stable, on the verge of hop (bad ride), or experiencing hop.

The test engineer operating the second tractor in the train controlled each test run. With radio communication, he helped the test tractor operator coordinate start-up of the train. Once underway in the gear selected for the test run, data collection was started. Then the test engineer would increment the draft load in small steps by means of a knob controlling the towed electrical retarder. It is important to note here that the loading was entirely controlled by the test engineer in the instrument tractor and not by the test tractor operator who was only responsible for steering, reporting on slip, ground speed, and engine speed displays, and commenting on stability. Sometimes the test engineer would tap the brakes of the instrument tractor to create a jerk that might induce power hop. After the first few test runs, this was found to be unnecessary because hop would occur entirely on its own without stimulus.

MFWD Test Example

Experimental time traces of the pull generated by the John Deere 4450 MFWD tractor modeled in Case 1 and Case 2 previously are shown in Figures 25 and 26. On concrete, the maximum pull-to-weight ratio can exceed 1.0 as is shown in both figures. For reference, the front inflation pressures in Case 1 are 220 kPa (32 psi) and the rear inflation pressures are 110 kPa (16 psi). The small spikes that appear near the maximum pull level in Case 1 occurred

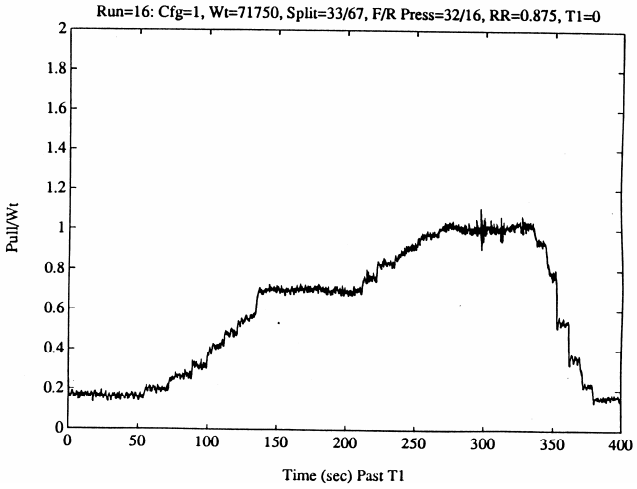

Figure 25. Time trace of gradually increased drawbar load for Case 1; no hop.

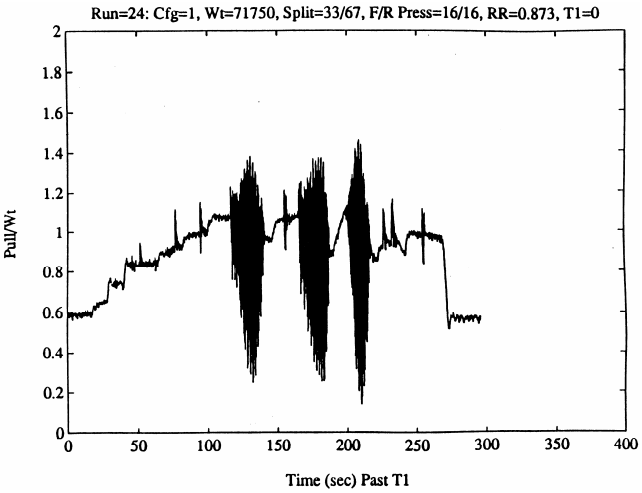

Figure 26. Time trace of gradually increased drawbar load for Case 2; power hop occurs.

when the test engineer tapped the brakes of the instrument tractor to try to induce hop, but the test tractor was totally stable. When the test was repeated with all inflation pressures set at 110 kPa (16 psi) corresponding to Case 2 of the model, violent power hop occurred three times as shown in Figure 26. Once power hop occurred, it was necessary to reduce the drawbar load substantially to regain stability.

Thus the mathematical model and experimental test results agree that the tractor is stable with high front inflation pressures (Case 1) and power hops with all inflation pressures equal (Case 2). These initial tests also confirmed that drawbar load is the main parameter controlling when power hop will occur on a tractor whose weight distribution and tire inflation pressure settings are such that hop can occur. These early test experiences also represented a major step forward in understanding how to consistently produce power hop in a test situation.

Summary of Test Results on Concrete

Experimental power hop tests of MFWD and 4WD tractors were all conducted in the following manner. For a given combination of front and rear tire sizes, a total tractor weight and static weight split (fore-aft balance) was created by using a combination of front and/or rear ballast elements. Cast iron weights were used predominantly, but in some cases liquid ballast in tires was used alone or in conjunction with the cast weights. Front and rear static axle loads were measured on platform scales. Then a series of test runs was made with various combinations of front and rear inflation pressures. In each test, the draft load was initially near zero or some relatively small amount. The test engineer would then gradually increase the draft load in small increments until the tractor either power hopped or achieved the maximum pull attainable on the surface. Each test was repeated at least once and all were recorded on video tape. The goal of each test run was to determine if the tractor was stable or power hopped along with acquiring the pull and slip data described previously for the given combination of inflation pressures. Thus each test run produced a simple primary result—"yes" it did hop or "no" it did not. The approximate slip at which hop commenced was noted in the data and on the video tape. Then the ballast was adjusted to produce another total weight and weight split case and the entire process repeated. From the late summer of 1989 through the mid-1990s, over 1200 such test runs on concrete and on a variety of soils were conducted.

Initially the focus of the experiments was on verification of the mathematical model using a John Deere 4450 MFWD tractor as a base vehicle with several different weights, weight splits, and pitch moment of inertia variations. Six different ballasting combinations were used. These produced weight splits ranging from 24/76 to 53/47, total masses ranging from 7315 kg to 10,273 kg, and pitch moments of inertia ranging from 10,500 kg-m^2 to 28,100 kg-m^2.

The mathematical model was exercised for each of the six experimental test configurations. In every instance, the model and test results were in complete agreement regarding which inflation pressure combinations led to power hop and which resulted in a stable tractor.

Later in 1989 and early in 1990, a John Deere 8450 4WD tractor was also modeled and tested on concrete as shown in Figure 27. Again there was 100% agreement between the mathematical model and the test results as to which front and rear inflation pressure combinations resulted in a stable tractor and which combinations led to power hop.

Figure 27. John Deere 8450 power hop testing on concrete in 1990.

These results on concrete, where the front and rear stiffnesses are essentially due to the tires alone and mathematically well defined, provide strong confirmation that the mathematical model captures the essence of power hop. This confirmation of theory with experiment proves that power hop is an example of a self-excited vibration. The source of energy that sustains the vibration is the engine driving the wheels which generate the traction forces that directly influence the pitch motion.

All of the model and test results on concrete for both MFWD and articulated 4WD tractors showed that power hop could be controlled by raising the front inflation pressures and lowering the rear inflation pressures by sufficient amounts and never by the opposite approach. In other words, to control power hop on firm surfaces, the tractor needs "high" stiffness in front and "low" stiffness in the rear. For MFWD tractors this was the accepted practice developed from prior ad hoc field experiences and still is in use today. However, for 4WD tractors, it was a new result in 1990.

The conventional approach used to control power hop of 4WD tractors in the field had been to raise the rear inflation pressures. It didn't always work, but it usually improved the situation somewhat. But in every 4WD case tested on concrete, on paved surfaces, and on firm soils, power hop was never controllable by raising the rear inflation pressures. It was always controllable by raising the front and reducing the rear. As will be discussed in more detail later, there are some soil conditions and some operating conditions where the recommended 4WD power hop control procedure calls for higher inflation pressures in the rear and lower in the front. However, the only way to control power hop of 4WD tractors operating on firm soils or paved surfaces is to use the stiff front-soft rear combination of inflation pressures.

Field Test Experiences: MFWD Tractors

In the late fall of 1989, after the initial tests of the 4450 MFWD tractor on the concrete track were completed, the tractors and test equipment were shipped to the Firestone Proving Grounds in Fort Stockton, Texas, to continue testing in the Caliche soil conditions that Firestone engineers had found to be conducive to power hop. The soil was very dry and loose on top as shown in Figure 28, but was hard underneath. It was easy to induce power hop as the drawbar load was gradually increased with appropriate combinations of inflation pressures. A typical vehicle pull-slip curve for this Caliche soil is shown as Figure 29. The fact that the curve saturates at such a low pull-to-weight ratio indicates that it is much more difficult to generate traction on Caliche than on typical Corn Belt soils.

As with the tests on concrete, hop was consistently controlled with high front and low rear inflation pressures. The inflation pressure combinations for stability or power hop predicted by the model were not always identical to the test results as they had been on concrete, but they were within ±0.5 kPa (4 psi) and usually closer. This is due to the lack of an experimental and/or analytical method for measuring and/or predicting the combined soil-tire stiffness and damping.

Figure 28. MFWD power hop testing at Firestone Fort Stockton, Texas, Proving Grounds, 1989.

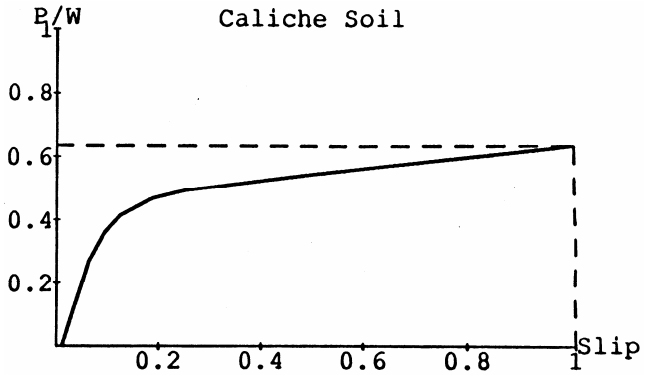

Figure 29. Vehicle pull-slip curve for Caliche soil.

At the time these tests were conducted, the lowest allowable inflation pressure for both radial and bias ply tires was 83 kPa (12 psi) per The Tire and Rim Association standards. Accordingly, in most of these tests the rear tires were set no lower than this. However, with the concurrence of Firestone engineers participating in the tests, there were some tests run with the rears as low as 55 kPa (8 psi). This clearly made it easier to control power hop and appeared to improve the pulling capability of the tractor. Even so, at the time it was assumed that the 83 kPa (12 psi) lower limit had to be respected for customer usage. This in itself was a long stretch down from the typical inflation pressures of 124-165 kPa (18-24 psi) being used routinely by most tractor owners in the 1980s.

The question of allowable inflation pressures also arose with regard to the front tires. The upper limit on inflation pressures was 165 kPa (24 psi) or 207 kPa (30 psi) depending on the ply (bias) or star (radial) load rating of the tires in question. Often when raising the front inflation pressures to control power hop, the upper limit was reached before control was achieved. Ultimately the principal tire companies supplying OEM agricultural tires in North America in 1990 (Bridgestone/Firestone, Goodyear, and Pirelli-Armstrong) all agreed to allow as much as 41 kPa (6 psi) above the maximum pressure imprinted on the sidewall of radial front MFWD tires *for power hop control only—not to carry more load*. This was usually enough to suppress power hop, and it continues to be a part of the current published recommendations.

In one brief test series, bias ply rear tires were installed. Little difference was noted in the inflation pressures required to control power hop in comparison to those required with radial tires.

It is interesting to note that the front and rear inflation pressure combinations required to suppress power hop on this Caliche soil with a loose surface were essentially the same as those required on concrete in spite of the vast differences in the vehicle pull-slip curves for the two.

One of the most revealing experiments conducted in this same field at Fort Stockton by Firestone engineers earlier in 1989 dealt with the influence of liquid ballast in tires of MFWD tractors. The most typical ballasting methods farmers used on their MFWD tractors at that time were front suitcase weights or 75% liquid fill in the front tires and 75% liquid fill in the inner rear tires. Liquid ballast had a lower cost than cast rear wheel weights so it was popular. Farmers installed it in the inner rear tires, which were seldom removed, and left it out of the outer rear dual tires, which were often removed and reinstalled at least annually.

Table 2. Effect of liquid ballast amount and location on controllability of power hop of a John Deere 4450 MFWD tractor* (after Brodbeck, 1989).

14.9R30 front tires	18.4R42 rear tires (inner and dual)	Inflation pressures required for no hop, kPa (psi), front and rear
Air	Air inner, air outer	241 kPa (35 psi) front, 69 kPa (10 psi) rear
Air	75% liquid inner, air outer	Still hopped at 379 kPa (55 psi) front, 55 kPa (8 psi) rear
75% liquid	75% liquid inner, air outer	Still hopped at 276 kPa (40 psi) front, 55 kPa (8 psi) rear
90% liquid	75% liquid inner, air outer	207 kPa (30 psi) front, 83 kPa (12 psi) rear
75% liquid	Air inner, air outer	207 kPa (30 psi) front, 83 kPa (12 psi) rear
*All masses approximately 9979 kg (22,000 lb.). All weight splits approximately 38% front/62% rear.		

Figure 30. 4WD power hop testing in the San Joaquin Valley of California, 1990.

Handling liquid-filled tires is quite difficult, requiring a crane, a forklift, or a loader. Thus it was absolutely necessary to determine the effect of liquid ballast on power hop control.

The five different combinations of liquid and cast ballast as shown in Table 2 were tested. It is striking to see that with the second and third combinations, the most popular setups used by farmers, it was not possible to control power hop while staying within the maximum pressure limits on the front tires and minimum pressure limits on the rear tires. No wonder that farmers were so upset with the tractor and tire manufacturers over the inability to control power hop in those early days.

Liquid fill in the front tires has a positive influence on power hop control. Since the liquid is incompressible, the tire is stiffer at a given inflation pressure with liquid than when dry as will be discussed later in this Lecture. High front stiffness and low rear stiffness is needed for power hop control, so the liquid in the front is aiding while the stiffening effect of liquid in the rear is detrimental.

Field Test Experiences: 4WD Tractors

Early Experiences—1990

A major series of tests with a John Deere 8760 4WD tractor, as shown in Figure 30, was conducted in the San Joaquin Valley of California in the summer of 1990. The power level was set at the factory standard 224 kW (300 engine hp). The test field had previously been in seed alfalfa for several years. The last irrigation was in late March and no rain had fallen since that time when the tests were conducted in August and September. Thus this highly compactable clay-silt soil was extremely hard and dry. After harvesting the alfalfa seed, the field had been tilled about 208 mm (8 in) deep with a stubble disk and then land planed. This produced very hard and dry clods ranging from approximately 20-75 mm ($^3/_4$-3 in.) in size along with some fines. A reasonable term to describe this top layer of clods is "rubble." Tractor tire marks were no more than approximately 20 mm ($^3/_4$ in) deep except at extreme slip conditions. Thus the soil behaved almost like a hard surface even though it was "cloddy" in appearance and structure. The vehicle pull-slip curve shown in Figure 31 gives a good indication of just how difficult it is to generate traction on such a surface since saturation occurs at a pull-to-weight ratio of only about 0.52. As a result, tractors used in this area are typically ballasted to very high levels for heavy tillage operations.

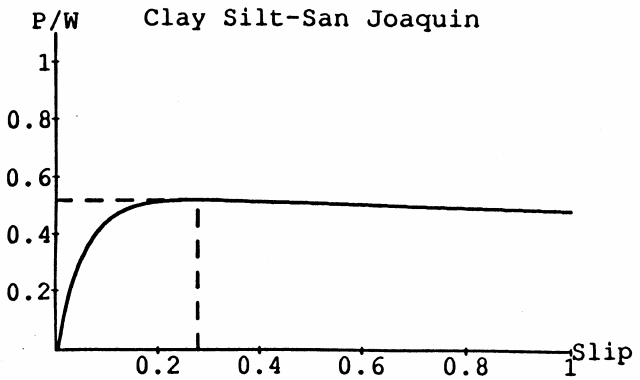

Figure 31. Vehicle pull-slip curve for clay-silt soil of the San Joaquin Valley.

The primary test variables included tire size and the amount and location of liquid ballast (water only) and cast ballast. Some bias ply tires were also included. In all but a few cases, the weight split was maintained at or near 55% front and 45% rear since that was the existing John Deere recommendation for 4WD tractors pulling towed implements. Tractor weight to horsepower ratios ranged from 75 kg/kW (123 pounds per engine horsepower) to 91 kg/kW (150 pounds per engine horsepower) with most of the tests being run at 84 kg/kW (138 pounds per engine horsepower). These are very high in comparison to the total ballasted tractor weights recommended for most soils, but typical of the levels used on this type of soil in California.

The front/rear tire inflation pressure combinations selected for testing started with the lowest allowable on the front and on the rear to carry the static axle loads with 83 kPa (12 psi) being the lowest minimum in most cases. Then the front pressures were increased in 28 kPa (4 psi) increments while maintaining the rear pressures at the minimum. Next the process was reversed by raising the rear pressures incrementally while holding the front at the minimum. Finally both the front and rear minimum pressures were raised by 28 kPa (4 psi) or sometimes more to operate in a condition with both front and rear overinflated. As a practical matter, the process was actually reversed from that just described. The maximum pressure on front or rear was initially set and then reduced incrementally by bleeding air for succeeding test runs to speed the process of conducting the tests.

When conducting these tests, two new types of instabilities were observed in addition to power hop. The first may be described as a "roll" about the fore-aft longitudinal axis of either the front bogie or the rear bogie. This was given the name "duckwalk" due to its appearance. The second instability was an oscillation in which the front and rear bogies oscillated about the vertical steering hinge axis and was thus named "yaw." These instabilities typically occurred when the slip was more than approximately 15%. Application of the tractor differential lock would sometimes cause duckwalk to switch to yaw. Sometimes these instabilities were too severe to be tolerated but usually they were just annoying. They tended to be more likely to occur and more violent when there was liquid ballast in the tires. We are aware that duckwalk and yaw have been observed on numerous other 4WD tractors operating in the San Joaquin Valley, but we did not encounter them in any other soils while conducting power hop tests over the years. They have not been reported as a significant issue by farmers, so we have not pursued any further study of them.

The fundamental result in these tests regarding the influence of inflation pressures on power hop control is that operating both the front and rear at the minimum pressures required to support the static axle loads or with the fronts somewhat higher than that resulted in stability. If the front pressures were raised extremely high, duckwalk, yaw, and sometimes power hop would occur. On the other hand, if the front pressures were held at the minimum and the rear pressures raised, the tractor would always power hop. Raising both the front and rear simultaneously usually resulted in loss of stability especially with liquid ballast in the tires. Thus, on this very hard soil, the tractor stability behavior was exactly like that on concrete with the exception that on concrete very high front pressures did not lead to instability.

The tire sizes used in these tests were 18.4R42, 20.8R42, 20.8-42 bias, and 24.5R32, all with the tractor set up for duals. It was easier to control power hop with the 20.8 cross-section tires, which are taller than the 18.4 cross-section tires. The 20.8 tires were also more tolerant of liquid ballast than the 18.4 tires in hop control. For reference, the 20.8 tires are 102 mm (4 in) taller and have a greater cavity volume than the 18.4 tires so the minimum inflation pressures to support the static axle loads are a bit lower. The smaller diameter, but significantly wider 24.5R32 tires provided excellent stability control when dry and heavily ballasted with cast weight, but they lost this excellence when 75% liquid fill was used in the inners. Power hop occurred with bias ply tires, but usually there were more inflation pressure combinations for stability than with comparable radial tires.

In all tests with liquid fill ballast, the standard practice at that time of filling to the top of the rim by placing the valve stem at the 12 o'clock position was used. This fills approximately 75% of the cavity volume with liquid. Furthermore, the common practice at that time of using liquid ballast in only the inner tires was used for comparison with the same axle weights obtained using cast wheel weights. Some tests with liquid ballast in all four fronts or all four rears were also conducted with 18.4R42 tires.

The ability to control power hop, duckwalk, and yaw was easiest with no liquid ballast in the tires. For all three tire sizes, liquid ballast tended to precipitate more duckwalk and yaw than cast ballast. In general, the negative influences of liquid ballast were less with bias ply tires than with radial tires. With liquid ballast in only the front tires or only the rear tires, power hop could be controlled, but over a smaller range of inflation pressures than with cast ballast. With liquid ballast in both front inner and rear inner tires, the number of inflation pressure combinations that controlled power hop was the smallest.

RJT—During the summer of 1990 the Alberta Farm Machinery Research Centre, or AFMRC, also began a series of tests that developed into the Centre's first power hop control study. AFMRC was approached by Caterpillar Tractor with a request to compare the rubber belt equipped Challenger tractor to a comparable size radial tire equipped 4WD tractor. Caterpillar wanted independent verification of the performance of the machine, anticipating higher power delivery efficiency and freedom from power hop problems with the rubber belt system. Initial tests run in

July, comparing performance in the field of a Challenger 65 to a Case-IH 9250 4WD were AFMRC's first serious encounter with power hop and provided a good learning experience. The Case-IH was equipped with 20.8R38 radial tires, set according to the load inflation recommendations of the day. The soil conditions were such that it was difficult to make the tractor power hop (for the most part it did not), leaving the question of tracks as an acceptable solution to power hop unanswered.

As the season progressed, AFMRC and Montana State University personnel cooperated to continue power hop work using farmer-owned tractors that were reported to be experiencing hop problems. One of the early successes was a radial tire equipped John Deere 4955 MFWD. This tractor had a severe power hop problem that was controlled by adding the front-end loader frame to bring the weight distribution to 40/60 front to rear and by raising the tire pressures in the front and lowering them in the rear. The group then visited a number of radial dual equipped 4WD tractors with power hop problems in central Alberta and in the Havre, Montana area. The tractors ranged in power from 185 kW (250 hp) to 390 kW (525 hp). Each tractor was run through a series of pressure and weight tests, evaluating what seemed to reduce the tendency to hop. Changes included adding and removing cast ballast, adding and removing liquid ballast, and raising and lowering tire pressures, but always remaining within the then-correct load inflation table ranges (never below 83 kPa (12 psi)). Overall the tests showed that moving the weight split closer to 50/50 helped somewhat, changing ballast type between liquid and cast sometimes helped and sometimes hurt, and reducing the front tire pressures and increasing the rear tire pressures helped substantially.

All these tests were run in farm fields, with trailed implements serving as the load units, and using some form of the AFMRC onboard instrumentation system to record tractor performance values during the tests. This became the standard procedure that was used for all subsequent AFMRC tractor, traction, and power hop testing.

Refining the Details

JCW—In the process of assimilating all of the implications of the results of the test experiences with MFWD and 4WD tractors in 1989 and 1990 as well as the results of the mathematical model, it became clear that further experimental investigations were required. There were a number of questions and unexplored issues that had to be dealt with before making further hop control recommendations to farmers.

First, did the San Joaquin soil represent such an extreme case that the results might not be applicable elsewhere? Second, was there a more reasonable way to deal with the negative effects of liquid ballast that had shown up in tests? Third, how much did tire size influence the ability to control power hop? The influence of fore-aft weight balance (static weight split) of 4WD tractors had not been studied very much in the tests on soils, but the mathematical model and the results of MFWD tests indicated it was important. Would this importance be confirmed in the field for 4WD tractors? But the most difficult question of all was how to deal with the extremely high tire inflation pressures required to control power hop in some situations. Could both front and rear inflation pressures be lowered from the extremes and still achieve power hop control? In the few instances where tests had been run with inflation pressures less than the minimum of 83 kPa (12 psi), there was a clear improvement in power hop controllability. Could the tables be extended downward to lower pressures and thus to lower stiffnesses of the tires? Would rim slip occur with inflation pressures lower than 12 psi?

During the winter of 1990 and early spring of 1991, a number of discussions were held with tire engineers from Bridgestone/Firestone and Goodyear to deal with these questions. They were eager to contribute their expertise and capabilities to help further the development of a comprehensive approach to power hop control. After all, farmers were blaming the tire manufacturers as much as the tractor manufacturers for the problem.

Progress on two major issues depended on significant input from the tire engineers. The first was to extend the load-inflation pressures downward for experimental purposes, and the second was to quantify the effect of liquid ballast on tire stiffness.

Privately, these tire engineers had actually been considering the possibility of reducing the lower limit in the load-inflation pressure tables for dual and triple tires to improve traction and ride, but they had been reluctant to do so based on the long history of using 83 kPa (12 psi) as the lower limit in all types of farm tractor tires. However, the possibility that this might help improve power hop controllability served as a powerful incentive to try it experimentally.

The Tire and Rim Association standards (Tire and Rim a) call for tires of a given size, travel speed, and construction to support a tabulated set of loads corresponding to a series of specified inflation pressures (hence the name "load-inflation pressure" tables). The loads in the tables are to be interpreted as the static loads on the tires when the tractor is ballasted and field ready. The increase in loads due to weight transfer when operating have been accounted for by the tire manufacturers in testing the tires and when preparing the tables.

While it is not obvious by inspection of the load-inflation pressure tables, the static deflection of the loaded tire is approximately the same for all load-pressure pairs for a given tire size and construction. For single tires, this deflection is called the Rated Deflection (RD) of the tire. Thus each inflation pressure shown in a load-inflation pressure table is a Rated Deflection Pressure (RDP). These are

the minimum inflation pressures that can be used without the potential of serious damage to the tire.

The RD of an 18.4R42 tire is approximately 79 mm (3.1 in), and the RD of a 20.8R42 tire, which is 102 mm (4 in) greater in diameter than an 18.4R42, is approximately 97 mm (3.8 in). At Rated Deflection, the tire has the longest usable contact length and greatest contact area. This results in the greatest tractive capacity and least soil contact pressure. If the inflation pressure in a tire exceeds the RDP, the contact length will shrink reducing tractive capability, and the contact area will also shrink increasing soil contact pressure. On the other hand, if a tire is inflated with less than the RDP for a given load, it will be overdeflected and could potentially fail. When tires are used as duals, the loads corresponding to rated deflection are 88% of the loads for singles, and for triples the loads are 82%. These reductions provide a safety factor to account for the potential of high loading should an individual tire temporarily carry all or most of the weight on uneven terrain.

Considering these facts, it seems obvious that tires should be operated at Rated Deflection Pressures. However, as a matter of practice prior to 1992, there were two barriers, one technical and one psychological, that prevented this from happening in the field. When radial tires are inflated with a Rated Deflection Pressure, there is a bold "cheek" in the sidewalls just above the contact patch which makes some people think that the tire is underinflated. Such a cheek would indicate underinflation on bias ply tires, which were the most commonly used tires on tractors until the mid-80s, but it indicates correct inflation for radial tires. Furthermore, farmers usually set inflation pressures by "eyeball," and seldom referred to a chart or table.

Figure 32 shows rear and side views of dual radial tires set at Rated Deflection Pressures. The white lines are superimposed on the photo to highlight the sidewall boundaries. In addition to the large sidewall cheeks, there is a long footprint, and the lugs touching the ground make contact all the way out laterally to the ends of the bars. These characteristics are, in fact, responsible for the superior performance of radial tires over comparable bias ply tires, which have much shorter contact lengths. In contrast, Figure 33 shows the results of overinflation of radial tires (and correct inflation of bias ply tires). The sidewalls are almost vertical above the contact patch, the footprint length is much shorter, and the lugs in contact with the ground do not touch laterally all the way to the ends. This is the same appearance as that of a properly inflated bias ply tire. If radial tires are overinflated instead of using Rated Deflection Pressures, their performance diminishes and approaches that of bias ply tires. As examples of the effect on performance see Turner (1993a) and Zoz (1994), where 55 kPa to 68 kPa (8 to 10 psi) overinflation of radial tires reduced their power delivery efficiency by 4 to 7%.

The technical barrier to the use of Rated Deflection Pressures prior to 1992 was the 83 kPa (12 psi) lower limit.

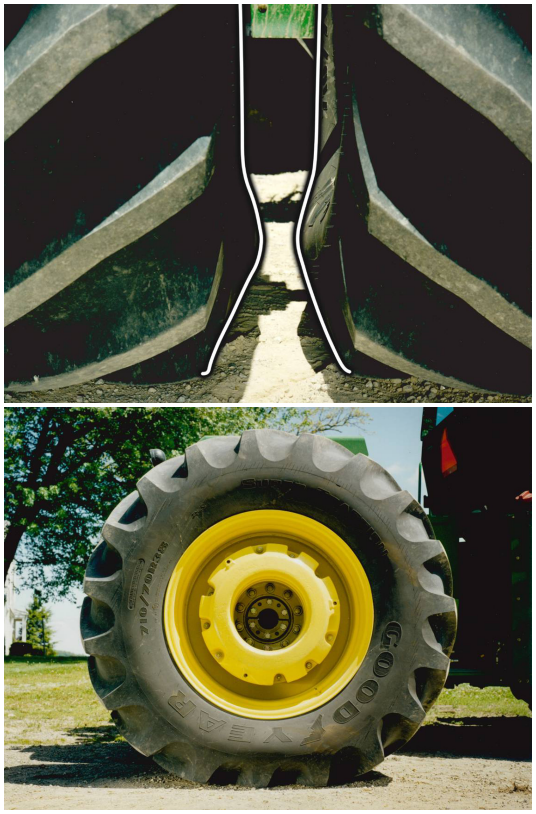

Figure 32. Radial tires inflated correctly with Rated Deflection Pressures.

Figure 33. Overinflated radial tires.

Table 3. Extended load-inflation pressure table for 20.8R42 dual tires (extracted values).

	New Lower Limit ↓	Old Lower Limit ↓		
Inflation Pressure	41 kPa (6 psi)	83 kPa (12 psi)	124 kPa (18 psi)	165 kPa (24 psi)
Tire Load	14.6 kN (3290 lb)	22.2 kN (5000 lb)	28 kN (6290 lb)	33.4 kN (7520 lb)

The static load per tire on tractors equipped with dual or triple tires is often much less than the load in the tables corresponding to 83 kPa (12 psi). Therefore, in adhering to the 83 kPa (12 psi) limit, the tires were actually overinflated. This limits the minimum attainable tire stiffness and reduces the range of stiffness difference available to control power hop when it does occur.

In the spring of 1991, tire engineers tentatively extended the tables downward to 41 kPa (6 psi) for experimental purposes. An excerpt from a current table for 20.8R42 dual tires is shown in Table 3. It is important to note that the tire deflection and footprint shape are essentially the same in the lower extended range as for the higher Rated Deflection Pressures. Therefore, it was not necessary to alter tire design and construction since the effective operating range was just expanded while keeping the deflection the same.

In dealing with the issue of liquid ballast, the most basic information needed was the set of load-deflection curves parameterized on inflation pressure with various amounts of liquid fill. From these, the stiffness as a function of load could be derived by differentiation. Figure 34 shows the influence of liquid fill on stiffness of an 18.4R42 tire (Wiley, 1992). The original load-deflection data from which these curves were derived was generated first by Bridgestone/Firestone engineers (see also Lopp, 1992). The 75% level (which was the most common level used) is achieved by filling to the top of the rim with the valve stem straight up. The 38% level is half that amount and is achieved by placing the valve stem at the 4 o'clock position and filling to that level. At high inflation pressures, the volume of liquid has little effect on tire stiffness. However, at low inflation pressures, the stiffness is lowest with air only and increases significantly with increasing fill level.

Inspection shows that stiffness increases more rapidly above 38% fill than below it. The same total amount of ballast can be obtained by filling the inner and outer dual tires to the 38 % level as with a 75% fill on the inner, but the end result is lower combined tire stiffness and a potential improvement for power hop control when liquid ballast is used.

RJT—Taylor (1996) performed an investigation of the influence of liquid ballast on the static stiffness of a radial tire. His results showed the stiffness change to be largely

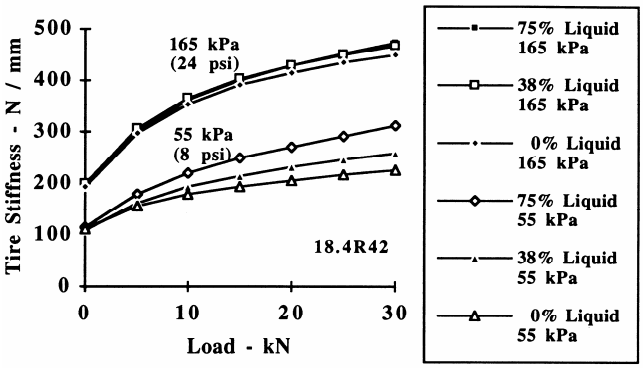

Figure 34. Influence of liquid fill on tire stiffness on a firm surface.

proportional to the static head of the liquid and to a lesser degree to the tire volume reduction from tire deflection. As the static head increased, the pressure at the base of the tire increased and the stiffness increased proportionally. Considering this liquid ballast effect, tire stiffness would increase both as more liquid is added, and from using a more dense liquid solution (calcium chloride solution versus water).

First Field Experiences with Lower Inflation Pressures

JCW—The first opportunity to apply the experimental tables came late in May of 1991. John Deere field service personnel had received reports of significant power hop problems with several relatively new 8760 4WD tractors operating on steep slopes near Walla Walla, Washington and just across the Columbia River in Oregon. John Deere and Goodyear engineers along with John Deere field service personnel traveled to the area for a week to apply the new tables to tractors operating in these extreme conditions.

Figure 35 shows one of these customer tractors operating near The Dalles, Oregon. The late afternoon shadows in the photo help give an indication of the steepness of the slopes which the customer said exceeded 45%. In this area, wheat is harvested with self-leveling hillside combines. This tractor was equipped with 20.8R42 radial tires that the customer was operating with 138 kPa (20 psi) in the front and 165 kPa (24 psi) in the rear. This was the first tractor he had ever owned with radial tires, and he had set the inflation pressures high since this had been his practice with bias ply tires. With these pressures, the tractor exhibited violent power hop when trying to pull up hills and in turns. Based on the experimental tables, the rear tires only required 55 kPa (8 psi). The front pressures were left at 138 kPa (20 psi) to follow the hop control recipe of stiff front and soft rear. This totally controlled power hop, and the tractor was able to pull the 9.75 m (32 foot) chisel plow up the hills that it had not been able to do with the high rear inflation pressures.

Figure 35. Early experience in controlling 4WD power hop with lower inflation pressures (The Dalles, Oregon, 22 May 1991).

Power hop was also controlled with this approach on three other similar tractors operating in this area that same week. This was a very gratifying experience not only for the customers but also for the engineers and service personnel involved.

Comprehensive 4WD Power Hop Tests—1991

To carefully evaluate interactions of all the important variables of 4WD power hop control and to operate in more typical soil conditions, an extensive series of tests was conducted near Denver, Colorado, in the late summer and early fall of 1991. The central focus was, of course, on applying the experimental extended load-inflation pressure tables. In order to achieve the agreement of all tire manufacturers on using these tables, it was important that they participate directly in the tests to witness the results. Thus engineers and marketing personnel from Bridgestone/Firestone, Goodyear, and Pirelli-Armstrong (now Titan) all worked side by side with John Deere engineers in conducting the tests. This collaborative effort was very important in helping to ultimately bring about major changes in tractor ballasting and tire inflation practices for both the tractor industry and the farm tire industry.

The major test variables were:

- tractor ballast type (cast weights and/or liquid ballast in tires),
- tractor fore-aft center of gravity location (static weight split), and
- tire size.

For a given tire size and total tractor weight, a matrix of ballast types and weight splits was used to examine the interaction of effects on power hop control. Most of these interaction effects were studied using a John Deere 8760 tractor with an uprated engine at 254 kW (340 eng hp) as shown in Figure 36. This tractor was equipped with

Figure 36. 4WD power hop test equipment in Colorado, 1991.

20.8R42 dual tires for most tests and with 18.4R46 duals on a few tests. Some tests were also conducted with a John Deere 8960 tractor equipped with the then new 710/70R38 size tires. It had an uprated engine at 276 kW (370 eng hp). For each configuration, inflation pressures were varied systematically to search for front and rear inflation pressure combinations which resulted in power hop or in a stable tractor.

To expedite cast ballast changes for most tests, special weight racks for the front of the tractor and for the 3-point hitch were designed to hold up to 40 standard 47 kg (100 lb) suitcase weights each. The test equipment, instrumentation, and data acquisition were all essentially the same as described previously.

Drawbar pull, transmission input shaft torque, true ground speed, and tractor rear axle speed were measured and recorded for all tests with the 20.8R42 and 18.4R46 tires. The tractor used for the tests of the 710/70R38 tires did not have a torque meter installed.

The soil conditions were ideal for power hop to occur readily. Wheat had been harvested and the field disked to a depth of 100-150 mm (4-6 in) several weeks before the tests started and no rain had fallen. Some volunteer wheat had begun to emerge. The soil was very loose and mellow in the disked layer. Pickup trucks and human footprints were approximately 50 mm (2 in.) deep, so it was very soft and compressible in the tilled layer and very hard below it.

The test procedures, data acquisition, radio communication, and video taping were all the same as described for previous tests.

From time to time, testing with the electrical retarders was temporarily discontinued, and the test tractor operated with a chisel plow in the same field. In all cases, the tractor behaved the same (hopped or was stable) with the implement as with the retarders.

Interpretaton of Typical Test Results

For each ballasting and weight split combination, front and rear inflation pressures were varied principally along the left and lower borders of a matrix, an example of which is shown in Table 4. The lower left corner cell indicates that both front and rear tires are inflated to their respective Rated Deflection Pressures from the experimental tables. When the total weight or weight split is changed, the Rated

Table 4. Typical test matrix for a given ballast configuration and weight split using 4WD tractor, 254 kW (340 engine-hp); 18,320 kg (40,400 lb) 55/45 split; 72 kg/kW (119 lb/eng hp); 20.8R42 duals fronts, dry rears, all 38% liquid fill; Rated Deflection Pressures 90 kPa (13 psi) front and 62 kPa (9 psi) rear. Test results indicated as % slip at which power hop started.

Front Pressures, (psi) kPa							
	(28) 193	Hop 12%					
	(24) 165	Hop 6-10%					
	(20) 138	Hop 18-20%		Hop 12-20%			
	(16) 110	Stable to 25% **	Stable to 25%				
	(13) 90	Stable to 25% **	Mild Hop 17-25%	Hop 10-13%	Hop 10%	Hop 10%	Hop 10%
		62 (9)	90 (13)	110 (16)	138 (20)	165 (24)	193 (28)
	Rear Pressures, kPa (psi)						
** indicates downshift to a lower gear was required to prevent engine stall							

Deflection Pressures change, so the reference pressures in the lower left cell and all others change from one test to the next. Inflation pressure increments of 28 kPa (4 psi) were used. Some tests were run with both the front and rear inflation pressures above Rated Deflection Pressures. Usually the combinations were selected along the diagonal as shown in Table 4.

The comment in each cell indicates the basic stability result for the front and rear inflation pressure combination represented. If hop occurred below approximately 20% slip, the level at which it started is shown. The tractor would be considered unusable with those inflation pressures. When hop first occurred when slips were greater than 20%, the cell shows the result as "Stable to the indicated level." The tractor would be usable up to that point in actual field operating conditions.

The most typical result obtained in testing each ballasting and weight split configuration in this test series was that the tractor was most stable when the front and rear tires were operated at Rated Deflection Pressures—the lower left corner of the matrix. There are other soil moisture, soil texture, and operating conditions where raising the front or raising the rear inflation pressures is required to control power hop. Today, the stiffness contributed by the soil in the series spring combination of tire and soil is unpredictable on all but firm soils. It must be the case that soil stiffness varies widely depending on soil moisture, soil texture, and possibly other unknown factors. There is no question but that both soil stiffness and soil damping significantly influence power hop and hop controllability, but obviously, humans cannot control the soil. They can only manipulate the influences of the tractor and the tires in power hop control, and the specific requirements will vary from one soil condition to another.

Overall Results Summary Matrix— 20.8R42 Dual Tires

The test matrix shown in Table 5 was used to investigate the interactions of ballast configuration and weight split with total tractor weight being held constant within practical limitations at 18,320 kg (40,400 lb). Cast ballast was used on the front and/or rear weight racks to maintain total tractor weight and weight split in each case. Each cell in this matrix corresponds to a complete sequence of tests with various inflation pressures as shown in Table 4. The cells in Table 5 provide a synopsis of the overall test series results.

Influence of Liquid Ballast Amount and Location

The negative influence of liquid ballast on the ability to control power hop is dramatically shown in the test results of Table 5. Examining the first row, the old standard practice of filling the inner front and inner rear tires to the 75% level, all inflation pressure combinations led to power hop for all three static weight splits tested. This parallels the same result found by Brodbeck (1989) for an MFWD tractor.

The next two rows show that as liquid is removed from the front, the situation improves. However, notice that power hop control is not as good with 75% fill in all four rear tires as with just two. This suggests that with more liquid ballast on an axle, power hop sensitivity is increased.

The fourth row of the matrix reveals that with the 38% fill in all rear tires, power hop control is becoming a bit easier and now even includes the extremely "nose-heavy" weight split of 62/38.

Finally, with no liquid in any tire, the tractor achieves its greatest range of stability and is the least sensitive to inflation pressure deviations from Rated Deflection Pressures.

Table 5. Overall results summary matrix for 20.8R42 tires on 4WD tractor @ 254 kW (340 eng hp); 18,320 kg (40,400 lb); 72 kg/kW (119 lb/eng hp). Static weight splits expressed as % front/% rear. Inflation pressure pairs expressed as front pressures-rear pressures. RDPs = Rated Deflection Pressures. Soft compressible soil disked 100-150 mm (4-6 in) deep.

Liquid Ballast Location, % Fill	45/55 Split RDPs 62-90 kPa (9-13 psi)	50/50 Split RDPs 76-76 kPa (11-11 psi)	55/45 Split RDPs 90-62 kPa (13-9 psi)	62/38 Split RDPs 110-55 kPa (16-8 psi)
Front Inners 75% Rear Inners 75%	Not tested	All hop	All hop	All hop
Front All Dry Rear Inners 75%	Not tested	Stable to 25-40% slip at RDPs only.	Stable to 35% slip at RPDs and slightly higher front pressures.	All hop
Front All Dry Rear All 75%	Not tested	Stable only to 20% slip at RDPs and slightly higher front pressures.	Stable only to 21% slip at RDPs.	Not tested
Front All Dry Rear All 38%	Not tested	Stable to 35% slip at RDPs and up to 62 kPa (9 psi) above rated in fronts. Also stable with rears slightly higher than rated.	Stable to 25% slip at RDPs and slightly higher front pressures.	Stable to 25% slip at RDPs and slightly higher front pressures.
Front All Dry Rear All Dry	Stable to 45% slip for RD and all higher front pressures. Also stable with rears slightly higher than fronts.	Stable to 40% slip at RDPs. Stable to 30% slip with fronts up to 34 kPa (5 psi) higher than rated. Stable to 28% slip with rear slightly higher than rated.	Stable to 40% slip at RDPs. Stable to 30% slip with fronts as much as 48 kPa (7 psi) above rated.	Stable to 27% slip at RDPs only.

These dramatic results provided great impetus to start the process of helping wean farmers away from using liquid ballast or at the very most to use no more than 38% fill in all rear dual or triple tires of tractors used in tillage operations. These recommendations remain today, and the on-farm use of liquid ballast has decreased.

RJT—The liquid ballast effect has been a more positive experience in AFMRC's field tests. On 4WDs, AFMRC has sometimes found just the addition of liquid to the rear tires (typically up to the 40% fill mark) will provide enough stiffening to control power hop without raising inflation above Rated Deflection Pressures. Similarly on MFWDs the addition of liquid to the front tires (typically to the 75% fill or above) is often enough to control power hop without raising front pressures.

Influence of Tractor Fore-Aft Center of Gravity Location

JCW—An overall examination of Table 5 reveals that the range of stability increases as the percentage of static weight on the front axle is decreased. This is completely in keeping with the predictions of the mathematical model and consistent with other field experiences, i.e., the more "nose-heavy" the tractor, the more likely it is to experience power hop and the more difficult it is to control.

Most 4WD tractors are sold without a 3-point hitch and PTO, which means that the static weight on the front axle of the unballasted tractor is around 60% or more of the total. This was, in fact, regarded as desirable by some of the pioneers who first built 4WD tractors, and it was adopted by many manufacturers thereafter. Their logic behind this choice of static weight split was that under average drawbar load, weight transfer would result in approximately equal front and rear axle loads and thereby generate about equal amounts of pull per axle. The implicit assumption was that this was "optimum." This concept was easily accepted by tractor engineers and by farmers.

Figure 37 shows plots of both pull-to-weight ratio and power delivery efficiency data for the weight splits and inflation pressures shown in the lower right three cells of the bottom line of the matrix in Table 5. Power delivery efficiency is the ratio of drawbar power to engine power.

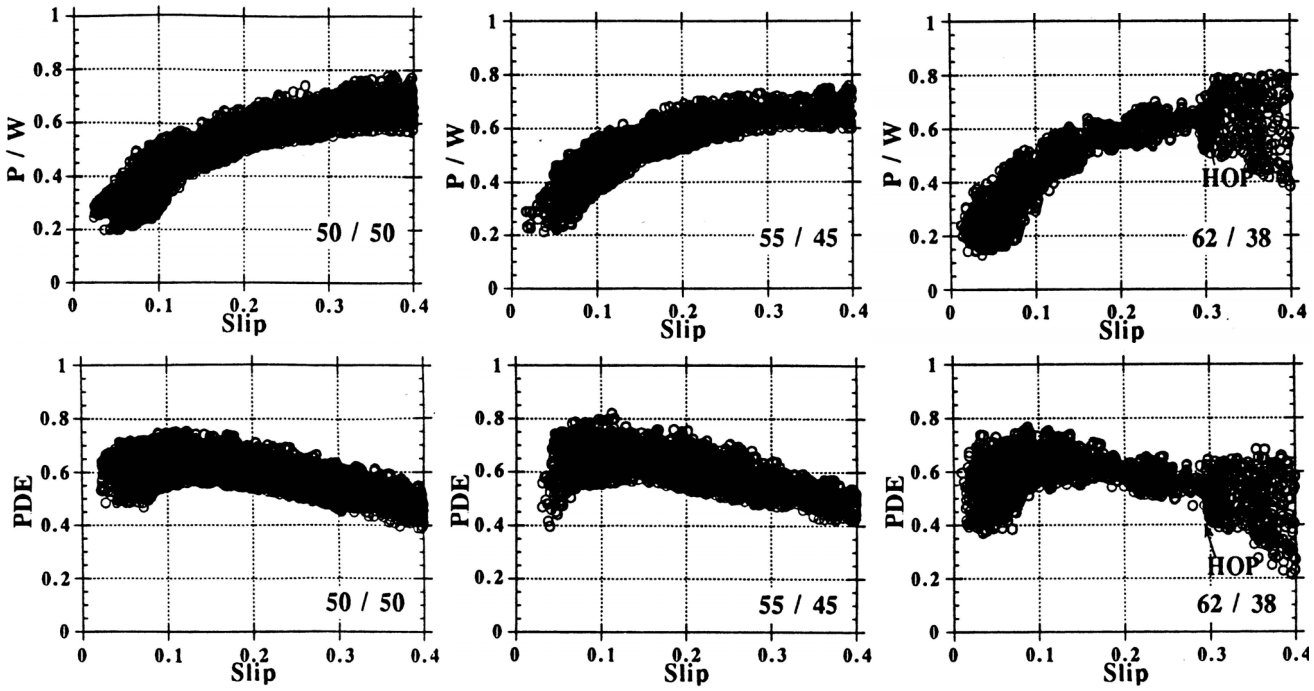

Figure 37. Comparison of 4WD tractor performance measures at three static weight splits. Conditions: 4WD tractor @ 254 kW (340 eng hp), 18,320 kg (40,400 lb), 72 kg/kW (119 lb/eng hp); static weight split; Rated Deflection Pressures (front-rear) of 50/50 76-76 kPa (11-11 psi); 55/45 90-62 kPa (13-9 psi); 62/38 110-55 kPa (16-8 psi). P/W = pull ratio = drawbar pull/tractor weight. PDE = power delivery efficiency = drawbar power/engine power.

This concept was introduced by Reed Turner (Turner, 1993a; Zoz et al., 2002), as an alternative to tractive efficiency for full scale field tests since it is much easier to measure and provides the essential information for comparing tractor performance under various conditions.

Inspection of the three pull-slip plots and the three efficiency plots in Figure 37 shows no fundamental differences among the three weight splits. As of the time these tests were conducted in 1990, no other test results comparing tractive performance of 4WD tractors with various weight splits had been published. Later results of tests of a model 4WD tractor in a soil bin were presented by Gu and Kushwaha (1992). Then field tests using the same three weight splits were reported by Turner (1993a). All researchers found the same results, i.e., that the traction and performance measures were the same for all weight splits. So the old argument to ballast a 4WD tractor to a 60/40 weight split for best tractive performance does not appear to be valid. Furthermore, such a high front weight split makes power hop control very difficult.

The test with 45% front and 55% rear was conducted primarily to confirm the trend toward greater stability with a lower percentage of weight on the front axle. Although this weight split clearly provided the greatest resistance to power hop, there is a valid reason to avoid it—the potential for overloading components of the rear power train of the tractor. On typical articulated 4WD tractors, the front and rear power train components are usually the same size and often the same part numbers. This helps keep the manufacturing costs lower than if different front and rear sizes were used and is a major reason that the cost of 4WD tractors per unit of engine power is less than that of MFWD tractors. So, the recommended weight split range for practical power hop control of 4WD tractors was selected to be 51 to 55% on the front axle. This has proven to be an essential requirement for power hop control of 4WD tractors operating in soil conditions where it is likely to occur. In such conditions, with no more than 55% on the front, power hop can usually be controlled, but often it is almost impossible if the front percentage is higher than 55%.

We note here that weight split has much more influence on power hop sensitivity in 4WD tractors than in MFWD tractors. It is clear from field experiences, but also can be seen from the mathematical model. Using the static weight splits of 35/65 for MFWD tractors and 55/45 for 4WD tractors, the Hop Functions become:

$$k_f(0.65) - k_r(0.35) > 0$$

is sufficient for MFWD stability, and

$$k_f(0.45) - k_r(0.55) > 0$$

is sufficient for 4WD stability. Dividing the first by 0.65, the second by 0.45, and rearranging each, we obtain

$$k_f > 0.54k_r$$

is sufficient for MFWD stability, and

$$k_f > 1.22k_r$$

is sufficient for 4WD stability. Recall that as pull increases,

the front stiffness decreases and the rear increases. Thus it is much more difficult for a 4WD tractor to satisfy the inequality.

RJT—As noted above, AFMRC also investigated the effect of weight split on tractor performance and power hop. These tests compared ratios of 60/40, 55/45, and 50/50, using single, dual, and triple 20.8R42 radial tires on a 242 kW (325 hp) Ford New Holland 946 ballasted to 61 kg/kW (100 lbs/eng hp). Tests were run in a dry clay-loam soil in a well-worked secondary tillage condition with the tire inflation pressures set correctly. The weight splits showed no significant differences in peak pull or in power delivery efficiency but, as would be expected, showed significant differences in the power split front to rear. The ratio moved from 52% of the total at the 60/40 split to 46% at 55/45 and to 42% at 50/50. In this test sequence, power hop was only an issue at the 50/50 weight splits on the duals and triples. This hop was controlled by increasing the rear inflation pressures

Effect of Inflation Pressure on Performance

JCW—In virtually all tests, a downshift of the powershift transmission by one or two gears was needed to prevent engine stall at high pull levels when the tires were all set at Rated Deflection Pressures or with the front tires slightly higher. This is an indication that the tractive performance was greatest with these pressures. This was definitely shown to be the case in later tests by Zoz and Turner (1994), Upadhyaya and Lancas (1994), Lancas et al. (1995a), Lancas et al. (1995b, 1996, 1997), Zoz (1997), and Zoz and Grisso (2003). However, in 1991, the effect of overinflation on performance was not well recognized.

As indicated from the results in Table 5, power hop occurred very readily in this soil. While operating with Rated Deflection Pressures in both front and rear usually provided the greatest resistance to hop, any time both front and rear were raised simultaneously, power hop occurred. However, in some cases the tractor was stable with the front raised

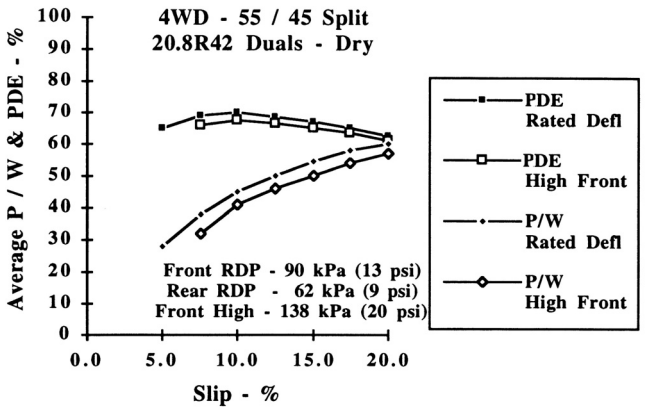

Figure 38. Performance comparison of Rated Deflection Pressures and a higher front pressure. P/W = pull ratio = drawbar pull/tractor weight; PDE = power delivery efficiency = drawbar power/engine power

while keeping the rear at rated. One such case is shown in Figure 38. With an increase of front pressures by only 48 kPa (7 psi) above rated, the peak power delivery efficiency decreased by approximately 4.4%. The corresponding reduction in pull at that point is approximately 9%. While this decrease is significant, it is far smaller than the drop that would result in the typical high pressures front and rear used by farmers at that time which was a primary factor contributing to power hop. The test results, however, are clear: the best performance and best power hop control in this soil occurred when both the front and rear tires are set at Rated Deflection Pressures.

Influence of Tire Size

Tire size relative to tractor weight and power level has a very significant influence on sensitivity to power hop and the ability to control it. This was not at all well understood by engineers, marketing personnel, dealers, or farmers prior to the results of the 1991 tests. A common practice at the time was to use the least expensive tires that would support the ballasted weight of the tractor with due consideration given to using larger sizes with increased engine power. On 4WD tractors in particular, a wide range of tire size options from minimal to very large is offered by all tractor manufacturers. The bottom line price of a 4WD tractor can vary widely depending on tire size, and often customers selected a minimal size to try to squeeze tractor cost to the lowest possible amount. It was tacitly assumed that if the tires could simply support the weight of the tractor and get it across the field under load, they were adequate. The influence of tire size on power hop control was essentially unknown prior to 1991.

Some of the most definitive demonstrations of the influence of tire size came in the 1991 tests. In addition to the 20.8R42 tires used in the tests just discussed, the row crop size 18.4R46 was tested on the 8760 4WD tractor set to 254 kW (340 eng hp). While the outside diameter is the same as the 20.8R42 tire, the rim diameter is 102 mm (4 in) larger, and, obviously, the tire is narrower. The net result is that 18.4R46 tires have less internal air volume and thus require higher Rated Deflection Pressures to carry the same loads as 20.8R42 tires. The consequence is that they are stiffer and pose more difficult problems with power hop control as shown in Table 6. This table corresponds to the last row in Table 5, i.e., no liquid ballast. The only difference is the tire size.

Practical power hop control was barely achieved at the 50/50 static weight split and required higher front inflation pressures than rated. Hop was controlled at the 45/55 split, but as discussed previously, this is not a practical solution based on the potential for overloading the rear power train components.

Earlier in 1991 after the experimental load-inflation tables were first created, Loran Lopp, then Chief Engineer of Farm Tires at Goodyear, hypothesized that the stiffnesses

Table 6. Overall results summary matrix for 18.4R46 tires. Refer to Table 5 for other details.

Liquid Ballast Location & % Fill	45/55 Split RDPs 83-110 kPa (12-16 psi)	50/50 Split RDPs 97-97 kPa (14-14 psi)	55/45 Split RDPs 110-83 kPa (16-12 psi)	62/38 Split RDPs 13-62 kPa (20-9 psi)
Front All Dry Rear All Dry	Stable to 30% slip for RDPs and all higher front pressures. Ride choppy.	Marginally stable at RDPs with hop at 15-25% slip. Stable to 25% slip with fronts slightly higher than rated and rear at rated.	All hop	All hop

for dual or triple radial tires would probably be too high for practical power hop control if the Rated Deflection Pressure was more than 97 kPa (14 psi) (see Lopp, 1992). These test results seem to confirm his hypothesis. Current recommendations for selecting dual or triple tire sizes on MFWD and 4WD tractors now include this as the "14 psi Rule." Specifically, when selecting a tire size for dual or triple applications on the rear of MFWD tractors or for all tires of 4WD tractors, the required inflation pressure to support that ballasted static weight of the tractor should be no more than 14 psi. If more inflation pressure than this is required, the tractor will likely experience power hop problems and may not be controllable by standard procedures.

In addition to the 1991 test results from 18.4R46 *dual* radial tires, numerous on-farm power hop experiences have shown that this tire is not well suited to 4WD tractors doing high-draft tillage operations. Triples are required for reasonable results. Consequently, this caveat is included in the current recommendations for tire sizing based on engine power.

The final tire tests in this series were of a size that had just been introduced, the 710/70R38. It has the same overall diameter as the other two tires tested, but is much wider and on a smaller-diameter rim. Thus it has a huge air cavity in comparison to the other two and, consequently, can operate at much lower inflation pressures to carry the same loads. Of course, this means the stiffness is much lower than the other tires as well, which is very desirable for power hop control.

The 710/70R38 dual tires in this test series were mounted on a John Deere 8960 4WD tractor with power uprated to 276 kW (370 eng hp). It was ballasted with cast weights to 19,500 kg (43,000 lb) or 71 kg/kW (116 lb/eng hp) and a static weight split of 54/46. Rated Deflection Pressures were 55 kPa (8 psi) front and 48 kPa (7 psi) rear. The tractor was stable to more than 40% slip at Rated Deflection Pressures and at all higher front pressures. It did power hop with 110 kPa (16 psi) front and 83 kPa (12 psi) rear. At the conclusion of this test series, the inflation pressures were reset to the Rated Deflection Pressures front and rear and the tractor operated in the same field with a 12 m (40 foot) chisel plow set to maximum depth. It easily pulled the implement at ground speeds of 12.6 to 13 km/hr (7.8 to 8.1 mph), surprisingly high speeds for a tractor towing this size of chisel plow. The ride was smooth and comfortable, and there was no sign of power hop.

The wide range of differences in results with the three tire sizes in the same field in this test series helped establish the concept that 4WD tractors need tall, soft tires to deliver top performance along with the ability to control power hop. Over the next several years, the 710/70R38 tire was widely accepted as an ideal tire for large 4WD tractors. It was the largest diameter tire that would fit existing tractors, but as power levels were increased, tractors were redesigned to accommodate even larger diameter tires (Brodbeck, 2004).

RJT—During the summer and fall of 1991 AFMRC also continued tests comparing rubber belt tracks to radial tire equipped 4WD tractors, investigating both track versus tire performance and tire power hop performance. The project proceeded as a joint effort with cooperation from Caterpillar, Deere, Case-IH, Firestone, and Montana State University (Turner, 1993b).

Tests were run in Alberta using a Challenger 65 compared to a Case-IH 9250 (articulated) and a Case-IH 9260 (fixed frame 4-wheel steering), both equipped with 20.8R42 radial tires. These combinations were tested in sandy, clay loam, and heavy clay soils in both primary and secondary tillage. On the rubber tire tractors, tests were run using the new lower pressure "soon to be recommended" load inflation tables and ballasted to 54/46 front to rear ratios using various combinations of cast weight and liquid ballast. With the new lower inflation pressure settings, power hop did not occur and was not an issue.

Tests were run in Montana using two Challenger 75's, one with 700 mm (27.5 inch) wide tracks and one with 890 mm (35 inch) wide tracks, and two John Deere tractors with various tire setups as shown in Table 7. All setups were tested in a dry and firm clay loam soil in both primary and secondary tillage with tire inflations set using the new lower load inflation tables, and ballasted with various combinations of liquid and cast ballast.

Power hop was a major issue throughout the testing and the fixes reached for the various setups were somewhat varied. With the single radial tire sets (an allowable but marginal use for single tires at these power levels), on the

Table 7. Montana tire test combinations.

Tractor and Tire Test Combinations		
Tractor	Eng kW	Tire Setups
Deere 8760	224	20.8 R42 duals 20.8-42 bias duals 25.5 R32 singles
Deere 8960	276	20.8 R42 duals 20.8 R42 triples 710/70 R38 duals 710/70 R38 singles

24.5 R32 tires the best hop control resulted from high front and correct rear inflation with cast or liquid ballast. Using 710/70 R38 tires as singles, the only acceptable hop control resulted from correct front and high rear inflation. With dual and triple radial tires the best hop control resulted from correct front and high rear inflation when there was liquid ballast in the rear. There was one instance with cast only ballast where the best control resulted from high front and correct rear and two with cast only ballast where the best control resulted from correct front and high rear. At this test site, the bias ply tires were the only tire set that showed no tendency to power hop with either type of ballast. While they showed slightly lower power delivery efficiency, they were clearly superior in power hop control.

Overall, heavier ballasted tractors experienced less problems with power hop than lighter tractors at the same power level. The heavier tractors were less likely to hop, and when they did, the hop was less severe than it was on the lighter tractors. This may have been simply a function of the force required to move the additional mass, or it may have been because the heavier tractors operated at lower slip levels.

While the type of ballast used (cast or liquid) had no effect on power delivery efficiency (PDE) or peak pull, it did have an effect on power hop. Some tractor and tire combinations with cast ballast at the rear were less prone to experience power hop than those with liquid ballast at the rear. Other combinations with liquid at the rear were much less prone to hop than the same combinations with cast at the rear. In general, when power hop did occur, it was controlled more easily and with smaller adjustments on tractors with liquid ballast than on tractors with cast ballast.

Tire inflation pressure had a large effect on both power hop and on tractor performance. The highest PDEs were obtained with the tire pressures set at the proposed lower Rated Deflection Pressures. Any pressure increases reduced the PDEs for any of the tire sets. With any of the tires, when (or if) hop occurred, it was always possible to control or remove it within the working range of the tractor by changing tire inflation pressure. The basic approach was to soften the tires on one end of the tractor and to stiffen them on the other. To minimize the effect on PDE, it was important to increase the stiffness of the tires on whichever end of the tractor was already the stiffer end. Typically this was the front tires on a tractor with cast ballast and the rear tires on a tractor with liquid ballast. As the inflation pressure was increased on one end of a tractor, the overall PDE decreased and the more the pressure was raised, the more the PDE decreased. Measurements showed that raising tire inflation pressure on either end of a tractor decreased the total PDE by about 30% of the amount that the PDE would have been decreased by raising the inflation pressure the same amount on both ends. Raising the tire pressure on the stiffest end of the tractor minimized the impact on PDE by minimizing the amount of tire pressure increase required for hop control.

Measuring Power Hop

Initial Documentation Efforts

Documentation of power hop has been a problem. Customers, researchers, and service personnel were able to report that a tractor was hopping (sometimes bouncing, jumping, or some other expression) but could not adequately describe the magnitude of the problem. Additionally, there was not always agreement that what was being experienced at a given instance was truly power hop, and not vibration, rough ride, or some other phenomenon. The most common initial measurement was simply a yes/no record, as decided by someone who "knew" power hop. This progressed to a video record of the hop and most "measurements" of power hop in early test work were documented using a video camera, occasionally supplemented with driver or passenger audio comments. This worked reasonably well as long as the video was available for observation or reporting, but even so it was difficult to quantify one hop against another, and it was cumbersome to maintain, keep track of, and share the records.

A Qualitative Scale

The testing that began in 1991 reinforced the need to be able to measure and describe power hop both qualitatively and quantitatively. With parallel tests occurring in different areas and recognition developing that there were differing degrees of hop, it was important to be able to communicate the specific hop levels that were occurring and to be able to compare them to hop at other sites or with other units. With that in mind, AFMRC and Deere field test personnel developed a basic hop description matrix to better describe and document what was being observed. The matrix considered how easy it was to get hop started, how easy it was to maintain the hop, and the relative severity of the hop. This was refined the following year to provide a five-level scale that was used along with ground speed and pull level to characterize and report the various hop occurrences. The scale was published as a card (shown in Table 8) and distributed as a hop characterization reference to various interested parties.

Table 8. Power hop definition card.

TRACTOR POWER HOP LEVELS

Level	Description	Starts	Stays	Hop Level
1	**NONE** Tractor shows no tendency to hop	No	No	None
2	**FLEETING** Hop difficult to start and dies out quickly	Difficult	Dies out	Low
3	**MILD** Hop difficult to start but will continue at a low level	Difficult	Sustains itself	Low
4	**DISTINCT** Hop starts easily and continues without increasing	Easily	Sustains itself	Medium
5	**SEVERE** Aggressive hop that starts easily and increases to uncomfortable levels	Easily	Sustains itself	High

Reed Turner/Frank Zoz
25 Aug 1993

Quantifying Hop Levels

In research done in later years, hop measurement progressed beyond this qualitative matrix to a true quantitative measurement that was derived from acceleration time histories. Vertical accelerometers, usually at the front axle but occasionally at the rear, were typically used during engineering tests to document when power hop was taking place. The accelerometer time history traces were plotted following the tests to define where hop began and to make statements about the magnitude of the hop. Zoz (2007) reported the calculation of real time RMS acceleration levels taken during a series of tests on a 4WD tractor in the late 1990s. Raw accelerations were RMS averaged over 1.5-second intervals, providing data points that could be plotted along with PDE and other tractive performance data as the test was run. This data provided the opportunity to measure and document power hop performance concurrent with other tractor and traction performance data. Figure 38 shows a plot from Zoz (2007) for a tractor experiencing power hop. PDE and front axle RMS vertical acceleration

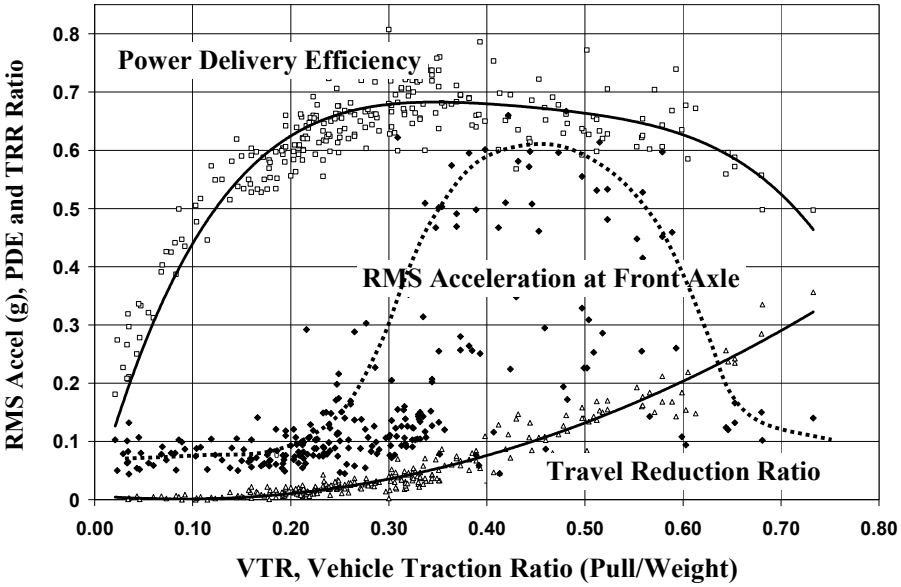

Figure 38. Power hop definition graph showing power delivery, travel reduction, and power hop using 710/70R38 duals at correct inflation pressures.

are plotted against vehicle traction ratio (VTR or pull-to-weight ratio). At around 0.3 VTR, power hop starts. The RMS acceleration data clearly delineates the beginning and indicates the magnitude of the hop as VTR increases.

As there is no common location defined on a tractor for mounting accelerometers, some judgment by the test engineer is still required to decide what level of RMS acceleration should be considered as the onset of power hop.

Practical Applications of the Results

Going Public

JCW—At the conclusion of the comprehensive tests near Denver, Colorado, in October, 1991, engineers from the three tire manufacturers who had participated in the tests and Deere personnel all agreed that the extended load-inflation pressure tables had provided a key breakthrough in helping control power hop and that the tables should be released to the public as soon as possible. In addition, they all agreed that new guidelines on tire sizing, weight split, and use of liquid ballast reflecting the results of the tests just completed should be incorporated into field service bulletins at the same time the new tables were released.

In December, 1991, at the ASAE Winter Meeting in Chicago, Reed Turner of the Alberta Farm Machinery Research Centre convened an informal evening meeting to discuss the tests that had just been completed. He invited representatives from all major tractor manufacturers and tire manufacturers, researchers, and representatives from the agricultural news media. At that meeting, Bridgestone/Firestone, Goodyear, and Pirelli-Armstrong (now Titan) announced their intentions to support the new tables and power hop control recommendations. All three published the tables and new guidelines during the first three months of 1992. At the same time, Deere published service bulletins for dealers and began preparing handbooks on optimizing performance that were ultimately included with the operators manuals of all John Deere agricultural MFWD and 4WD tractors.

Further Field and Test Experiences

After the new information was made available in 1992, it was not as vigorously applied by dealers and farmers as hoped. Indeed, major changes in thinking and in practices were required, and change is always difficult. However, steady progress was made as it was applied by tractor field service personnel and by farm tire engineers in response to power hop complaints. The most difficult aspect was that, initially, they were all working with tractors already in the field, the majority of which fell short of the new guidelines by having undersized tires, not enough ballast, too much liquid ballast, or liquid in the wrong places.

It was generally straightforward to control power hop in customer MFWD tractors by getting the liquid ballast leveled out at 38% fill or less in all four rear tires and then setting the inflation pressures by the new tables. Some customers were willing to replace liquid with cast weight, which made it even easier. The major hurdle was in assuring customers that the tires would not fail with the lower inflation pressures if the rules for inflating based on known axle weights were followed carefully. Of course, following the rules means increasing the rear inflation pressures when mounted 3-point hitch implements are used. Initially, this need to change inflation pressures with the type of implement being used was met with resistance, but as more and more dealers and farmers observed the positive benefits of using the correct pressures, acceptance increased.

As has been mentioned previously, dealing with power hop in 4WD tractors is inherently more difficult than with MFWD tractors. In addition, most 4WD tractors experiencing power hop problems in the field in the early 1990s had been purchased with minimal tires and ballasted with liquid ballast. Thus it was difficult, sometimes impossible, to get hop under control on these tractors. Field demonstrations with tractors set up by the new guidelines were the most effective means of getting the message out. Then, when the next tractor purchase was made by a customer who had witnessed the demonstration, ordering the right tires and ballast, and setting the inflation pressures by "the book" instead of by eye, was not such a shock. For more comments about helping people change their minds on this subject, see Wiley (1995).

Three important technical refinements to the 1991 rules came about as a result of numerous experiences with customer tractors. The first observation was that with 4WD tractors, in particular, power hop tends to occur more frequently at higher travel speeds. While many operators were content with travel speeds less than 8.0 km/hr (5 mph), by the mid-90s, more and more expected to operate at 11 to 13 km/hr (7 to 8 mph). This ultimately led to inclusion of different hop control recommendations based on average travel speeds above or below approximately 8.8 km/hr (5.5 mph).

A second observation from field experiences was that for very lightweight 4WD tractors, based on weight per engine horsepower (kg/eng hp), power hop tends to occur more frequently than with average or heavier tractors. A caveat pointing this out and a suggested minimum level was then incorporated into the ballasting recommendations for 4WD tractors.

The third refinement is probably the most surprising and mystifying. All of the Deere formal tests of 4WD tractors on a variety of soils showed that operating both front and rear tires at Rated Deflection Pressures or with the fronts higher controlled power hop. Raising the rear pressures above rated usually induced power hop. However, when operating in other *soft* soil conditions with faster speeds and different implements on customer farms, sometimes power hop could be controlled by raising the rear pressures

while keeping the fronts at Rated Deflection Pressures. Thus, raising either the front or the rear while keeping the opposite end at Rated Deflection Pressures controls hop in many *soft* soil conditions. However, if the soil is *firm* (or the test is on a paved surface), raising the front is the only means of controlling power hop.

It is natural to ask why raising the rear pressures should work. Although a lot of thought has gone into this question, there is no clear and compelling answer. Conjectures about the total front and rear stiffness and damping provided by stiff tires on soft soil versus soft tires on soft soil seem plausible but remain unsubstantiated. Thus it is simply accepted as a fact of life. Power hop can be controlled without knowing the answer, anyway.

RJT—AFMRC field testing on 4WD tractors in both soft and firm soils found raising rear inflation pressures to often be an effective method to control power hop. In most cases, when raising the rear pressures worked, so did raising the front pressures, but raising the rear sometimes worked better and often required smaller pressure increases than raising the front. Three factors that might explain this can be considered. First, while the net stiffness and damping of the tire and soil combination has a significant effect on power hop performance in the field, the contribution to the stiffness and damping provided from a specific soil is not well understood. Second, AFMRC tests used a tillage tool rather than a load unit to provide tractive load, and the differences between the two (horizontal and stable pull, isolated source and significantly greater mass than the tractor) may affect the results. Third, AFMRC used calcium chloride solution rather than water as ballast, typically in the rear tires. These and/or other areas to yet be identified may suggest opportunities for additional research in understanding the differences between front and rear control.

In considering why raising rear pressures works in the field, it is interesting to note that the published higher speed recommendations for 4WD tractors closely fit the results from AFMRC field tests. The northern Great Plains area where AFMRC tests were typically run is an area where lighter ballasted tractors and higher speed operations are more the norm.

Power hop control on 4WD tractors is basically a two-step process. The first step is to begin with all the tires set correctly at Rated Deflection Pressures. The second step, if power hop is a problem, is to increase the stiffness on one end of the tractor. This is typically done by raising tire inflation pressures on one end of the vehicle, but can also be done by adding liquid ballast, equalized in the tires, on one end. Which end is most appropriate to work with can be difficult to predict in advance. It is common to work first on whichever end is the stiffer, commonly the front for tractors ballasted with cast, and the rear for tractors ballasted with liquid, but it is often worthwhile to experiment with both ends and settle on the one which requires the least total stiffening. The implement and the field operation can also affect this, sometimes as much or more than the vehicle or the ground condition.

A problem with raising pressures on either end to control power hop is the impact of this on tractor productivity. Any time inflation pressures are raised above the Rated Deflection Pressures, tractive efficiency, power delivery efficiency, and fuel efficiency are negatively affected (Turner, 1995). This productivity effect provides another good reason to experiment with both front and rear to select the one that requires the least increase in pressure and hence has the least impact on efficiency. In softer soils in particular, AFMRC has found increasing the rear stiffness usually provides hop control with the least reduction of efficiency, possibly because the rear tire runs in a track defined and firmed by the front tire.

A few comments about bias tires are appropriate. Bias ply tires have generally shown less power hop problems than equivalent radials, probably because of the higher stiffness of their sidewalls. When bias tires have experienced hop problems, the hop was typically controlled with smaller pressure adjustments than for radials. While bias tires typically have 5 to 7% lower power delivery efficiency than radials, in instances where radials hop and have to be controlled through inflation pressure increase, this difference narrows and in some instances may even disappear. It has not been uncommon to observe customers "living with" occasional hop on bias ply tires rather than adjusting for it, because it was a more uncommon or rare occurrence. This is usually not an option with radials. In the early 1990s, work was done to develop bias belted tire designs that would allow operation at the lower pressure and larger footprints of radial ply tires, yet still provide the power hop control of bias tires. By 1995, Trelleborg was marketing a series of these tires and company publications suggested they were an effective alternative for efficient power delivery with no power hop problems. Tests at the Alberta Farm Machinery Research Centre (Turner, 1999) showed the tires could operate at similar inflation pressures and ground pressures as equivalent-sized radials. They proved to have less hop problems than radials, but still had lower power delivery efficiencies, similar to those of standard bias ply tires.

Another area of concern that arose as the new load inflation tables were adopted was actual "flat" tires. Existing tires set at the new lower inflation pressures tended to have substantially more problems maintaining inflation. There were several causes, but the most serious one resulted from the tube quality used in the tube-type tires of the day. When subjected to the additional flexing of the tires resulting from the increased sidewall deflections, the tubes tended to chafe, wear, and split or leak. Once improved natural rubber or "radial tire quality" tubes filtered through the pipeline, and as it began to be more common to mount tires tubelessly, this problem went away. A secondary cause was just the fact that a 14 kPa (2 psi) air loss or pressure inaccu-

racy on a 41 kPa (6 psi) tire was a much greater change than a 14 kPa (2 psi) loss on a 138 kPa (20 psi) tire. Customers and operators had to acquire more accurate low-pressure tire gauges and accept the responsibility of checking and maintaining all tire pressures more often than they had typically done in the past. This is an ongoing education and extension process, even now, 15 years after the load inflation table pressure reductions.

One puzzling characteristic that has been observed in AFMRC tests, and reported by other researchers, is the capability to go "beyond" power hop in a tractor. It is possible (though not particularly practical) to operate some tractor configurations beyond their power hop range. When a tractor initially experiences power hop, the normal tendency for the operator is to slow down or reduce the pull in order to get out of or stop the hop. With some configurations, it is possible instead to substantially increase the pull and have the hop subside, or to start out at that high pull level and not begin to hop. This can be seen in the data shown in Figure 38; as VTR reaches 0.6 and above, the hop disappears. While this is not a useful or acceptable approach to the control of power hop, it suggests that there are factors in play which have not yet been identified or understood.

JCW—After the introduction of the lower inflation pressure tables, several researchers examined the influence of using these lower pressures on soil compaction. Upadhyaya et al. (1994) and Lancas et al. (1995a, 1995b, 1996, 1997) conducted their research in soils of the San Joaquin Valley of California. Raper et al. (1995a, 1995b) and Bailey et al. (1996) did their studies both in a soil bin and in Alabama soils. Abu-Hamdeh et al. (1997) studied compaction in Ohio soils. Kirby et al. (1997a, 1997b) examined the soil compaction in Australian soils. Turner et al. (1997, 2001) tested in the soils of Southern Alberta. All found that compaction was significantly reduced with the lower but correct inflation pressures in comparison to higher pressures that had typically been used by farmers. These results are very important in that they emerged consistently across so many different soil types and were based on a wide range of measurement systems. Operating tires at Rated Deflection Pressures is the most important thing farmers can do to minimize compaction of their soils by tractors and equipment.

Specific Guidelines to Optimize Power Hop Control and Tractor Performance

The essential elements of the guidelines for controlling power hop and optimizing performance have not changed since the early 1990s, but several refinements have been added based on both extensive field experience and further testing. The current guidelines are being applied successfully throughout the world. While there may be minor differences in the recommendations issued by various tractor and tire manufacturers, there is basic agreement on the fundamentals. The first author helped in the formulation and refinements of the recommendations by John Deere which are presented below. These represent the ultimate practical outcomes of the research on power hop reported herein.

An important aspect of these recommendations is that they start at the time the options are being selected when a customer and dealer are working out the details of ordering a new tractor to be built. The decision on tire size is very critical because it is usually economically impractical to upgrade later to a larger size if the initial choice was for tires that prove to be too small. Ordering the tractor to be ballasted on the assembly line to achieve the right weight split and total weight overcomes the many problems that can occur if done later on the farm or in a dealer's shop. In those situations, determining how much ballast is needed and where it needs to be located to achieve the correct balance and total weight is not easy.

MFWD Tractors: Initial Setup

Minimum Tire Sizes

Select the tallest tires that will fit under the fenderwells for optimum traction. For best power hop control, the dual or triple drive tires must not require more than 97 kPa (14 psi) to support the ballasted rear axle load on the tractor. Tires that require even less are better. Front tires are selected based on the required MFWD gear ratio which usually means the front Group Number will be five less than the rear. Each Group Number identifies a standard outside diameter of a tire (see Tire and Rim b.) For MFWD row crop tractors in North America that use dual or triple tires, the current (2007) recommendations used by John Deere are:

PTO horsepower	Minimum dual or triple rear tires
120-150	480/80R42 duals or larger (Group 46) 73" diameter
150-225	480/80R46 duals or larger (Group 47) 77" diameter
225-275	480/80R50 duals or larger (Group 48) 81" diameter

For tractors outside of North America that operate on large single tires, the current (2007) recommendations are:

Engine horsepower	Minimum single rear tires
Up to 225	620/70R42 single tires or larger (Group 47) 1.95 m diameter
225-275	650/65R42 single tires or larger (Group 47) 1.95 m diameter
275 and higher	650/85R38 single tires or larger (Group 48) 2.05 m diameter

Ballasting Guidelines

Tractor total weight-to-power ratio is based on anticipated travel speed for heaviest draft operations. The required balance (weight split) depends on whether or not the tractor is used exclusively for integral implements or is used for both towed and integral. Heavy and high draft 3-point hitch mounted implements typically require a higher percentage of tractor weight on the front axle than shown below, but power hop is not an issue with them. For MFWD tractors *without* front suspensions used interchangeably between towed draft implements and integral implements, the maximum recommended percentage of tractor weight on the front axle is 35% for power hop control. For MFWD tractors *with* front axle suspensions, the maximum can be over 40% and depends on tractor manufacturer.

Cast ballast wheel weights are preferred over liquid in tires. Since liquid is incompressible, it increases the stiffness of tires which can make it difficult or impossible to control power hop. If liquid ballast must be used, fill all rear tires with equal amounts not to exceed 40%, i.e., with the valve stem in the 4 o'clock position.

Using North American power and speed units, the recommendations used by John Deere for MFWD tractors *without* suspensions and pulling towed implements are:

Speed	Weight-to-Power Ratio	Balance
Over 5.5 mph	120 lb/PTO hp	35-30% on front axle
4.6 to 5.5 mph	130 lb/PTO hp	
Less than 4.5 mph	145 lb/PTO hp	

The corresponding recommendations for MFWD tractors *without* suspensions outside North America are:

Speed	Weight-to-Power Ratio	Balance
Over 8.7 km/h	46 kg/eng hp	35-30% on front axle
8.7 to 7.2 km/h	50 kg/eng hp	
Less than 7.2 km/h	56 kg/eng hp	

Inflation Pressures for Towed Implement Operations

Using weight tables in the operators' manual provided by the tractor manufacturer, determine the static weight on each axle of the ballasted tractor. If these tables are unavailable, weigh each axle on platform scales. With these two weights, the correct pressures (Rated Deflection Pressures) for the tires on each axle can be found in the extended load-inflation pressure tables which have been published since 1992. They are normally included in the tractor operators' manual or they can be found in handbooks provided by tire manufacturers. Set these pressures using an accurate gauge. It is very important that all tires on a given axle be inflated to the same pressure. If the tractor is switched to an integral 3-point hitch implement, the rear pressures must be raised to accommodate the increased load in transport. If operating on very steep hillsides, increase the rear tire inflation pressures by 0.4 bar (6 psi) to help assure that the tires do not dismount from the rims on sideslopes.

MFWD Tractors: Power Hop Control Procedure

MFWD Tractors without Suspensions

Starting from the correct initial tractor setup outlined above, if power hop occurs, raise the front inflation pressures to increase front stiffness. If necessary, remove some or all front suitcase weights to help move the tractor center of gravity rearward. The step-by-step procedure recommended by John Deere follows.

1. If power hop occurs, make sure that all rear tires are inflated equally at the rated pressure for the rear axle static load.
2. Then if power hop occurs, increase the front inflation pressures by 0.4 bar (6 psi).
3. If power hop continues, increase the fronts by another 0.4 bar (6 psi). Continue to increase the front pressures as needed up to a maximum of 0.4 bar (6 psi) above the maximum pressure rating for the front tires (imprinted on the sidewalls). Usually 0.4-0.8 bar (6-12 psi) above the starting pressure is all that will be required to control power hop.
4. If power hop still persists, remove all front suitcase weights. Leave the high inflation pressure from the previous step in the front tires.
5. If power hop still persists, install 75% liquid fill in the front tires to increase stiffness. Re-inflate to the maximum pressure as indicated above.

The last two steps will usually be unnecessary.

MFWD Tractor with Suspensions

The discussion of the details for suspended tractors follows in a later section. However, for the sake of completeness and continuity, the procedure is stated here. Suspended tractors are not nearly as likely to experience power hop as unsuspended tractors.

Starting from the correct initial tractor setup outlined above, if power hop occurs, increase the amount of weight (suitcases) carried on the front of the tractor chassis frame. Do not add weight to the suspended tires or rims. Raise the front inflation pressures to carry the additional front chassis weight. This is all that is usually necessary to bring power hop under control.

4WD Tractors: Initial Setup

Minimum Tire Sizes

Select the tallest tires that will fit under the fenderwells for optimum traction. For best power hop control, dual or triple tires must not require more than 97 kPa (14 psi) to support each ballasted axle of the tractor. Avoid 480 (mm)

or 18.4 (in) cross-section *dual* tires on 4WD tractors for heavy tillage operations. These tires have relatively small air volumes making it very difficult or impossible to control power hop. For these cross-section sizes, triple tires are required for satisfactory power hop control. For 4WD tractors in North America that use dual or triple tires, the current (2007) recommendations used by John Deere are:

Engine horsepower	Minimum dual or triple tires
Up to 300	520/85R42 duals or larger (Group 47) 77" diameter
300 to 350	620/70R42 duals or larger (Group 47) 77" diameter
350 to 400	710/70R38 duals or larger (Group 47) 77" diameter
400 to 450	710/70R42 duals or larger (Group 48) 81" diameter
450 to 530	800/70R38 duals or larger (Group 48) 81" diameter

For tractors outside of North America that operate on large single tires, the current (2007) recommendations are:

Engine horsepower	Minimum single tires
350 to 400	710/70R38 single tires or larger (Group 47) 1.95 m diameter
400 to 450	710/70R42 single tires or larger (Group 48) 2.05 m diameter
450 to 530	800/70R38 single tires or larger (Group 48) 2.05 m diameter

4WD Ballasting Guidelines

Power hop incidence and power hop control of 4WD tractors are particularly sensitive to weight split. Ballasting the tractor influences both total tractor weight and the fore-aft balance, but of these two end results, balance is the most important for power hop control. For 4WD tractors used with standard towed tillage and seeding implements, no more than 55% of the static ballasted weight should be on the front axle. Tractors used to tow scrapers that generate high vertical drawbar loads and tractors used for deep ripping with an integral ripper should have 65-70% of the weight on the front axle. Power hop does not typically occur in these applications.

Power hop is also influenced by the weight-to-power ratio. While in certain applications some farmers considerate it desirable to operate very light tractors of less than 45 kg/eng hp (100 lb/eng hp) at high field speeds, these tractors seem to be more susceptible to power hop. Thus, users should be aware of this characteristic when they choose to operate very lightweight tractors.

As with MFWD tractors, cast weight is preferred over liquid ballast in tires. However, if liquid ballast must be used, it should never be installed in the front tires (except possibly for scraper applications) and all rear tires must be filled equally to no more than the 40% level.

Using North American power and speed units, the recommendations used by John Deere for 4WD tractors pulling standard towed implements (not scrapers) are:

Speed	Weight-to-Power Ratio	Balance
Over 5.5 mph	100 lb/eng hp	55-51% on front axle
4.6 to 5.5 mph	110 lb/eng hp	
Less than 4.5 mph	120 lb/eng hp	

The corresponding recommendations for 4WD tractors outside of North America are:

Speed	Weight-to-Power Ratio	Balance
Over 8.7 km/h	45 kg/eng hp	55-51% on front axle
8.7-7.2 km/h	50 kg/eng hp	
Less than 7.2 km/h	56 kg/eng hp	

Inflation Pressures for Towed Implement Operations

The comments above for setting inflation pressures in MFWD tires apply to 4WD tractors as well.

4WD Tractors: Power Hop Control Procedure

Starting with the correct initial tractor setup outlined above, if power hop occurs, increase the inflation pressure of either the rear or the front tires to increase stiffness. Never raise both at the same time. Either the front or the rear tires must be at Rated Deflection Pressures. The step-by-step procedure recommended by John Deere follows.

If power hop occurs, assure that all front tires are inflated equally at the Rated Deflection Pressure for the front axle static load and that all rear tires are inflated equally at the Rated Deflection Pressure for the rear axle static load. Then if power hop still occurs, use the following procedure.

1. If driving faster than 8.8 km/h (5.5 mph) or if operating on soft soils, increase the rear pressures in 0.4 bar (6 psi) increments until power hop is controlled. In certain field conditions, it may be necessary to go 83 to 124 kPa (12 to 18 psi) above the Rated Deflection Pressure before power hop is controlled.. Use differential lock on slopes.
2. If driving less than 8.8 km/h (5.5 mph) or operating on very firm soils where the lugs get minimal penetration, raise the front inflation pressures in 0.4 bar (6 psi) increments as described above. Do not use this procedure when operating on steep hillsides. Instead, use the previous procedure.

Usually *either* of the above procedures will control power hop. The major exception is that only the second procedure works when the soil is firm.

Power Hop in Tractors with Front Suspensions

RJT—The uncertainties of dealing with power hop assisted in driving the development of alternate traction approaches from industry, such as rubber belt track machines and suspension systems for rubber tire tractors. While not the only impetus, each system has at various times been advertised as a method of dealing with the problem.

JCW—Front suspensions on MFWD tractors are a relatively new innovation, but the number of tractors sold with suspension systems is increasing rapidly throughout the world. The suspension improves ride quality both on the road at high speeds and in rough field conditions. It has the added benefit of significantly reducing the sensitivity of the tractor to power hop. Power hop can still occur with suspended front axle tractors, but it is not nearly as likely as with unsuspended axle MFWD tractors. The suspension reduces the need to be as careful in ballasting and using the correct inflation pressures so that the tractor is more "forgiving" with regard to power hop incidence and control.

RJT—During the summer of 2002, AFMRC ran a series of tests to evaluate the effect of a front suspension on the performance and ride of MFWD tractors, equipped with various combinations of front and rear radial single and dual tires. Power hop became a significant issue during these tests, and provided an opportunity to learn a number of things about hop on vehicles with front suspension.

Tests showed that power hop could be excited with or without the front suspension but that the hop frequency and motion was affected by the suspension. With the test vehicle, it was possible to switch the front suspension on and off, making it easy to quickly observe the effect of the suspension on the various setups. With the front suspension off, the tractor behaved as a normal MFWD tractor—it could go into a vigorous and typical MFWD hop. The same fixes that would control hop on a normal MFWD (liquid and higher inflation pressure in the front tires) would control this hop. When the front suspension was re-enabled on the "hop fixed" tractor, it would still go into a hop mode, depending on the speed and pull, but at a somewhat lower frequency and amplitude than that of the unsuspended tractor. Removing the hop fix by lowering the front pressures and removing the liquid in the front tires did not affect this hop. Because the front tires were effectively "outside" the suspended system and thus isolated from the hopping tractor, any changes made to them had no effect on the hop. With the front suspension operating, the hop appeared to be driven from the rear tires. In extreme cases, the front suspension did exactly the opposite of what it was designed to do. The tractor would oscillate wildly in a power hop mode, and the front suspension would work in reverse to remove that motion entirely from the front wheels so that they alone were completely stable. An example of this motion is included in the video on the DVD.

To control the suspended tractor hop, it was necessary to find ways to influence parameters "inboard" of the suspension system. Two field adjustments were found to help. Adding suspended front weight to the tractor (by adding cast weights on the front weight bar) and effectively shifting the center of gravity of the suspended part forward reduced the tendency to hop somewhat, but would not remove it completely throughout the effective working range. Raising the inflation pressure in the rear tires was effective in controlling the hop throughout the working range, with or without the change in front weight. Moving to larger front and rear tires in an effort to lower the allowable correct pressures and thus reduce the overall stiffness made power hop occur more easily and the resultant hop was more difficult to control.

AFMRC also had a short experience with a fully suspended MFWD tractor. In a limited amount of testing in a soft soil condition, the tractor showed no tendency to power hop. It was possible to put the tractor into a whole vehicle resonance mode by running at an angle across a uniformly ridged field and adjusting both the ground speed and path angle (excitation frequency) until the tractor frame and cab began to resonate, with the suspension behaving somewhat like the front suspension discussed above (wheels stable, tractor bouncing), but it was not a true power hop.

JCW—It is important to emphasize that the mathematical model developed herein does not apply to tractors with suspensions. Models could be, and should be, developed that incorporate the additional degrees of freedom, suspended masses, and suspension control system characteristics. The suspension systems are not just simple passive spring and shock absorber arrangements, so the analysis will be considerably more involved than that for unsuspended tractors.

There has been a limited amount of experimentation with a 4WD tractor with a suspended front axle. While it was very successful in suppressing power hop in hop-prone soils, the expense of adding the suspension was deemed too much to be viable at the time the experiment was concluded. However, as power levels continue to increase, suspended 4WD tractors may ultimately be accepted in the marketplace just as was the case with MFWD tractors.

RJT—Examples of another design in the marketplace are the fully suspended 4WD tractors such as the JCB Fastrac and similar models. In the past, these have been available at relatively low power levels, targeted at a transport market along with a limited field work market, and little has been said or published about power hop related issues on them. As high end models now approach the 220 kW (300 hp) power level, there may yet be power hop applicable information to learn from these suspension systems as well.

Future Research and Development Recommendations

Soil-Tire Interaction Models

JCW—There is essentially no information available on how to represent the stiffness and damping properties of the tire-soil combination either while the tire is simply rolling or when it is delivering traction. Some very limited experiments on the influence of the soil on combined soil/tire stiffness and damping have been conducted by Prof. Dr.-Ing. H. Göhlich and his students at the Technical University of Berlin, Institute of Agricultural Engineering (see Meyer et al., 1988). Ideally, what is needed is a portable system capable of accepting very large tires (both current and future) that could be transported to any place in the world for testing on a variety of soils. Accommodation of dual tires is most likely necessary since the soil under both tires will simultaneously influence the combined stiffness and damping. The system must also be able to accommodate smaller diameter front tires for MFWD tractors. Possibly a second machine for smaller diameter tires would be needed to provide the sensitivity required. Tire manufacturers typically have trailers like this that can accommodate over-the-road truck tires, but nothing approaching the size required for tractor tires.

The output of these experiments needs to be mathematical representations of stiffness, damping, and traction characteristics simultaneously parameterized on load, torque, inflation pressures, and key soil characteristics. It is obvious that the initial development and the on-going support of such a system would require a substantial amount of resources and long-term commitments. This is probably the reason no such system exists today. One possible approach to consider is a consortium of tractor manufacturers, tire manufacturers, and research organizations.

If such results were available, more accurate predictions of power hop could be made, but that would only be one basic application. Of much more importance, future detailed mathematical models of tractors to simulate performance characteristics, ride characteristics, and stability will require such detailed tire-soil interaction models to achieve the accuracy of results that will be required. Further advances in finite and discrete element based methods may provide the basis for these models.

Tire Changes

RJT—Current radial tire designs are recognized as one of the best methods to engage soil and deliver tractive power into it. Unfortunately they also contribute significantly to the problem of power hop through their present tire stiffness and damping ratios. Work has been done with bias belted and other tire sidewall designs, and with rubber belts in efforts to develop devices that deliver power to the ground but have stiffness and damping ratios that do not allow power hop. What is needed are modifications to tire design and construction that add appropriate power hop control stiffness and damping into the structure while maintaining ground contact profiles that allow maximum effectiveness in power transfer. This could result in tires with sidewalls or cross sections quite different in design and construction from what we are familiar with today.

Power Hop Modeling Extensions

Rubber tires exhibit a variety of potential spring actions. The various efforts at modeling power hop with tires have typically concentrated on describing and analyzing one or another of these possible springs along with the mass of the system the spring suspends. Certainly the most effective model to date uses the vertical spring and the masses of the system. It would be appropriate to investigate the addition to this vertical spring mass model of a representation of tangential and/or torsional spring forces and associated masses. This may enable a greater understanding of some of the current model versus field anomalies and suggest possible less fuel inefficient methods of controlling power hop.

JCW—The linearized mathematical model described in the Appendix has been used with the root locus stability approach mainly to predict the effect of inflation pressure (and hence vertical stiffness) and weight distribution on the potential for the development of hop. Further work using this approach could identify the sensitivity of hop development to other model parameters such as vertical damping and thus provide a broader understanding of the relative importance of these parameters for hop control. As mentioned, the basic approach used in the linearized model can be incorporated into a multibody dynamics model with appropriate attention to numerical integration error control for time domain simulation. Such an approach allows nonlinear effects such as the tires losing ground contact to be studied if desired. In addition, more detailed tire-soil modeling may indicate the use of finite and/or discrete element based methods.

Practical On-Board Inflation Systems

Once a tractor is set up properly, power hop control of unsuspended tractors basically amounts to adjustment of inflation pressures. It would be very convenient to be able to do this manually from the tractor seat or by automatic control. In addition to power hop control adjustments, the ability to quickly raise or lower the inflation pressures of the rear tires to accommodate heavy 3-point hitch implements for road transport is obviously highly desirable.

On-board inflation systems are routinely used for logging trucks and certain military trucks. They are also available as an accessory for agricultural tractors with no more than four tires. However, for tractors with dual or triple front and rear tires, there are challenges in designing such systems to minimize the amount of time required to either inflate or deflate.

Suspension System Tuning

An attractive possibility for enhancing power hop control of tractors with front suspension systems is to provide the capability for tuning the suspension stiffness and damping characteristics. This might simply be a knob that the operator adjusts manually or a more sophisticated automatic control system that makes the adjustments based on sensed acceleration data.

For this suspension approach as well as for the on-board inflation system described above, the fundamental concept is that "adjustments" are made to accommodate changes in soil and/or operating conditions. For power hop control, a single "setting" will not necessarily work for all soil and operating conditions. However, this is not so unusual in agricultural machines. Consider, for example, a modern combine with its myriad of controls to either manually or automatically fine-tune the separator settings to attain minimum crop loss. The same can be contemplated for tractors of the future.

Conclusions

Power hop has been a matter of interest in MFWD and 4WD tractors for over half a century. At this time, the understanding of how to control it is basically complete. To a great extent, this is the result of extensive collaborative efforts with tire company engineers who provided a key ingredient—the new load-inflation pressure tables with lower inflation pressure limits. Although the lower inflation pressures for radial tires were essential for power hop control, they are having far broader implications for farmers worldwide who now are reaping the benefits of increased traction, improved field productivity and fuel efficiency, reduced soil compaction, and smoother-riding tractors.

It has been shown conclusively herein that power hop is an example of a self-excited vibration. Based on the generality of the mathematical model and the results it reveals, it is reasonable to assert that the self-excited vibration called power hop in tractors can occur in other vehicles towing draft loads as well. The model shows it is an inherent characteristic of vehicles with tires generating traction to tow draft loads. Any traction formulation based on a "friction-like" concept will ultimately lead to an unsymmetric stiffness matrix, and, thus, to the possibility of a self-excited system. Of course, in vehicles with suspension systems, the details will be different, but in a fundamental sense, the mere process of generating traction with tires creates the possibility for the vehicle to become self-excited given the right circumstances.

Because self-excited vibrations are an unusual and uncommon phenomenon, they are often misunderstood by those not familiar with them. One common characteristic of self-excited systems is that there is typically no single source or element that leads to the instability. It is the interaction of all of the elements of the system subjected to a steady input (speed, load, or power) which can lead to the large amplitude motions. By adjusting appropriate parameters, self-excited systems can be "tuned" away from particular instabilities, but the possibility of self-excitation cannot be completely eliminated without fundamentally altering the construction of the system itself.

For example, consider the simple front casters on a grocery cart, a system that can exhibit self-excited vibrations. If the cart is pushed at a steady forward speed, normally nothing happens, but at a certain "critical speed," one or both casters will begin to shimmy. By altering the caster trail angle, the critical speed can be either raised or lowered, but there will always be a critical speed at which shimmying will start. If the caster angle is designed so that the critical speed is higher than could be reached by any human pushing the cart, then all users of the cart will think it is just fine and not pay any attention to the casters at all. To them the system appears completely stable even though it would become unstable at some speed higher than the user could achieve.

The same applies with regard to power hop. Most tractors do not experience power hop, but it is always lurking as a possibility given the right soil and operating conditions. Its occurrence is partially dependent on parameters related to the tractor and tires which can be controlled by humans, but also is highly dependent on soil conditions beyond the control of humans. Not only that, but soil moisture and texture conditions can change from one field to the next and from one type of tillage operation to the next. Thus, a key part of power hop instability is only controlled by Mother Nature, and she is fickle. This is a source of frustration for farmers who complain that their tractor was doing just fine in one field, but then power hopped in another. One combination of inflation pressures will not necessarily work everywhere.

We now know how to make the adjustments to control power hop, but for the most part there is no single adjustment that will work for all situations. Furthermore, it requires stopping the tractor to make inflation pressure or ballast adjustments. Hopefully, in the future, we can make life simpler for the tractor operator. Two possibilities are on-board inflation systems and "tunable" front suspension systems. Either could be manually or automatically controlled.

RJT—While we understand the basic principles, and we know how to make adjustments to control power hop, there are still things that we do not fully understand—the mysteries, as it were. Examples include the effects of increased ground speed on effective power hop control, the demonstrated capability of pulling through and beyond the power hop regime, and the operating condition related variability of our presently understood control methods. The very fact that we propose something that adversely affects tractor efficiency as the most reliable solution to power hop suggests that we still have work to do. Yes, we should make it

easier to control power hop using what we now understand, but hopefully we will also seek solutions that remove the capability for the problem to occur while improving the capability of traction devices to do what we expect of them. The ultimate solution would be a "factory fix" design such that, as delivered from the factory, no power hop could occur and no customer interaction would be required.

Acknowledgements

JCW—Bernard Romig, David Smith, Nicolae Orlandea, and Tibor (Ted) Berenyi, former colleagues of the first author when at the Deere & Company Technical Center, Moline, Ilinois, all made significant contributions to the research on power hop. Edmund Wegscheid, also of the Deere & Company Technical Center, developed the data acquisition software and was the first test engineer involved in the power hop experiments of 1989 and 1990. Later in 1990 and 1991, Vern Hovenga of the Technical Center aided with the instrumentation and data collection efforts. Dennis A. Bowman of the John Deere Waterloo Product Engineering Center designed the remote tractor operator's platform and control system. He and Larry Anderson of the Product Test and Evaluation Group at the Waterloo Product Engineering Center arranged test equipment and locations, and both participated directly in much of the test work. Frank Zoz of the same Group participated in later tests as well. Kenneth Brodbeck of Bridgestone/Firestone first demonstrated a practical approach for conducting repeatable power hop tests on dry soil, and he participated extensively in the field tests. Loran Lopp of the Goodyear Tire and Rubber Company led the effort to revise the tire load-inflation pressure tables downward and make them a Tire and Rim Association standard. The support of engineering and marketing personnel from Bridgestone/Firestone, Goodyear, and Pirelli-Armstrong (now Titan) in technical interchanges as well as in laboratory and field testing was key to bringing about the revised load-inflation pressure tables. The efforts of Larry Scura, Richard Michael, and David Olson of the John Deere Waterloo Product Engineering Center who produced some of the earliest analytical studies of power hop are also gratefully acknowledged.

RJT—Ministers, managers, and engineers of the Alberta Provincial Agriculture Department supported the project through all its various stages, providing manpower and funding for the common good of understanding and solving the problem of power hop. AFMRC/Agtech staff over the years showed patience, resolve, and innovation as they developed and provided the test capabilities needed as (and sometimes before) the engineers even learned they needed them. Patient farmers throughout Alberta, Montana, California, and Texas provided field access, chisel plows, and occasionally tractors and drivers for the sake of the tests, with never a complaint and always an interest. Lynn Stilger, Greg Clouse, and Tom Welch, professors and instructors at Montana State University–Northern assisted with testing and site and vehicle location throughout the various phases. Larry Haugen of Case-IH, Allen Rider of New Holland, Dave Janzen, Jeff Moore, and Mel Busch of Caterpillar (who didn't even have a hop problem), Ken Brodbeck of Firestone, and Dave Weed and Drew Shorter of Goodyear all assisted in providing and supporting various pieces of equipment and products needed and used in the tests. Frank Zoz of Deere, Lon Shell of Southwest Texas State University, and Lou Leviticus and Leonard Bashford of the Nebraska Tractor Test Lab assisted with commentary, opinions, and analysis as the test information and knowledge grew.

JCW and **RJT**—The research on power hop that led to this publication and Lecture would not have been possible without the significant efforts of these men. Their contributions are sincerely appreciated.

References

Abu-Hamdeh, N. H., T. G. Carpenter, R. K. Wood, and R. G. Holmes. 1997. Soil compaction of four-wheel drive tractors and tracked tractors under various draft loads. SAE Paper No. 952098. Also in *Belt and Tire Traction in Agricultural Vehicles,* 45-63.Warrendale, Pa.: Society of Automotive Engineers, Inc.

Al-Deen, H. H., J. B. Liljedahl, and W. Soedel. 1977. Jumping phenomena of tractors. ASAE Paper No. 771524. St. Joseph, Mich.: ASAE.

Al-Deen, H. H., J. B. Liljedahl, and W. Soedel. 1978. Jumping phenomena of tractors. In *Proc. of the 6th International Congress of the ISTVS,* 403-436.

ANSI/ASAE. 2003 (Dec). S296.5: General Terminology for Traction of Agricultural Traction and Transport Devices and Vehicles. St. Joseph, Mich.: ASABE.

Bailey, A. C., R. L. Raper, E. C. Burt, T. R. Way, and C. E. Johnson. 1996. Soil stresses under a tractor tire at various loads and inflation pressures. *J. Terramechanics* 33(1): 1-11.

Billah, K. Y., and R. H. Scanlan. 1991. Resonance, Tacoma Narrows Bridge failure, and undergraduate physics textbooks. *American J. Phys*. 59(2): 118-124. Available at: www.ketchum.org/wind.html.

Bolotin, V. V. 1963. *Non-Conservative Problems of the Theory of Elastic Stability*. New York, N.Y.: Macmillan.

Bolotin, V. V. 1964. *The Dynamic Stability of Elastic Systems*. San Francisco, Calif.: Holden-Day.

Brenninger, M. M. 2002. Stufenlos geregelter Allradantrieb für Traktoren (Continuously variable control of four-wheel drive for tractors). PhD thesis. TU München 2002. Fortschritt-Berichte VDI Series 12, No. 256. Düsseldorf, Germany: VDI-Verlag 2003.

Brixius, W. W. (a.k.a. C. M. Hollis). 1987. Traction prediction equations for bias-ply tires. ASAE Paper No. 871622. St. Joseph, Mich.: ASAE.

Brodbeck, K. N. 1989. MFWD power hop test results. Firestone Tire & Rubber Company presentation given at the John Deere Product Engineering Center, Waterloo, Iowa.

Brodbeck, K. N. 2004. Choosing the right tire. *ASAE Distinguished Lecture Series, Tractor Design No. 28*. St. Joseph, Mich.: ASAE. Available at: asae.frymulti.com/data/pdf/6/crt2004/Lecture28.pdf.

Burt, E. C., A. C. Bailey, T. R. Way, R. K. Wood, C. E. Johnson, and D. C. Erbach. 1997. Soil-tire interface pressures and deformation as related to traction instability. In *Proc. of the 3rd International Conference on Soil Dynamics*, 59-66. Haifa, Israel: Technion-IIT.

Den Hartog, J. P. 1956. *Mechanical Vibrations*. New York, N.Y.: McGraw-Hill.

Dessèvre, D. 2005. Experimental characterization and numerical modeling of the "power hop" phenomenon. VDI-Berichte Nr. 1895, 125-130. Düsseldorf, Germany: VDI-Verlag.

Erickson, L. R., W. E. Larsen, and S. J. Rust. 1982. Four-wheel drive tractor axle and drawbar horsepower: Field evaluation and analysis. ASAE Paper No. 821057. St. Joseph, Mich.: ASAE.

Erickson, L. R., and W. E. Larsen. 1983. Four-wheel drive tractor field performance. *Trans. ASAE* 26(5): 1346-1351.

Feldman, B. J., 2003. What to say about the Tacoma Narrows Bridge to your introductory physics class. *The Physics Teacher* 41(2). Available at: www.umsl.edu/~feldmanb/pdfs/tacoma_bridge.pdf.

Garciano, L. O., R. Torisu, J. Takeda, and K. Sakai. 2002. Repeated jump, impact and bouncing phenomenon of farm tractors from the nonlinear dynamics perspective. In *Int'l. Proc. of the ASAE Conference on Automation Technology for Off-Road Equipment*, 270-278. St. Joseph, Mich.: ASAE. Available at: asae.frymulti.com/ request.asp?search=1&JID=1&AID=10016&CID=atoe2002&v=&i=&T=2.

Goering, C. E., M. L. Stone, D. W. Smith, and P. K. Turnquist. 2003. *Off-Road Vehicle Engineering Principles*. St. Joseph, Mich.: ASAE. Available at: asae.frymulti.com/textbook.asp?confid=orvp2003.

Grad, K. 1996. Zur Steuerung und Regelung des Allradantriebs bei Traktoren (Control of four-wheel drive for tractors). PhD thesis. TU, München 1996. Fortschritt-Berichte VDI Series 14, No. 82. Düsseldorf, Germany: VDI-Verlag 1997.

Gu, Y., and R. L. Kushwaha. 1992. Dynamic load distribution and tractive performance of a model tractor. ASAE Paper No. 921018. St. Joseph, Mich.: ASAE.

Harris, C. 2002. *Harris' Shock and Vibration Handbook*. 5th ed. McGraw-Hill.

Kirby, E. F., J. B. Liljedahl, and D. W. Smith. 1968. Investigation of tractor jumping when pulling. ASAE Paper No. 68132. St. Joseph, Mich.: ASAE.

Kirby, J. M., and F. M. Zoz. 1997a. Stress under belts and radial tires with various weight distributions. SAE Paper No. 972733. Also in *Belt and Tire Traction in Agricultural Vehicles,* 101-108. Warrendale, Pa.: Society of Automotive Engineers, Inc.

Kirby, J. M., S. Mockler, and F. M. Zoz. 1997b. Influences of varying axle load and tyre pressure on soil stresses and resulting compaction. SAE Paper No. 952096. Also in *Belt and Tire Traction in Agricultural Vehicles,* 21-30. Warrendale, Pa.: Society of Automotive Engineers, Inc.

Kutzbach, H. D., and H. Schrogl. 1987. Dynamic behavior of rolling tractor tires. In *Proc. of the 9th International ISTVS Conference*, 457-464.

Lancas, K. P., S. K. Upadhyaya, and M. Sime. 1995a. Traction and soil compaction due to low/correct inflation pressure for radial ply tractor tires. In *Proc. of the 5th North American ISTVS Conference/Workshop*, 11-21.

Lancas, K. P., A. G. Santos Filho, and S. K. Upadhyaya. 1995b. Implication of using low/correct inflation pressure for radial ply tractor tires. Agricultural Equipment Technology Conference Paper No. 95056. St. Joseph, Mich.: ASAE.

Lancas, K. P., S. K. Upadhyaya, M. Sime, and S. Shafii. 1996. Overinflated tractor tires waste fuel, reduce productivity. *California Agric.* 50(2): 28-31.

Lancas, K. P., A. G. Santos Filho, and S. K. Upadhyaya. 1997. Performance of low/correct pressure radial ply tires. ASAE Paper No. 971026. St. Joseph, Mich.: ASAE.

Liljedahl, J. B. 1974. Tractor tire vibrations. *Agricultural Engineering* August: 19. St. Joseph, Mich.: ASAE.

Lopp, L. 1992. Optimum tractor tire performance, ASAE Paper No. 921587. St. Joseph, Mich.: ASAE.

Meyer, W., T. Siefkes, and H. Göhlich. 1988. Dynamic properties of agricultural tires. In *Proc. of the AG-ENG Meeting—1988*, 146-151.

MSC Software. 2007. ADAMS (Automated Dynamic Analysis of Mechanical Systems). Ann Arbor, Mich. Available at: www.mscsoftware.com.

Meirovitch, L. 1967. *Analytical Methods in Vibrations*. New York, N.Y.: Macmillan.

Orlandea, N. V., 1973. *Node Analogous, Sparsity Oriented Methods for Simulation of Mechanical Dynamic Systems*, PhD thesis. Ann Arbor, Mich.: The University of Michigan.

Orlandea, N. V., M. A. Chace, and D. A. Calahan. 1977. A sparsity-oriented approach to the dynamic analysis and design of mechanical systems: Part 1. *Trans. ASME, J. Eng. for Industry* 99(3): 773-779.

Orlandea, N. V. 1988. Simulation of 4WD tractor hop on soft soils. ASAE Paper No. 883030. St. Joseph, Mich.: ASAE.

Pacejka, H. B. 2005. *Tire and Vehicle Dynamics,* 25-30. 2nd ed. Warrendale, Pa.: Society of Automotive Engineers.

Panovko, Y. G., and I. I. Gubanova. 1965. *Stability and Oscillations of Elastic Systems*. New York, N.Y.: Consultants Bureau.

Raper, R. L., A. C. Bailey, E. C. Burt, T. R. Way, and P. Liberati. 1995a. Inflation pressure and dynamic load effects on soil deformation and soil-tire interface stresses. *Trans. ASAE* 37(3): 763-768.

Raper, R. L., A. C. Bailey, E. C. Burt, T. R. Way, and P. Liberati. 1995b. The effects of reduced inflation pressure on soil-tire interface stresses and soil strength. *J. Terramechanics* 32(1): 43-51.

Renius, K. T., and R. Resch. 2005. Continuously variable tractor transmissions. *ASAE Distinguished Lecture Series, Tractor Design No. 29*. St. Joseph, Mich.: ASABE. Available at: asae.frymulti.com/data/pdf/6/cvtt2005/ lectureseries29rev.pdf.

Rocard, Y. 1957. *Dynamic Instability*. Crosby Lockwood & Son, London.

Rocard, Y. 1960. *General Dynamics of Vibrations*. New York, N.Y.: Frederick Ungar.

Sakai, K., A. J. Bukta, A. Sasao, and S. Shibusawa. 1998. Application of OGY control method on chaotic vibrations for tractor-implement systems: Nonlinear dynamics and chaos on bouncing tractor. ASAE Paper No. 981086. St. Joseph, Mich.: ASAE.

Sakai, K., A. Sasao, and S. Shibusawa. 1999. Nonlinear dynamics of bouncing and power hop. ASAE Paper No. 991066. St. Joseph, Mich.: ASAE.

Scanlan, R. H., and R. Rosenbaum. 1968. *Aircraft Vibration and Flutter*. New York, N.Y.: Dover Publications.

Schlosser, J. F., L. Márquez, and P. Linares. 2001. Development of methodology to predict power hop due to axle ratio differences of front wheel assist tractors. *Cienc. Rural*. 31(6) Santa Maria Nov/Dec 2001. Available at: www.scielo.br/scielo.php?script=sci_arttext&pid=S0103-84782001000600011.

Sohoni, V. N., and D. W. Smith. 1995. Stability analysis of a 4-wheel drive tractor using ADAMS. In *Technical Note—Proc. of 1995 ADAMS Users Conference*, Ann Arbor, Mich. Available at: www.mscsoftware.com/ support/library/conf/adams/na/1995/UC950029.PDF.

Smith, D. W., T. A. Berenyi, R. A. Light, N. V. Orlandea, B. E. Romig, J. C. Wiley, N. Portillo, S. E. O'Brien, and D. J. Hertema. 1982. Automated simulation and display of mechanism and vehicle dynamics. ASAE Paper No. 825019. St. Joseph, Mich.: ASAE.

Taylor, R. K, and M. D. Schrock. 1996. Influence of liquid ballast on the static stiffness of agricultural traction tires. SAE Paper No. 961780. Warrendale, Pa.: SAE. Available at: www.sae.org/technical/papers/961780.

Tire and Rim (a). Any year. *Year Book*. Copley, Ohio: The Tire and Rim Association, Inc. Available at: www.us-tra.org.

Tire and Rim (b). Any year. *Engineering Design Information for Ground Vehicle Tires*. Copley, Ohio: The Tire and Rim Association, Inc. Available at: www.us-tra.org.

Turner, R. J. 1993a. A simple system for determining tractive performance in the field. ASAE Paper No. 931574. St. Joseph, Mich.: ASAE. Available at: www1.agric.gov.ab.ca/$department/deptdocs.nsf/all/eng9927.

Turner, R. J. 1993b. Single, dual and triple tires and rubber belt tracks in prairie soil conditions. ASAE Paper No. 931516. St. Joseph, Mich.: ASAE. Available at: www1.agric.gov.ab.ca/$Department/deptdocs.nsf/all/eng8282.

Turner, R. J. 1995. Comparison of two and four track machines to rubber tire tractors in prairie soil conditions. SAE Paper No. 952097. Warrendale, Pa.: SAE. Available at: www1.agric.gov.ab.ca/$Department/deptdocs.nsf/all/eng8073.

Turner, R. J., L. R. Shell, and F. M. Zoz. 1997. Field performance of rubber belted and MFWD tractors in Southern Alberta soils. SAE Paper No. 972730. Also in *Belt and Tire Traction in Agricultural Vehicles*, 75-85. Warrendale, Pa.: Society of Automotive Engineers, Inc. Available at: www1.agric.gov.ab.ca/$Department/deptdocs.nsf/all/eng8133.

Turner, R. J., and R. L. Raper. 2001. Soil stress residuals as indicators of soil compaction. ASAE Paper No. 011063. St. Joseph, Mich.: ASAE. Available at: www1.agric.gov.ab.ca/$Department/deptdocs.nsf/all/eng8299.

Upadhyaya, S., and K. P. Lancas. 1994. How to get the most from radial ply tractor tires: A guide to select the correct inflation pressure. Davis, Calif.: Biological and Agricultural Engineering Department, University of California. Available at: www.energy.ca.gov/process/pubs/trac.pdf.

Volfson, B. P., and M. Estrin. 1983. The slip-stick phenomenon in vehicle ride simulaton. *Computers in Engineering 1983* (1): 229-235. New York, N.Y.: ASME.

Volfson, B. P. 1986. Simulation of off-road vehicle hop phenomena: Part 1. ASME Winter Annual Meeting. New York, N.Y.: ASME.

Volfson, B. P. 1988. Simulation of off-road vehicle hop phenomenon: Part 2. SAE Paper No. 885129. SAE, Warrendale, Pa.: Society of Automotive Engineers.

Volfson, B. P. 1999. Comparison of two simulation models of tire-surface interaction. In *Proc. 13th Intl. Conf. of the ISTVS*, 311-318.

Wiley, J. C., B. E. Romig, N. Orlandea, T. A. Berenyi, and D. W. Smith. 1979. Automated simulation and display of mechanism and vehicle behavior. In *Proc.of the Fifth World Congress on Theory of Machines and Mechanisms,* 680-683.

Wiley, J. C., B. E. Romig, L. V. Anderson, and F. M. Zoz. 1992. Optimizing dynamic stability and performance of tractors with radial tires. ASAE Paper No. 921586. St. Joseph, Mich.: ASAE.

Wiley, J. C. 1995. Down to earth breakthrough. *Resource* (September 1995) St. Joseph, Mich.: ASAE.

Wolfram, 2007. *Mathematica: A System for Doing Mathematics by Computer*. Champaign, Ill.: Wolfram Research, Inc. Available at: www.wolfram.com.

Zhuang, J. and Q. Wang. 1990. A simulation of the unstable state tractive dynamics of a 4WD vehicle on sand. In *Proc. of the 10th International Conference of the ISTVS*, 425-435.

Ziegler, H. 1968. *Principles of Structural Stability*. Waltham, Mass.: Ginn Blaisdell.

Zoz, F. M., and W. W. Brixius (a.k.a. C. M. Hollis). 1979. Traction prediction for agricultural tires on concrete. ASAE Paper No. 791046. St. Joseph, Mich.: ASAE.

Zoz, F. M., and R. J. Turner. 1994. Effect of correct pressure on tractive efficiency of radial-ply tires. ASAE Paper No. 941051. St. Joseph, Mich.: ASAE. Available at: www1.agric.gov.ab.ca/$Department/deptdocs.nsf/all/eng8081.

Zoz, F. M. 1997. Belt and tire tractive performance. SAE Paper No. 972731. Also in *Belt and Tire Traction in Agricultural Vehicles*. Society of Automotive Engineers SP-1291. Warrendale, Pa.: SAE. Available at: filebox.vt.edu/users/rgrisso/Dist_Lecture/REFERENCES/Belt_and_Tire_Tractive_Performance.pdf.

Zoz, F. M., R. J. Turner, and L. R. Shell. 2002. Power delivery efficiency: A valid measure of belt and tire tractor performance. *Trans. ASAE* 45(3): 509-518. Available at: asae.frymulti.com/request.asp?search=1&JID=3&AID=8817&CID=t2002&v=45&i=3&T=2.

Zoz, F. M., and R. D. Grisso. 2003. Traction and tractor performance. *ASAE Distinguished Lecture Series, Tractor Design No. 27*. ASAE, St. Joseph, Mich.: ASAE. Available at: asae.frymulti.com/request.asp?search=1&JID=6&AID=16586&CID=ttp2003&v=&i=&T=2.

Zoz, F. M. 2007. The cause of power hop. ASABE Paper No. 071110. St. Joseph, Mich.: ASABE. Available at: asae.frymulti.com/request.asp?search=1&JID=5&AID=22913&CID=min2007&v=&i=&T=1.

Appendix: Development of the Mathematical Model

Jack C. Wiley (retired) and David W. Smith (retired)
Deere & Company Technology Center, Moline, Illinois

The System Model: Basic Assumptions

The system model considers the motions of a four-wheel-drive tractor in its plane of forward motion. The tractor has neither a front nor a rear suspension system other than the effects of the tires. Either a row crop MFWD tractor configuration or an articulated 4WD tractor configuration can be represented by appropriate choices of parameters. The tractor is pulling a draft load and moving at a constant velocity V. Three degrees of freedom are all measured from the operating point position and orientation as illustrated in Figure A-1.

These three degrees of freedom are:

x, the fore-aft translational motion (surge) of the center of gravity with respect to a coordinate system translating forward at the constant velocity V corresponding to the operating point forward velocity. With respect to the ground, the location of the center of gravity is given by $X = Vt + x$ where t is time. Thus a positive x displacement is in the direction of forward motion.

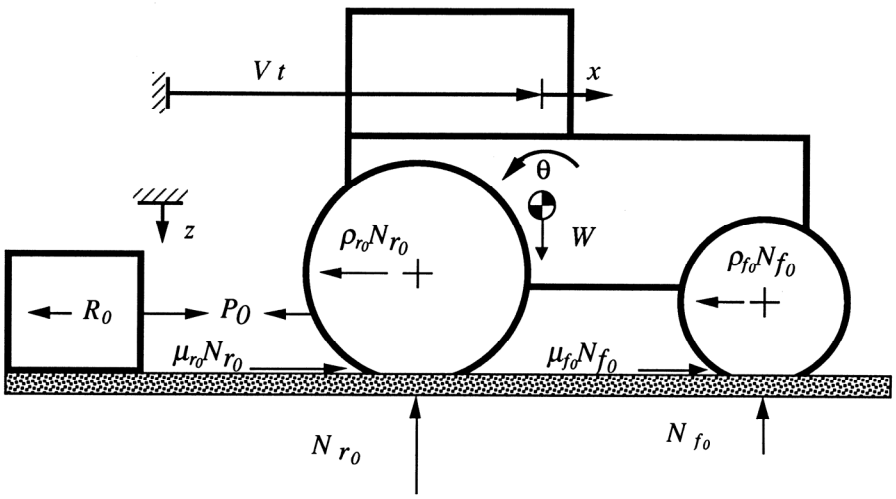

Figure A-1. Operating point free-body diagram.

z, the vertical translational motion of the center of gravity with respect to a datum located at the operating point height of the center of gravity above the ground surface. A positive z displacement is downward.

θ, the pitch rotational motion of the vehicle with a counterclockwise displacement being considered positive. This pitch motion is measured from the operating point pitch orientation of the vehicle.

Thus, all three degrees of freedom have zero displacements and velocities at the operating point position.

The choice of the degrees of freedom here is significant in that additional degrees of freedom could have been considered. It has been postulated by some that power hop might have a power train related cause such as engine torque variations created by the engine governor, torsional oscillations in the power train and/or torsional oscillations in the drive tires. If the power hop instability is directly related to these degrees of freedom and they are not considered, the model will not be capable of predicting power hop. However, as the subsequent development shows, the model with just these three degrees of freedom does predict power hop.

The next step in the development of the model is to create a free body diagram of the vehicle including all the external forces. In doing so, the drive wheel mechanics used in Chapters 13 and 14 of Goering et al. (2003) are used as illustrated in Figure A-2. Note two alternative but dynamically equivalent force systems are depicted. The force system on the left has an applied axle torque Q acting to drive the wheel forward leading to the creation of a gross tractive force $F = Q/r$ acting at a distance r (the wheel's rolling radius) from the center of the wheel which seeks to propel the vehicle forward. A motion resistance force TF also acting at the distance r opposes the forward motion as does the horizontal reaction force acting on the wheel from the vehicle chassis. At equilibrium, this reaction force must equal the sum of the other two horizontal forces or $F - TF = Q/r - TF$. This reaction force can be considered the net tractive force acting on the wheel and, together with the net tractive forces on the other drive wheels, provides the force required to move the vehicle forward under drawbar loading. The vertical force exerted by the chassis on the drive wheel is denoted as V which here includes the weight of the wheel. From equilibrium, the vertical force on the wheel from the ground (N) must equal V. Since the gross tractive force F was defined as Q/r, moment equilibrium requires that N must be translated forward a distance $e = (TF/N)\, r$. This relation follows from summing moments about the center of the wheel:

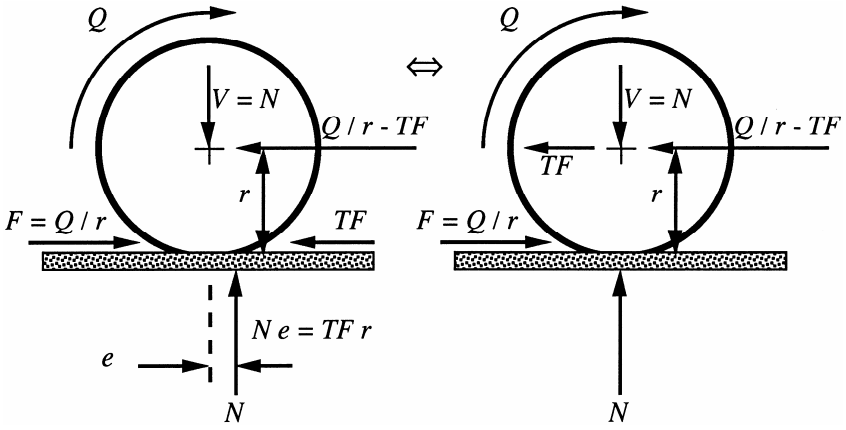

Figure A-2.Drive wheel free-body diagrams.

$$Q - F\,r + TF\,r - N\,e = 0$$

$$Q - (Q/r)\,r + TF\,r - N\,e = 0$$

$$Q - Q + TF\,r - N\,e = 0$$

$$TF\,r = N\,e \text{ or } e = (TF/N)\,r\,.$$

The free body diagram on the right side of Figure A-2 is dynamically equivalent to the one on the left but has the advantage of having the vertical ground reaction acting at the center of the wheel. The only changes from the free body diagram on the left is to move the motion resistance force vertically up to the wheel center while the vertical ground reaction is shifted horizontally backwards to act through the wheel center. With these moves, both TF and N now have a zero moment arm about the wheel center. But this situation is equivalent to that of the free body diagram on the left since from above $TF\,r - N\,e = 0$ or the sum of the moments of these two forces is always zero.

Defining the gross tractive coefficient $\mu = F/N = (Q/r)/N$ and the motion resistance coefficient $\rho = TF/N$, one can write $F = \mu N$ and $TF = \rho N$. Although the assumption of a friction-like relationship between the tractive and motion resistance forces and the normal force acting on a wheel is a common one, it should still be recognized as an assumption. As will be seen later, this assumption does directly influence the form of the linearized equations of motion and hence the prediction of power hop.

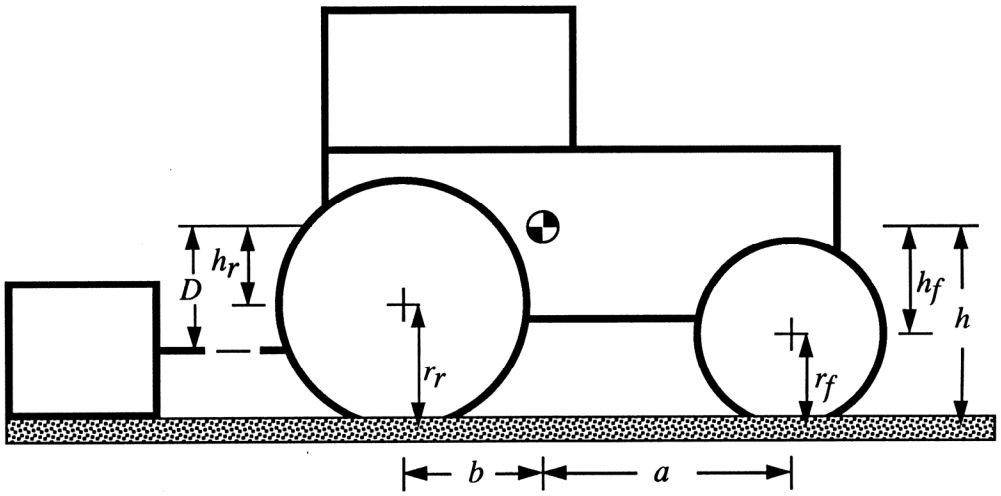

Figure A-3. Basic system geometry parameters.

This method of representing the gross tractive and motion resistance forces is used in the free body diagram shown in Figure A-1 where all the forces shown are those at the operating point as denoted by the subscript *o*. The subscripts *r* and *f* are used to denote a rear and a front drive wheel respectively. Note the alternative method of representing the forces on the drive wheels is used with the motion resistance forces acting at the wheel center height and the vertical ground reaction forces passing through the wheel centers. A horizontal drawbar pull force is exerted on the vehicle at the drawbar location from an implement depicted by the box on the left. Note the drawbar force is assumed to be horizontal with the vehicle operating on a flat surface (zero slope). An inclined drawbar force and operation on a slope could be added to the model to increase its generality but these effects are omitted here to simplify the analysis.

Figure A-3 depicts the basic geometry parameters locating the lines of action of the forces with respect to the center of gravity and the rolling radii of the wheels again using the subscripts *r* and *f* to denote rear and front.

Figure A-4 shows the operating point velocities: the forward velocity V already defined and the angular velocities of the front and rear drive wheels ω_f and ω_r. All three of these velocities are considered as constants for a given operating point condition. Note this would not be the case if rotational dynamics of the power train were included as additional degrees of freedom.

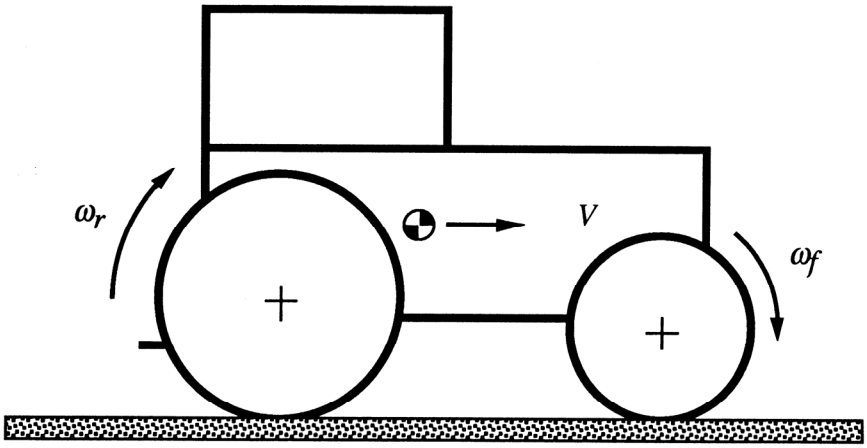

Figure A-4. Operating point velocities.

The Operating Point

The vehicle is in static equilibrium at the operating point under the action of a given drawbar load P_0 so we can write, using the forces shown in Figure A-1 and the geometry shown in Figure A-3,

$$\sum F_x = 0 = F_{f0} - TF_{f0} + F_{r0} - TF_{r0} - P_0 = \mu_{f0}N_{f0} - \rho_{f0}N_{f0} + \mu_{r0}N_{r0} - \rho_{r0}N_{r0} - P_0 \quad \text{(A-1)}$$

$$\sum F_z = 0 = W - N_{f0} - N_{r0} \quad \text{(A-2)}$$

$$\sum M_{cgy} = 0 = N_{f0}a - N_{r0}b + F_{f0}h - TF_{f0}h_f + F_{r0}h - TF_{r0}h_r - P_0D = N_{f0}a - N_{r0}b + \mu_{f0}N_{f0}h - \rho_{f0}N_{f0}h_f + \mu_{r0}N_{r0}h - \rho_{r0}N_{r0}h_r - P_0D \quad \text{(A-3)}$$

There are thus three equations of equilibrium in terms of six unknowns: N_{f0}, N_{r0}, μ_{f0}, ρ_{f0}, μ_{r0}, and ρ_{r0}. To obtain a solution, it is necessary to specify additional equations defining the gross tractive and motion resistance coefficients μ and ρ. Models both on soil and on concrete were utilized.

For soils, the tractive and motion resistance force equations developed by Brixius (1987) have seen widespread adoption and use and were used in this study. For radial tires, Brixius suggested the following equations:

$$F = \mu R = [0.88\,(1 - e^{-0.1B_n})\,(1 - e^{-9.5s}) + 0.0325]R$$

$$TF = \rho R = (\frac{0.9}{B_n} + 0.0325 + \frac{0.5s}{\sqrt{B_n}})R$$

where R is the normal force on an individual wheel, s is the slip of the wheel and B_n, the mobility number, is defined as:

$$B_n = \left(\frac{CIb_t d}{R}\right)\left(\frac{1 + 5\frac{\delta}{h_t}}{1 + 3\frac{b_t}{d}}\right)$$

where CI is the cone index of the soil on which the wheel is operating, b_t is the section width of the tire on the wheel, d is the unloaded overall diameter of the tire, δ is the tire deflection and h_t is the section height of the tire. Note these equations apply to an individual wheel so the normal force on an individual wheel can be found from the total normal force N on the front or rear axle by dividing by the number of tires (n_f or n_r) on that axle. For a given inflation pressure, the tire deflection δ is a function of the normal load R.

Thus the equations for the gross tractive and motion resistance forces add the following equations for describing the system:

$$R_{f0} = N_{f0} / n_f \tag{A-4}$$

$$R_{r0} = N_{r0} / n_r \tag{A-5}$$

$$\delta_{f0} = f(R_{f0}) \tag{A-6}$$

$$\delta_{r0} = g(R_{r0}) \tag{A-7}$$

$$B_{nf0} = \left(\frac{CI_f b_{tf} d_f}{R_{f0}}\right)\left(\frac{1 + 5\frac{\delta_{f0}}{h_{tf}}}{1 + 3\frac{b_{tf}}{d_f}}\right) \tag{A-8}$$

$$B_{nr0} = \left(\frac{CI_r b_{tr} d_r}{R_{r0}}\right)\left(\frac{1 + 5\frac{\delta_{r0}}{h_{tr}}}{1 + 3\frac{b_{tr}}{d_r}}\right) \tag{A-9}$$

$$TF_{f0} = \rho_{f0} N_{f0} = (\frac{0.9}{B_{nf0}} + 0.0325 + \frac{0.5s_{f0}}{\sqrt{B_{nf0}}})N_{f0} \tag{A-10}$$

$$TF_{r0} = \rho_{r0} N_{r0} = (\frac{0.9}{B_{nr0}} + 0.0325 + \frac{0.5s_{r0}}{\sqrt{B_{nr0}}})N_{r0} \tag{A-11}$$

$$F_{f0} = \mu_{f0} N_{f0} = [0.88\,(1 - e^{-0.1B_{nf0}})\,(1 - e^{-9.5s_{f0}}) + 0.0325]N_{f0} \tag{A-12}$$

$$F_{r0} = \mu_{r0} N_{r0} = [0.88\,(1 - e^{-0.1B_{nr0}})\,(1 - e^{-9.5s_{r0}}) + 0.0325]N_{r0} \tag{A-13}$$

Thus far, our system consists of the above ten equations plus the three equations of equilibrium making 13 equations in 14 unknowns $(R_{f0}, R_{r0}, N_{f0}, N_{r0}, \delta_{f0}, \delta_{r0}, B_{nf0}, B_{nr0}, TF_{f0}, TF_{r0}, F_{f0}, F_{r0}, s_{f0}, s_{r0})$.

To complete the solution for the operating point forces, an additional kinematic equation relating s_{f0} and s_{r0} is needed. The wheel slip s is defined as $s = 1 - V/(r\omega)$ so that $s_{fo} = 1 - V/(r_f\omega_{f0})$ and $s_{r0} = 1 - V/(r_r\omega_{r0})$. Solving both of these latter equations for V and equating the results, $V = r_f\omega_{f0}(1 - s_{f0}) = r_r\omega_{r0}(1 - s_{r0})$.

Solving for s_{f0} in terms of s_{r0} results in $s_{f0} = 1 - [(r_r\omega_{r0})/(r_f\omega_{f0})](1 - s_{r0})$.

Assuming a mechanical transmission connects an engine running at speed ω_{e0} to the front and rear axles with speed ratios of $G_f = \omega_{e0}/\omega_{f0}$ and $G_r = \omega_{e0}/\omega_{r0}$, $s_{f0} = 1 - [(r_r G_f)/(r_f G_r)](1 - s_{r0})$.

With G_f and G_r (or their ratio $G_f/G_r = \omega_{r0}/\omega_{f0}$) known, the above equation provides the desired relationship between s_{f0} and s_{r0}.

With the operating point forces determined, the axle torques $Q_{f0} = F_{f0}\, r_f$ and $Q_{r0} = F_{r0}\, r_r$ can be determined. Several alternatives are then available for determining the operating velocities. One approach is to assume that the vehicle's total axle power is available and calculate ω_{f0} using

$$Q_{f0}\omega_{f0} + Q_{r0}\omega_{r0} = \text{ axle power } = Q_{f0}\omega_{f0} + Q_{r0}(G_f/G_r)\omega_{f0}$$

$$\omega_{f0} = \frac{axle\ \ power}{Q_{f0} + Q_{r0}(G_f/G_r)}$$

$$\omega_{r0} = (G_f/G_r)\omega_{f0}\ .$$

Another approach requiring more power train information is to calculate the engine torque from the axle torques, the front and rear speed ratios for the transmission gear chosen, and the overall engine-to-axle power train efficiency. An engine torque-speed relation can then be used to find ω_{e0} and hence ω_{f0} and ω_{r0}.

Once the axle speeds have been determined, the forward speed V can be calculated:

$$V = r_f\omega_{f0}(1 - s_{f0}) = r_r\omega_{r0}(1 - s_{r0})\,. \tag{A-14}$$

The above set of 14 equations is nonlinear in nature so an iterative solution technique is required for a simultaneous solution to determine the operating point forces and velocities. The method outlined above is similar to that described in Sections 14.4 and 14.5 of Chapter 14 in Goering et al. (2003).

For operation on a concrete surface, the models developed by Zoz and Brixius (1979) for the traction and motion resistance forces were utilized. For the sake of brevity, the development of the corresponding equations is not reproduced here. The process is identical to that shown above for soil.

Linearized Equations of Motion

The next step is to derive the linearized differential equations of motion for small perturbations about the operating point. Summing forces in the x and z directions, we have

$$\sum F_x = m\ddot{x} = F_f - TF_f + F_r - TF_r - P$$

$$\sum F_z = m\ddot{z} = W - N_f - N_r\ .$$

In linearizing the pitch equation of motion, a common assumption is that the moment arms of the forces do not vary with the rotation angle θ thus assuming only the forces vary with θ. This assumption has the effect of omitting some linear terms that should be included for a rigorous analysis. The following derivation indicates how the moment arm effect should be included. But for purposes of brevity, only the linear moment arm terms for the normal forces are derived. A similar approach was used for the moment arms of the tractive and motion resistance forces.

Consider the front normal force acts at the center of the front wheels at a distance a in front of the center of gravity and at a distance h_f below it as indicated in Figure A-3. These two dimensions can be considered to be two sides of a right triangle with the hypotenuse g_f representing the distance between the center of the front wheels and the center of gravity ($g_f = \sqrt{a^2 + h_f^2}$, where $a = g_f\cos\theta_f$, $h_f = g_f\sin\theta_f$ where θ_f is the angle between side a and the hypotenuse). As the pitch angle θ varies, the moment arm of the front normal force N_f varies as well according to the relation $g_f\cos(\theta_f - \theta)$. Similarly the moment arm of the rear normal force varies according to $g_r\cos(\theta_r + \theta)$.

The resulting moment equation becomes

$$\sum M_{cgy} = I_{yy}\ddot{\theta} \cong N_f[g_f\cos(\theta_f - \theta)] - N_r[g_r\cos(\theta_r + \theta)] + F_f h - TF_f h_f + F_r h - TF_r h_r - PD\,.$$

Using the trigonometric identities for the cosine of the sum and difference of two angles,

$$\cos(\theta_f - \theta) = \cos\theta_f \cos\theta + \sin\theta_f \sin\theta$$
$$\cos(\theta_r + \theta) = \cos\theta_r \cos\theta - \sin\theta_r \sin\theta \quad .$$

But if θ is small, $\cos\theta \approx 1$ and $\sin\theta \approx \theta$, and

$$g_f \cos(\theta_f - \theta) = g_f(\cos\theta_f \cos\theta + \sin\theta_f \sin\theta) \cong g_f \cos\theta_f + (g_f \sin\theta_f)\theta = a + h_f\theta \ .$$

Similarly, $g_r \cos(\theta_r + \theta) = g_r(\cos\theta_r \cos\theta - \sin\theta_r \sin\theta) \cong g_r \cos\theta_r - (g_r \sin\theta_r)\theta = b - h_r\theta$.

$$\sum M_{cgy} = I_{yy}\ddot{\theta} \cong N_f(a + h_f\theta) - N_r(b - h_r\theta) + F_f h - TF_f h_f + F_r h - TF_r h_r - PD \ .$$

The next step is to express the above three differential equations in terms of the degrees of freedom (x, z, θ). The normal forces are modeled as a parallel spring-damper combination to reflect the tire's spring and damping properties. In doing so, the tire stiffness is taken as the slope (k_i, i = f or r) of its vertical load-deflection relation at the operating point deflection δ_{i0} as shown in Figure A-5.

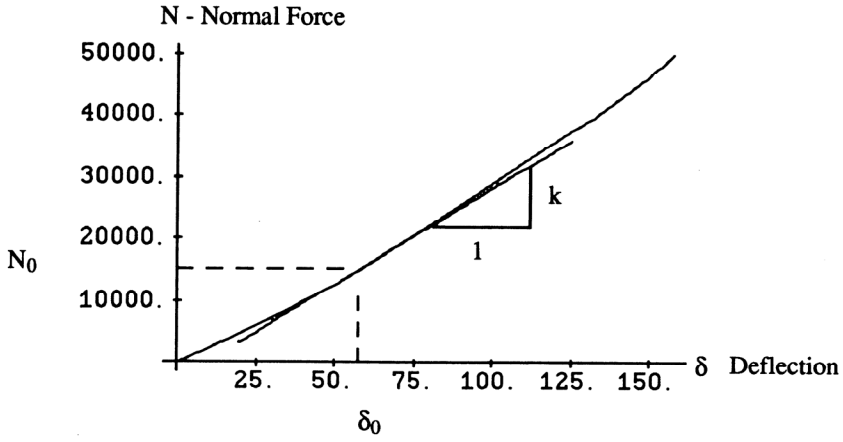

Figure A-5. Typical vertical load-deflection relationship of a tire on a firm surface.

This stiffness model is really valid only for operation on a firm surface. For operation in deformable soil conditions, the spring and damping values used should reflect the tire/soil combination. This is an important point to remember when comparing analytical and experimental results, i.e., they will be most accurate for operation on firm surfaces. Mathematical models describing the combined stiffness and damping effects of the tire/soil combination while tires are delivering traction on soft soils are unavailable.

For hard surfaces the normal force can then be expressed as

$$N_i = N_{i0} + k_i(\delta_i - \delta_{i0}) + c_i\dot{\delta}_i$$

where c_i is the viscous damping value. Note k_i and c_i represent the total vertical stiffness and damping at the front or rear axle. For springs (or dampers) in parallel (the case for multiple tires on an axle), the individual stiffnesses (damping rates) add to determine the equivalent total stiffness (damping) at the axle. The front tire vertical deflection from its operating point value ($\delta_f - \delta_{f0}$) can be expressed exactly as

$$\delta_f - \delta_{f0} = z + g_f \sin(\theta_f - \theta) - g_f \sin\theta_f \ .$$

Using the trigonometric identities for the sine of the sum and difference of two angles,

$$\sin(\theta_f - \theta) = \sin\theta_f \cos\theta - \cos\theta_f \sin\theta$$
$$\sin(\theta_r + \theta) = \sin\theta_r \cos\theta + \cos\theta_r \sin\theta$$

Then again using the approximation of $\cos\theta \approx 1$ and $\sin\theta \approx \theta$,

$$\delta_f - \delta_{f0} = z + g_f \sin(\theta_f - \theta) - g_f \sin\theta_f = z + g_f \sin\theta_f \cos\theta - g_f \cos\theta_f \sin\theta - g_f \sin\theta_f \cong$$
$$z + g_f \sin\theta_f - (g_f \cos\theta_f)\theta - g_f \sin\theta_f = z - (g_f \cos\theta_f)\theta = z - a\theta$$

Similarly, it can be shown that $\delta_r - \delta_{r0} \cong z + b\theta$. By differentiating the above exact expression for the front tire vertical deflection and using the classical small angle approximations, it can be shown that $\dot{\delta}_f = \dot{z} - a\dot{\theta}$. Similarly $\dot{\delta}_r = \dot{z} + b\dot{\theta}$ so that

$$N_f = N_{f0} + k_f(z - a\theta) + c_f(\dot{z} - a\dot{\theta})$$
$$N_r = N_{r0} + k_r(z + b\theta) + c_r(\dot{z} + b\dot{\theta}) \ .$$

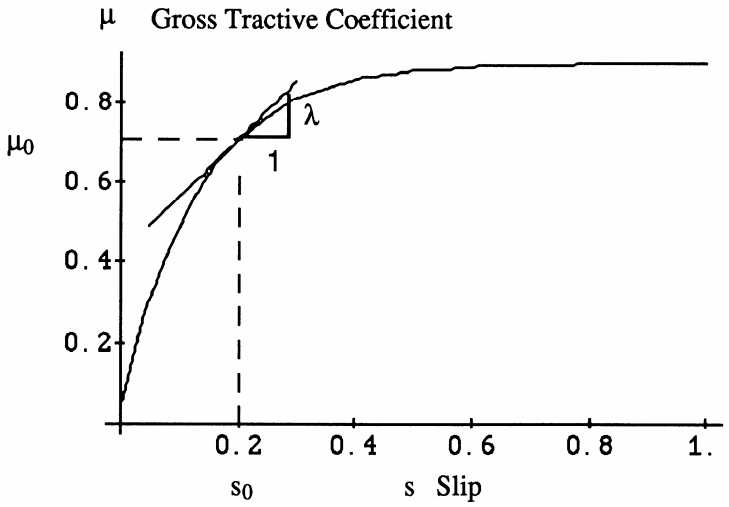

Figure A-6. Typical gross tractive coefficient variation with slip on soil.

The gross tractive force is considered to be the product of the gross tractive coefficient and the normal force. As shown in Figure A-6, the gross tractive coefficient is considered to be a function of wheel slip.

For small variations in slip, the gross tractive coefficient-slip relation can be linearized giving

$$F_i = \mu_i N_i = (\mu_{i0} + \lambda_i \Delta(slip)_i) N_i$$

where λ_i is the slope of the gross tractive coefficient-slip relation taken at the operating point slip, s_{i0}. The definition of slip s_i can be expanded to include the effects of the perturbation velocities as $slip_i = s_i = 1 - \dfrac{V + \dot{x} + h_i\dot{\theta}}{r_i(\omega_{i0} - \dot{\theta})}$

where the term $\dot{x} + h_i\dot{\theta}$ represents the linearized forward velocity of the axle center relative to the vehicle center of gravity which is itself moving forward with forward velocity V.

Then $$\Delta(slip)_i = \left.\frac{\partial(slip_i)}{\partial \dot{x}}\right|_{\substack{\dot{x}=0 \\ \dot{\theta}=0}} \dot{x} + \left.\frac{\partial(slip_i)}{\partial \dot{\theta}}\right|_{\substack{\dot{x}=0 \\ \dot{\theta}=0}} \dot{\theta}$$

$$\frac{\partial(slip_i)}{\partial \dot{x}} = -\frac{1}{r_i(\omega_{i0} - \dot{\theta})} \quad \text{and} \quad \left.\frac{\partial(slip_i)}{\partial \dot{x}}\right|_{\substack{\dot{x}=0 \\ \dot{\theta}=0}} = -\frac{1}{r_i\omega_{i0}}$$

$$\frac{\partial(slip_i)}{\partial \dot{\theta}} = -\frac{h_i}{r_i(\omega_{i0} - \dot{\theta})} - \frac{[V + \dot{x} + h_i\dot{\theta}]}{r_i(\omega_{i0} - \dot{\theta})^2} \quad \text{and} \quad \left.\frac{\partial(slip_i)}{\partial \dot{\theta}}\right|_{\substack{\dot{x}=0 \\ \dot{\theta}=0}} = -\frac{h_i}{r_i\omega_{i0}} - \frac{V}{r_i\omega_{i0}^2}$$

Thus $$\Delta(slip)_i = -\frac{\dot{x}}{r_i\omega_{i0}} - \left(\frac{h_i}{r_i\omega_{i0}} + \frac{V}{r_i\omega_{i0}^2}\right)\dot{\theta} \ .$$

Similarly, the motion resistance force is considered to be the product of the motion resistance coefficient and the normal force. As shown in Figure A-7, the motion resistance coefficient is considered to be a function of wheel slip.

For small variations in slip, the motion resistance coefficient-slip relation can be linearized giving

$$TF_i = \rho_i N_i = (\rho_{i0} + A_i \Delta(slip)_i) N_i$$

where A_i is the slope of the motion resistance coefficient-slip relation taken at the operating point slip, s_{i0}.

Considering a free body diagram of the implement, the drawbar pull force P acts to move the implement forward against the resistance R imposed by the soil. The resistance force R is commonly thought of as a function of forward velocity as shown in Figure A-8.

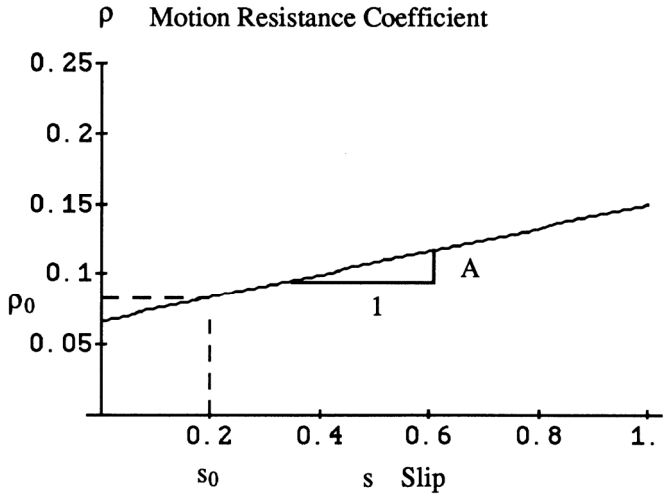

Figure A-7. Typical motion resistance coefficient variation with slip on soil.

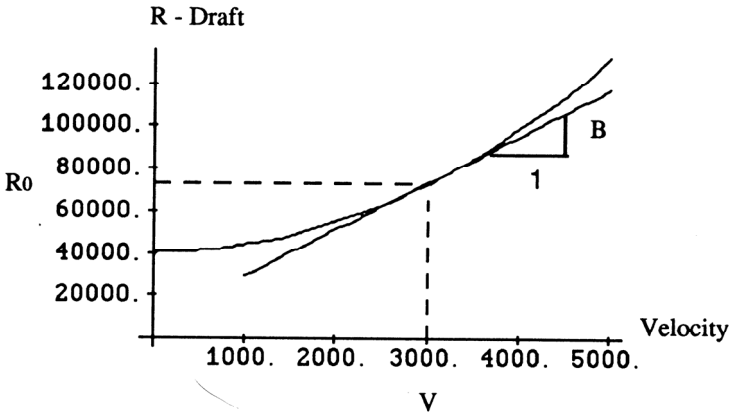

Figure A-8. Typical draft load variation with velocity.

B is the slope of the implement resistance-forward speed relation at the operating point velocity V. If R_0 is the resistance at forward speed V

$$R = R_0 + B(V + \dot{x} + D\dot{\theta} - V) = R_0 + B(\dot{x} + D\dot{\theta})$$

where $\dot{x} + D\dot{\theta}$ is the linearized forward velocity of the vehicle drawbar attachment point with respect to the center of gravity operating point forward velocity V.

Similarly the linearized fore-aft acceleration of the implement is $\ddot{x} + D\ddot{\theta}$ so that for an implement mass of m_I,

$$m_I(\ddot{x} + D\ddot{\theta}) = P - R = P - R_0 - B(\dot{x} + D\dot{\theta}) \ .$$

Solving for P, $P = m_I(\ddot{x} + D\ddot{\theta}) + R_0 + B(\dot{x} + D\dot{\theta})$.

The above relations for N_f, N_r, F_f, F_r, TF_f, TF_r, and P can be expressed in the form of the sum of the operating point force and a force variation about the operating value dependent on the system's three degrees of freedom:

$$N_f = N_{f0} + k_f(z - a\theta) + c_f(\dot{z} - a\dot{\theta}) = N_{f0} + N_{fv}$$

$$N_r = N_{r0} + k_r(z + b\theta) + c_r(\dot{z} + b\dot{\theta}) = N_{r0} + N_{rv}$$

$$F_f = \mu_f N_f = (\mu_{f0} + \lambda_f \Delta(slip)_f)N_f = (\mu_{f0} + \lambda_f \Delta(slip)_f)(N_{f0} + N_{fv}) =$$

$$(\mu_{f0} + \lambda_f[-\frac{\dot{x}}{r_f\omega_{f0}} - \dot{\theta}\left\{\frac{h_f}{r_f\omega_{f0}} + \frac{V}{r_f\omega_{f0}^2}\right\}])(N_{f0} + N_{fv})$$

$$F_r = \mu_r N_r = (\mu_{r0} + \lambda_r \Delta(slip)_r)N_r = (\mu_{r0} + \lambda_r \Delta(slip)_r)(N_{r0} + N_{rv}) =$$

$$(\mu_{r0} + \lambda_r[-\frac{\dot{x}}{r_r\omega_{r0}} - \dot{\theta}\left\{\frac{h_r}{r_r\omega_{r0}} + \frac{V}{r_r\omega_{r0}^2}\right\}])(N_{r0} + N_{rv})$$

$$TF_f = \rho_f N_f = (\rho_{f0} + A_f \Delta(slip)_f)N_f = (\rho_{f0} + A_f \Delta(slip)_f)(N_{f0} + N_{fv}) =$$

$$(\rho_{f0} + A_f[-\frac{\dot{x}}{r_f\omega_{f0}} - \dot{\theta}\left\{\frac{h_f}{r_f\omega_{f0}} + \frac{V}{r_f\omega_{fo}^2}\right\}])(N_{f0} + N_{fv})$$

$$TF_r = \rho_r N_r = (\rho_{r0} + A_r \Delta(slip)_r)N_r = (\rho_{r0} + A_r \Delta(slip)_r)(N_{r0} + N_{rv}) =$$

$$(\rho_{r0} + A_r[-\frac{\dot{x}}{r_r\omega_{r0}} - \dot{\theta}\left\{\frac{h_r}{r_r\omega_{r0}} + \frac{V}{r_r\omega_{r0}^2}\right\}])(N_{r0} + N_{rv})$$

$$P = R_0 + m_I(\ddot{x} + D\ddot{\theta}) + B(\dot{x} + D\dot{\theta}) = P_0 + P_v \ .$$

The operating and variable forces are indicated in the free body diagram of Figure A-9.

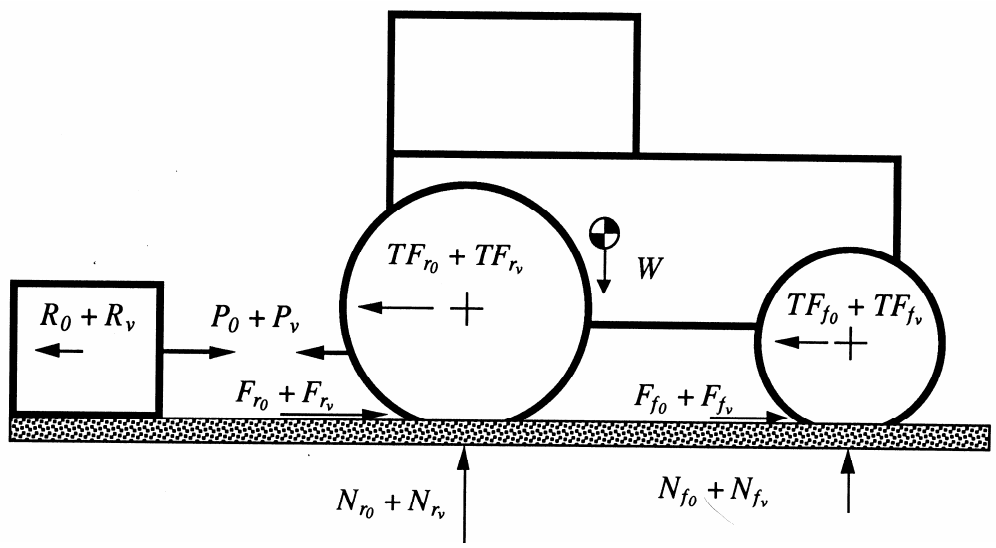

Figure A-9. Operating point forces and variable forces during disturbed motion.

Substituting the above relations in the differential equation of motion for the variation x in the forward motion:

$$\sum F_x = m\ddot{x} = F_f - TF_f + F_r - TF_r - P$$

$$= \mu_{f0}N_{f0} - \lambda_f[\frac{\dot{x}}{r_f\omega_{f0}} + \dot{\theta}\left\{\frac{h_f}{r_f\omega_{f0}} + \frac{V}{r_f\omega_{f0}^2}\right\}]N_{f0} + \mu_{f0}N_{fv} - \lambda_f[\frac{\dot{x}}{r_f\omega_{f0}} + \dot{\theta}\left\{\frac{h_f}{r_f\omega_{f0}} + \frac{V}{r_f\omega_{f0}^2}\right\}]N_{fv}$$

$$- \rho_{f0}N_{f0} + A_f[\frac{\dot{x}}{r_f\omega_{f0}} + \dot{\theta}\left\{\frac{h_f}{r_f\omega_{f0}} + \frac{V}{r_f\omega_{fo}^2}\right\}]N_{f0} - \rho_{f0}N_{fv} + A_f[\frac{\dot{x}}{r_f\omega_{f0}} + \dot{\theta}\left\{\frac{h_f}{r_f\omega_{f0}} + \frac{V}{r_f\omega_{fo}^2}\right\}]N_{fv}$$

$$+ \mu_{r0}N_{r0} - \lambda_r[\frac{\dot{x}}{r_r\omega_{r0}} + \dot{\theta}\left\{\frac{h_r}{r_r\omega_{r0}} + \frac{V}{r_r\omega_{r0}^2}\right\}]N_{r0} + \mu_{r0}N_{rv} - \lambda_r[\frac{\dot{x}}{r_r\omega_{r0}} + \dot{\theta}\left\{\frac{h_r}{r_r\omega_{r0}} + \frac{V}{r_r\omega_{r0}^2}\right\}]N_{rv}$$

$$- \rho_{r0}N_{r0} + A_r[\frac{\dot{x}}{r_r\omega_{r0}} + \dot{\theta}\left\{\frac{h_r}{r_r\omega_{r0}} + \frac{V}{r_r\omega_{r0}^2}\right\}]N_{r0} - \rho_{r0}N_{rv} + A_r[\frac{\dot{x}}{r_r\omega_{r0}} + \dot{\theta}\left\{\frac{h_r}{r_r\omega_{r0}} + \frac{V}{r_r\omega_{r0}^2}\right\}]N_{rv}$$

$$-[P_0 + m_I(\ddot{x} + D\ddot{\theta}) + B(\dot{x} + D\dot{\theta})] \ .$$

From fore-aft force equilibrium at the operating point condition, we have

$$\sum F_x = 0 = F_{f0} - TF_{f0} + F_{r0} - TF_{r0} - P_0 = \mu_{f0}N_{f0} - \rho_{f0}N_{f0} + \mu_{r0}N_{r0} - \rho_{r0}N_{r0} - P_0 \ .$$

In addition, the terms $\lambda_i[\frac{\dot{x}}{r_i\omega_{i0}} + \dot{\theta}\left\{\frac{h_i}{r_i\omega_{i0}} + \frac{V}{r_i\omega_{i0}^2}\right\}]N_{iv}$ and $A_i[\frac{\dot{x}}{r_i\omega_{i0}} + \dot{\theta}\left\{\frac{h_i}{r_i\omega_{i0}} + \frac{V}{r_i\omega_{i0}^2}\right\}]N_{iv}$ are second order terms of the system displacements and velocities and can thus be neglected in a linearized analysis. Simplifying the resulting equation of motion,

$$[m + m_I]\ddot{x} + m_I D\ddot{\theta} + (\lambda_f - A_f)[\frac{\dot{x}}{r_f\omega_{f0}} + \dot{\theta}\left\{\frac{h_f}{r_f\omega_{f0}} + \frac{V}{r_f\omega_{f0}^2}\right\}]N_{f0}$$

$$-(\mu_{f0} - \rho_{f0})[k_f(z - a\theta) + c_f(\dot{z} - a\dot{\theta})]$$

$$+(\lambda_r - A_r)[\frac{\dot{x}}{r_r\omega_{r0}} + \dot{\theta}\left\{\frac{h_r}{r_r\omega_{r0}} + \frac{V}{r_r\omega_{r0}^2}\right\}]N_{r0}$$

$$-(\mu_{r0} - \rho_{r0})[k_r(z + b\theta) + c_r(\dot{z} + b\dot{\theta})]$$

$$+B\dot{x} + BD\dot{\theta} = 0 \ .$$

Simplifying the differential equation of motion in the vertical (z) direction,

$$\sum F_z = m\ddot{z} = W - N_f - N_r = W - N_{f0} - k_f(z - a\theta) - c_f(\dot{z} - a\dot{\theta}) - N_{r0} - k_r(z + b\theta) - c_r(\dot{z} + b\dot{\theta}) \ .$$

From statics, we have $W - N_{f0} - N_{r0} = 0$. Incorporating this relation and rewriting the above equation,

$$m\ddot{z} + k_f(z - a\theta) + c_f(\dot{z} - a\dot{\theta}) + k_r(z + b\theta) + c_r(\dot{z} + b\dot{\theta}) = 0 \ .$$

Finally, the differential equation for the pitch rotational motion becomes

$$\sum M_{cgy} = I_{yy}\ddot{\theta} \cong N_f(a + h_f\theta) - N_r(b - h_r\theta) + F_f h - TF_f h_f + F_r h - TF_r h_r - PD$$

$$= [N_{fo} + k_f(z - a\theta) + c_f(\dot{z} - a\dot{\theta})][a + h_f\theta]$$

$$-[N_{r0} + k_r(z + b\theta) + c_r(\dot{z} + b\dot{\theta})][b - h_r\theta]$$

$$+\left[\mu_{f0}N_{f0} - \lambda_f[\frac{\dot{x}}{r_f\omega_{f0}} + \dot{\theta}\left\{\frac{h_f}{r_f\omega_{f0}} + \frac{V}{r_f\omega_{f0}^2}\right\}]N_{f0}\right]h$$

$$+\left[\mu_{f0}N_{fv} - \lambda_f[\frac{\dot{x}}{r_f\omega_{f0}} + \dot{\theta}\left\{\frac{h_f}{r_f\omega_{f0}} + \frac{V}{r_f\omega_{f0}^2}\right\}]N_{fv}\right]h$$

$$-\left[\rho_{f0}N_{f0} - A_f[\frac{\dot{x}}{r_f\omega_{f0}} + \dot{\theta}\left\{\frac{h_f}{r_f\omega_{f0}} + \frac{V}{r_f\omega_{fo}^2}\right\}]N_{f0}\right]h_f$$

$$-\left[\rho_{f0}N_{fv} - A_f[\frac{\dot{x}}{r_f\omega_{f0}} + \dot{\theta}\left\{\frac{h_f}{r_f\omega_{f0}} + \frac{V}{r_f\omega_{fo}^2}\right\}]N_{fv}\right]h_f$$

$$+\left[\mu_{r0}N_{r0} - \lambda_r[\frac{\dot{x}}{r_r\omega_{r0}} + \dot{\theta}\left\{\frac{h_r}{r_r\omega_{r0}} + \frac{V}{r_r\omega_{r0}^2}\right\}]N_{r0}\right]h$$

$$+\left[\mu_{r0}N_{rv} - \lambda_r[\frac{\dot{x}}{r_r\omega_{r0}} + \dot{\theta}\left\{\frac{h_r}{r_r\omega_{r0}} + \frac{V}{r_r\omega_{r0}^2}\right\}]N_{rv}\right]h$$

$$-\left[\rho_{r0}N_{r0} - A_r[\frac{\dot{x}}{r_r\omega_{r0}} + \dot{\theta}\left\{\frac{h_r}{r_r\omega_{r0}} + \frac{V}{r_r\omega_{r0}^2}\right\}]N_{r0}\right]h_r$$

$$-\left[\rho_{r0}N_{rv} - A_r[\frac{\dot{x}}{r_r\omega_{r0}} + \dot{\theta}\left\{\frac{h_r}{r_r\omega_{r0}} + \frac{V}{r_r\omega_{r0}^2}\right\}]N_{rv}\right]h_r$$

$$-[P_0 + m_I(\ddot{x} + D\ddot{\theta}) + B(\dot{x} + D\dot{\theta})]\,D \ .$$

From statics, we have

$$\sum M_{cgy} = 0 = N_{f0}a - N_{r0}b + F_{f0}h - TF_{f0}h_f + F_{r0}h - TF_{r0}h_r - P_0D =$$
$$N_{f0}a - N_{r0}b + \mu_{f0}N_{f0}h - \rho_{f0}N_{f0}h_f + \mu_{r0}N_{r0}h - \rho_{r0}N_{r0}h_r - P_0D$$

As above, the terms $\lambda_i[\frac{\dot{x}}{r_i\omega_{i0}} + \dot{\theta}\left\{\frac{h_i}{r_i\omega_{i0}} + \frac{V}{r_i\omega_{i0}^2}\right\}]N_{iv}$ and $A_i[\frac{\dot{x}}{r_i\omega_{i0}} + \dot{\theta}\left\{\frac{h_i}{r_i\omega_{i0}} + \frac{V}{r_i\omega_{i0}^2}\right\}]N_{iv}$ are second order terms of the system displacements and velocities and can be neglected in a linearized analysis. In addition, terms such as θ^2 and $\theta\dot{\theta}$ are also second order terms and can be neglected. Using these results and simplifying,

$$I_{yy}\ddot{\theta} = N_{f0}h_f\theta + [k_f(z - a\theta) + c_f(\dot{z} - a\dot{\theta})]a$$

$$+ N_{r0}h_r\theta - [k_r(z + b\theta) + c_r(\dot{z} + b\dot{\theta})]b$$

$$+ (\mu_{f0}h - \rho_{f0}h_f)[k_f(z - a\theta) + c_f(\dot{z} - a\dot{\theta})]$$

$$+ (\mu_{r0}h - \rho_{r0}h_r)[k_r(z + b\theta) + c_r(\dot{z} + b\dot{\theta})]$$

$$+ (A_fh_f - \lambda_fh)[\frac{\dot{x}}{r_f\omega_{f0}} + \dot{\theta}\left\{\frac{h_f}{r_f\omega_{f0}} + \frac{V}{r_f\omega_{fo}^2}\right\}]N_{f0}$$

$$+ (A_rh_r - \lambda_rh)[\frac{\dot{x}}{r_r\omega_{r0}} + \dot{\theta}\left\{\frac{h_r}{r_r\omega_{r0}} + \frac{V}{r_r\omega_{r0}^2}\right\}]N_{r0}$$

$$- m_1D\ddot{x} - m_1D^2\ddot{\theta} - BD(\dot{x} + D\dot{\theta}) \ .$$

or rearranging the terms to the left hand side of the equation as was done above to put the equation in a standard form,

$$(I_{yy} + m_1D^2)\ddot{\theta} + m_1D\ddot{x} + BD(\dot{x} + D\dot{\theta}) - [N_{f0}h_f + N_{r0}h_r]\theta$$

$$-[k_f(z - a\theta) + c_f(\dot{z} - a\dot{\theta})]a + [k_r(z + b\theta) + c_r(\dot{z} + b\dot{\theta})]b$$

$$-(\mu_{f0}h - \rho_{f0}h_f)[k_f(z - a\theta) + c_f(\dot{z} - a\dot{\theta})]$$

$$-(\mu_{r0}h - \rho_{r0}h_r)[k_r(z + b\theta) + c_r(\dot{z} + b\dot{\theta})]$$

$$+ (\lambda_fh - A_fh_f)[\frac{\dot{x}}{r_f\omega_{f0}} + \dot{\theta}\left\{\frac{h_f}{r_f\omega_{f0}} + \frac{V}{r_f\omega_{fo}^2}\right\}]N_{f0} \ .$$

$$+ (\lambda_rh - A_rh_r)[\frac{\dot{x}}{r_r\omega_{r0}} + \dot{\theta}\left\{\frac{h_r}{r_r\omega_{r0}} + \frac{V}{r_r\omega_{r0}^2}\right\}]N_{r0} = 0$$

The next step is to rearrange and express the three equations of motion in a vector-matrix form:

$$[M]\begin{Bmatrix}\ddot{z}\\ \ddot{\theta}\\ \ddot{x}\end{Bmatrix} + [C]\begin{Bmatrix}\dot{z}\\ \dot{\theta}\\ \dot{x}\end{Bmatrix} + [K]\begin{Bmatrix}z\\ \theta\\ x\end{Bmatrix} = \begin{Bmatrix}0\\ 0\\ 0\end{Bmatrix} \qquad \text{(A-15)}$$

where [*M*], [*C*], and [*K*] are termed the mass, damping and stiffness matrices respectively. This yields the final equations governing small oscillations about the steady state operating point.

$$\begin{bmatrix} m & 0 & 0 \\ 0 & I_{yy}+m_I D^2 & m_I D \\ 0 & m_I D & m+m_I \end{bmatrix} \begin{Bmatrix} \ddot{z} \\ \ddot{\theta} \\ \ddot{x} \end{Bmatrix}$$

$$+ \begin{bmatrix} c_f + c_r & -c_f a + c_r b & 0 \\ -c_f a + c_r b & \begin{matrix} c_f a^2 + c_r b^2 + BD^2 \\ +(\mu_{f0} h - \rho_{f0} h_f) c_f a \\ -(\mu_{r0} h - \rho_{r0} h_r) c_r b \\ +(\lambda_f h - A_f h_f)(h_f + V/\omega_{f0}) N_{f0}/(r_f \omega_{fo}) \\ +(\lambda_r h - A_r h_r)(h_r + V/\omega_{r0}) N_{r0}/(r_r \omega_{ro}) \end{matrix} & \begin{matrix} BD \\ +(\lambda_f h - A_f h_f) N_{f0}/(r_f \omega_{f0}) \\ +(\lambda_r h - A_r h_r) N_{r0}/(r_r \omega_{r0}) \end{matrix} \\ -(\mu_{f0} h - \rho_{f0} h_f) c_f & \begin{matrix} BD \\ +(\mu_{f0} - \rho_{f0}) c_f a \\ -(\mu_{r0} - \rho_{r0}) c_r b \\ +(\lambda_f - A_f)(h_f + V/\omega_{f0}) N_{f0}/(r_f \omega_{fo}) \\ +(\lambda_r - A_r)(h_r + V/\omega_{r0}) N_{r0}/(r_r \omega_{ro}) \end{matrix} & \begin{matrix} B \\ +\dfrac{(\lambda_f - A_f)}{r_f \omega_{f0}} N_{f0} \\ +\dfrac{(\lambda_r - A_r)}{r_r \omega_{r0}} N_{r0} \end{matrix} \\ -(\mu_{r0} h - \rho_{r0} h_r) c_r & & \end{bmatrix} \begin{Bmatrix} \dot{z} \\ \dot{\theta} \\ \dot{x} \end{Bmatrix}$$

$$+ \begin{bmatrix} k_f + k_r & -k_f a + k_r b & 0 \\ -k_f a + k_r b & \begin{matrix} k_f a^2 + k_r b^2 \\ +(\mu_{f0} h - \rho_{f0} h_f) k_f a \\ -(\mu_{r0} h - \rho_{r0} h_r) k_r b \\ -(N_{f0} h_f + N_{r0} h_r) \end{matrix} & 0 \\ -(\mu_{f0} h - \rho_{f0} h_f) k_f & & \\ -(\mu_{r0} h - \rho_{r0} h_r) k_r & & \\ -(\mu_{f0} - \rho_{f0}) k_f & (\mu_{f0} - \rho_{f0}) k_f a & 0 \\ -(\mu_{r0} - \rho_{r0}) k_r & -(\mu_{r0} - \rho_{r0}) k_r b & \end{bmatrix} \begin{Bmatrix} z \\ \theta \\ x \end{Bmatrix} = \begin{Bmatrix} 0 \\ 0 \\ 0 \end{Bmatrix} \qquad \text{(A-16)}$$

Note that if the fore-aft (x) degree of freedom is not considered, the above equations simplify to those for the two degree of freedom (bounce z and pitch θ) system of Section 14.7 in Goering et al. (2003). As in that reference, the eigenvalues of the undamped system determine the system's natural frequencies and associated modes of vibration. However, a different tack was taken in this study in that the eigenvalues of the full set of equations, including the damping terms, were used to predict system stability.

For modeling the tractor operating on a concrete surface, Equation A-16 still applies but with the coefficients representing slopes of the various parameters for operation on soils replaced by the comparable slopes for the traction and motion resistance on concrete.

Analytical Stability Results

Closed-form results for the eigenvalues and eigenvectors are available by making one of the standard assumptions employed in the classical analysis of stability of dynamic systems, i.e., that the velocity-dependent forces are small in comparison to the inertial and stiffness forces (Bolotin, 1963; Ziegler, 1968). We will do this here by completely neglecting the damping matrix [C] in the general differential equations for perturbed motions and writing out the resulting three equations using the obvious subscript notation for the elements of the stiffness matrix.

$$m\ddot{z} + k_{11}z + k_{12}\theta = 0 \tag{A-17}$$

$$\left(I_{yy} + m_I D^2\right)\ddot{\theta} + m_I D\ddot{x} + k_{21}z + k_{22}\theta = 0 \tag{A-18}$$

$$m_I D\ddot{\theta} + (m + m_I)\ddot{x} + k_{31}z + k_{32}\theta = 0\ . \tag{A-19}$$

Now eliminate the surge acceleration $\ddot{x}$ from the last two equations by solving the third equation for $\ddot{x}$ and substituting the result into the second equation. This ultimately leads to

$$I'\ddot{\theta} + \left[k_{21} - k_{31}\frac{m_I D}{m + m_I}\right]z + \left[k_{22} - k_{32}\frac{m_I D}{m + m_I}\right]\theta = 0 \tag{A-20}$$

where $I' \triangleq I_{yy} + m_I D^2 \dfrac{m}{m + m_I}$ (A-21)

$$k_{11} = k_f + k_r \triangleq T_1 \tag{A-22}$$

$$k_{12} = -k_f a + k_r b \triangleq -T_2 \tag{A-23}$$

$$k_{21} = -k_f a + k_r b - \left(\alpha_f + \alpha_r\right) \triangleq -T_2 - \left(\alpha_f + \alpha_r\right) \tag{A-24}$$

$$k_{31} = -\left(\beta_f + \beta_r\right) \tag{A-25}$$

$$k_{22} = k_f a^2 + k_r b^2 + \left(\alpha_f a - \alpha_r b\right) - \left(N_{f0}h_f + N_{r0}h_r\right) \tag{A-26}$$

$$k_{32} = \left(\beta_f a - \beta_r b\right) \tag{A-27}$$

and $\alpha_f = \left(\mu_{f0}h - \rho_{f0}h_f\right)k_f > 0$ (A-28)

$$\alpha_r = \left(\mu_{r0}h - \rho_{r0}h_r\right)k_r > 0 \tag{A-29}$$

$$\beta_f = \left(\mu_{f0} - \rho_{f0}\right)k_f > 0 \tag{A-30}$$

$$\beta_r = \left(\mu_{r0} - \rho_{r0}\right)k_r > 0\ . \tag{A-31}$$

Now expand the coefficients of z and θ in (A-20) to get:

Coefficient of z = $-T_2 - T_3$ (A-32)

where $T_3 \triangleq \left(\alpha_f + \alpha_r\right) - \dfrac{m_I D}{m + m_I}\left(\beta_f + \beta_r\right)$. (A-33)

Coefficient of $\theta = T_4$ (A-34)

where $T_4 \triangleq k_f a^2 + k_r b^2 + \left(\alpha_f a - \alpha_r b\right) - \left(N_{f0}h_f + N_{r0}h_r\right) - \dfrac{m_I D}{m + m_I}\left(\beta_f a - \beta_r b\right)$. (A-35)

Rewriting (A-17) and (A-20) in terms of these definitions, we obtain two coupled linear differential equations governing the perturbed vertical displacement z and the pitch θ:

$$\ddot{z} + \frac{T_1}{m}z - \frac{T_2}{m}\theta = 0 \tag{A-36}$$

$$\ddot{\theta} - \frac{\left[T_2 + T_3\right]}{I'}z + \frac{T_4}{I'}\theta = 0\ . \tag{A-37}$$

To solve these, we assume periodic solutions of the forms

$$z = Ze^{st} \quad \theta = \Theta e^{st} \tag{A-38}$$

where Z and Θ are the eigenvector components corresponding to the eigenvalues s to be determined and t is the time. We note again that the stiffness matrix is unsymmetric due to the presence of the term T_3. Thus the eigenvalues may not be purely imaginary complex conjugate pairs as they would be if T_3 were zero.

Taking the required derivatives of the equations (A-38) and substituting into (A-36) and (A-37), we arrive at the following 2 linear equations for Z and Θ:

$$\left[s^2 + \frac{T_1}{m}\right]Z + \left[-\frac{T_2}{m}\right]\Theta = 0 \tag{A-39}$$

$$-\frac{\left[T_2 + T_3\right]}{I'}Z + \left[s^2 + \frac{T_4}{I'}\right]\Theta = 0\,. \tag{A-40}$$

Non-trivial solutions exist for these linear homogeneous equations if the determinant of the coefficients vanishes. Expansion of this determinant leads to

$$s^4 + \left[\frac{T_1}{m} + \frac{T_4}{I'}\right]s^2 + \left[\frac{T_1T_4}{mI'} - \frac{T_2^2}{mI'} - \frac{T_2T_3}{mI'}\right] = 0\ . \tag{A-41}$$

This is a quadratic in s^2 so the quadratic formula can be used to get

$$s_{1,2}^2 = -\frac{1}{2}\left[\frac{T_1}{m} + \frac{T_4}{I'}\right] \pm \frac{1}{2}\sqrt{\left[\frac{T_1}{m} + \frac{T_4}{I'}\right]^2 - 4\left[\frac{T_1T_4}{mI'} - \frac{T_2^2}{mI'} - \frac{T_2T_3}{mI'}\right]}\ . \tag{A-42}$$

If the discriminant inside the radical is positive, the two roots, s^2, will be strictly negative real numbers. Therefore the four eigenvalues s will be purely imaginary complex conjugate pairs. Each pair corresponds to a vibration mode without decay or growth.

However, if the discriminant is negative, the four eigenvalues, s, can be complex conjugate pairs with two having positive real parts. This indicates flutter instability of the system.

So the borderline between stable oscillations and flutter instability in this model which ignores velocity-dependent forces occurs when the discriminant is zero. For stability, it must be > 0.

$$\left[\frac{T_1}{m} + \frac{T_4}{I'}\right]^2 - 4\left[\frac{T_1T_4}{mI'} - \frac{T_2^2}{mI'} - \frac{T_2T_3}{mI'}\right] > 0 \text{ for stability.} \tag{A-43}$$

Upon expanding and regrouping terms this becomes

$$\left[\frac{T_1}{m} - \frac{T_4}{I'}\right]^2 + 4\frac{T_2^2}{mI'} + \frac{4T_2T_3}{mI'} > 0\,. \tag{A-44}$$

This is both a necessary and sufficient condition for stability. If T_2 and T_3 are simultaneously both positive or both negative, then clearly stability is assured. However, we have to determine the sign possibilities of T_2 and of T_3 before proceeding further. It is easily seen that T_2 can be either positive or negative. However, the sign of T_3 is not clear without further expansion of all of the terms embedded in that expression. From (A-33) as well as (A-28) through (A-31)

$$\begin{aligned} T_3 &\triangleq \left(\alpha_f + \alpha_r\right) - \frac{m_I D}{m + m_I}\left(\beta_f + \beta_r\right) \\ &= \left(\mu_{f0}h - \rho_{f0}h_f\right)k_f + \left(\mu_{r0}h - \rho_{r0}h_r\right)k_r - \frac{m_I D}{m + m_I}\left[\left(\mu_{f0} - \rho_{f0}\right)k_f + \left(\mu_{r0} - \rho_{r0}\right)k_r\right]\,. \end{aligned} \tag{A-45}$$

Rearranging and collecting terms yields

$$T_3 = \left[\mu_{f0}\left(h - \frac{m_I D}{m + m_I}\right) - \rho_{f0}\left(h_f - \frac{m_I D}{m + m_I}\right)\right]k_f + \left[\mu_{r0}\left(h - \frac{m_I D}{m + m_I}\right) - \rho_{r0}\left(h_r - \frac{m_I D}{m + m_I}\right)\right]k_r\ . \tag{A-46}$$

Referring back to the geometric definitions used in the model in Figure A-3, for practical tractor configurations the following inequalities hold:

$$h > D,\ h > h_f,\ h > h_r,\ h_f < D, \text{ and } h_r < D.$$

Now by examination of all terms in (A-46) using these inequalities, it is seen that T_3 is always positive for practical tractors.

Returning now to the stability condition equation (A-44) we see that it would be possible for T_2 to be negative and yet have the entire expression (A-44) be positive indicating stability. This would work out to be a very complicated stability criterion. However, for a simpler and more direct result, we can just set forth a sufficient, though not necessary, condition for stability, i.e., $T_2 > 0$, or $k_f a - k_r b > 0$ for stability.

We define this as the Hop Function,

$$H \triangleq k_f a - k_r b \,. \tag{A-47}$$

Then the *sufficient* condition for stability is as follows. If

$$H \triangleq k_f a - k_r b > 0 \tag{A-48}$$

throughout the pull-slip range of interest for this tractor/implement system with negligible velocity-dependent forces, power hop cannot occur. Note again that this was derived for tractors *without* suspension systems. In the discussion of analytical and experimental results, it will become evident that this criterion plays a very important role in the practical considerations of power hop control. However, it is also very important to note that this is *not a necessary* condition. In other words, this condition does not have to be satisfied for the tractor to be stable. It could be stable due to the presence of sufficient damping or to other system parameter combinations that simply do not allow any complex conjugate pair of eigenvalues to migrate to the right half plane (see Equation A-44).

Video Clips on the DVD

Jack C. Wiley and Reed J. Turner

Note: The author who supplied each video clip or photo is identified by his initials.

Power Hop Field Scenes

- **Power Hop in the 1970s (JCW)—**Power hop is documented for a variety of tractor configurations (MFWD, 4WD, and 2+2), several different tractor brands, and different chassis sizes being field tested by John Deere engineers in 1978 and 1979. Note that in the final scene of the IH 2+2 tractor, power hop occurs as the tractor climbs a slope without pulling any implement. The down slope component of its weight alone is enough "draft load" to induce power hop on this soil and slope. The poor quality of the video is the result of many generations of copies that preceded the final version on this DVD.
- **Deere Power Hop Test Highlights (JCW)—**This is a compilation of major events in the extensive power hop testing efforts jointly conducted by John Deere and the tire companies starting in September 1989 and continuing through October 1991.
- **Agtech Power Hop Test Highlights (RJT)—**This reviews the equipment and techniques used by the Alberta Farm Machinery Research Centre (subsequently the Agricultural Technology Centre) to evaluate and control power hop on tractors in farm fields. It also shows power hop of varying degrees on MFWD and 4WD tractors.
- **4WD Power Hop Control: Two Solutions (JCW)—**Power hop of this John Deere 8970 4WD tractor could be controlled either with high front inflation pressures or with high rear inflation pressures in the soft soil conditions found at this central Iowa location in 1991.
- **Power Hop with Suspended Front Axle MFWD (RJT)**—This shows the effect front axle suspension has on power hop on MFWD tractors. On unsuspended tractors, power hop is typically more vigorous and tends to come from the front of the tractor. With front suspensions, power hop is somewhat more muted and tends to come from the rear of the tractor but can cause problems for the suspension system. The last shot shows a vertical front suspension system working just opposite to its design intent on an MFWD tractor experiencing power hop. The suspension arms are pivoting at their outer ends and moving up and down at their inner ends instead of pivoting at their inner ends and moving up and down at their outer ends. As a result, instead of the wheels moving vertically while the tractor chassis motion is attenuated, the wheel motion is attenuated while the tractor chassis moves vertically.
- **The Ultimate Goal: A Stable Tractor (RJT)—**This shows a correctly set radial tire equipped 4WD tractor operating in the field as the load is slowly increased from 0 until the tractor is brought to a complete stop (100% slip). The tractor remains stable through the complete pull spectrum, showing no tendency to power hop at any pull or slip level and presents the ideal case.

Power Hop Simulation Scenes

- **4WD Power Hop Simulation: ADAMS, Early 1980s (JCW)—**These 3D simulations of a John Deere 8640 4WD tractor were produced at the Deere & Company Technical Center, Moline, Illinois, in 1981. Nicky Orlandea's original version of ADAMS was used to create the simulations. The three-dimensional graphic displays with hidden line removal were produced by a program named HAL created by Tibor (Ted) Berenyi. The animations were created by Bernard Romig by filming individual frames to display at a rate of 30 frames per second. The model was fully 3D and included tire, power train, and engine elements. The tire-soil interactions (traction and stiffnesses) were essentially the same as those used later in the two-dimensional model developed in the Distinguished Lecture paper. The 3D simulation clearly is capable of modeling power hop, but it required an enormous amount of effort and computing power (for its day) to produce each test run sequence.
- **Comparison of ADAMS Simulation to Colorado Field Tests in the Early 1990s (JCW)—**These 3D simulations of a John Deere 8760 4WD tractor were produced by David Smith of the Deere & Company Technical Center in 1992. Using the commercial version of ADAMS, he simulated conditions corresponding to some of the field tests that had been conducted in Colorado in the fall of 1991. For the cases simulated, the model and field tests agreed on which inflation pressure combinations led to power hop and which resulted in a stable tractor. An animated wire frame model of the tractor geometry is shown in the video. Note that the forces acting on the wheels and the drawbar load are shown as animated arrows whose length is proportion to force magnitude.
- **MFWD Hop Mode Shape Animation, 1989 (JCW)—**This animation shows the hop mode of the John Deere 4450 MFWD tractor, discussed in detail as Case 2 in the paper, just after hop starts. It was produced by Bernard Romig using *Mathematica*. The elongated oval in the video is the path of the tractor center of gravity. Note

that a mode shape represents only relative amplitudes—not absolute displacements. Thus the motions were created larger than might actually occur for the purpose of clarity of the animation. This animation is very similar to the motions exhibited by real tractors just after power hop begins.

Examples of Self-Excited Vibrations

- **Tacoma Narrows Bridge (JCW)—**The Tacoma Narrows Bridge scenes in this familiar clip show self-excited torsional vibrations induced by a steady 42 mph wind just prior to failure on November 7, 1940. For several weeks prior to this date, the bridge exhibited large vertical bending vibrations in winds of less intensity. These were not self-excited vibrations, but, rather, *forced* vibrations due to vortex shedding. Many textbooks have incorrectly described the Tacoma Narrows Bridge failure as being the result of a forced vibration. See the references on this in the Distinguished Lecture for a detailed discussion.
- **Galloping Power Lines (JCW)—**The very large amplitude oscillations of power transmission lines shown in this clip occurred after an ice storm. Wind blowing across the resulting "ice airfoil" cross sections of the wires created the self-excited vibrations. The ice on the wires is not visible due to the distance of the lines from the camera, but it is visible on the ground and at the base of the towers at the very beginning of the video clip. Near the end of the clip, bending trees illustrate the effect of strong cross wind.
- **Galloping Bridge Cables (JCW)—**On February 22, 1974, at approximately 7:30 a.m. as the first author crossed the I-280 Bridge over the Mississippi River at Davenport, Iowa, he noticed large amplitude vibrations of the suspension cables. A sleet storm the night before had created "airfoil" shaped cross-sections on the cables. Then the wind direction changed, resulting in aerodynamic flutter, a self-excited vibration. This tied-arch suspension bridge had just been opened for use the previous summer. At each panel point there are four cables each 2.25 inches in diameter spaced on a 12 inch by 16 inch pattern. The longest cables are approximately 100 feet in length. Of noteworthy interest, one of the four cables in each cluster usually exhibited far greater amplitudes than the other three. Movies of the phenomenon filmed from about 8:30 to 9:30 later that morning were sent to the Illinois Department of Transportation. Ultimately that department designed and installed a series of cross-clamps with five rubber isolators connecting the cables and cross bars to force all cables to move together and to provide some damping. These were positioned at two-thirds the height of the cables to provide asymmetry of cable length as well as to blend with the arches. No instability has been observed following sleet storms since the clamps were installed.
- **Airplane Nose Wheel Shimmy (JCW)—**This is a single photograph showing the wreckage of a burning aircraft on a runway. The path of the shimmying nose wheel that failed is clear from the wavy rubber marks on the runway. Caster wheel shimmy and trailer weaving are common examples of self-excited vibrations.

Example of Tractor Road Lope

- **Firestone Demo of Road Lope on MFWD Tractor (JCW)—**This video was provided by Ken Brodbeck of the Firestone Agricultural Tire Company. Road lope is a forced vibration that occurs when the rotation frequency of a wheel with sufficient geometric out-of-roundness of the tire, rim, dish, hub, axle, or a combination of these is near a pitch or bounce natural frequency of the tractor on its tires. In the video, the front wheel dishes are initially not centered relative to their rims, and the tractor exhibits road lope at the critical speed of 22 mph. The second section of the video illustrates how the wheels were reassembled to minimize the offsets. The third section shows the tractor running smoothly at 22 mph with the improved assemblies. A final section shows smooth ride at 25 mph.